ROBUST HIGH-FREQUENCY SOLVERS

by

Hasan Çağan Özen

B.S., Mathematics, Boğaziçi University, 2009

Submitted to the Institute for Graduate Studies in
Science and Engineering in partial fulfillment of
the requirements for the degree of
Master of Science

Graduate Program in Computational Science and Engineering

Boğaziçi University

2012

ACKNOWLEDGEMENTS

I would like to express my sincere gratitude to my advisor Fatih Ecevit who endured and guided me throughout my master studies. Without his motivations and enthusiasm, it would not have been possible to write the thesis.

I would like to thank Mehmet Burçin Ünlü and Ali Ecder for participating in my thesis committee.

I acknowledge the support from the Scientific Research Projects of Boğaziçi University through the project "Fast and convergent methods for high-frequency acoustic scattering" under the code 5548P.

I am also thankful to all of my officemates for a friendly atmosphere. My special thanks to Samet Keserci for being a sincere friend as well as a colleague in the path of pursuing the degree.

Filiz Carus who has been central for my happiness deserves special gratitudes. I would not be able to complete this work without her support.

Finally, I am truely indebted to my family for their support and patience during my education.

ABSTRACT

ROBUST HIGH-FREQUENCY SOLVERS

This work concerns the numerical solutions of the direct obstacle scattering problem in $\mathbb{R}^2$. To this end, we formulate the problem as an equivalent integral equation. We then review the fundamental numerical methods such as Nyström, collocation and Galerkin methods, for integral equations of the second kind. We establish convergence results and error estimates for these methods, and incorporate numerical examples considering different integral equations. Although these methods are very efficient for low frequencies, they can not be utilized for high frequency scenarios as the computational cost grows linearly with the wave number k. In this connection, we propose a robust convergent algorithm based on a Galerkin formulation utilizing the geometrical optics ansatz to adapt the approximation spaces to high frequency scattering (by convex obstacles) which overcomes this type of growth in complexity requiring only $\mathcal{O}(k^{\varepsilon})$, $\varepsilon > 0$, increase in the degrees of freedom to maintain a given accuracy. Numerical experiments demonstrate the efficiency of our method by exhibiting numerical errors and condition numbers in several scenarios.

ÖZET

SAĞLAM YÜKSEK FREKANS ÇÖZÜCÜLERİ

Bu çalışma iki boyutta direkt dalga saçılımı probleminin nümerik çözümleri ile ilgilidir. Bu amaçla, problem eşdeğer bir integral denklem olarak formüle edilmekte ve ikinci tür integral denklemler icin temel sayısal yöntemlerinden olan "Nyström", "collocation" ve "Galerkin" metotlari incelenmektedir. Daha sonra bu metotların yakınsaklık ve hata kestirimleri ispatlanmakta ve farklı integral denklemler ile örnekler yapılmaktadır. Bahsedilen metotlar düşük frekanslar için çok etkili olmalarına rağmen, hesaplama maliyeti dalga sayısı k ile lineer olarak arttığından dolayı yüksek frekanslı dalgalar için kullanılamazlar. Bu bağlamda, Galerkin formülasyonu temelli, yaklaşım uzaylarını geometrik optik kestirimi kullanarak yüksek frekans saçılmasına (dışbükey engellerden) adapte eden, sağlam ve yakınsak bir algoritma öneriyoruz ki bu algoritma verilmiş bir hassasiyeti korumak için, serbestlik derecesinde sadece $\mathcal{O}(k^{\varepsilon})$, $\varepsilon > 0$, artış gerektirerek karmaşıklıkta yukarıda bahsedilen tarzda büyümeyi gidermektedir. Nümerik deneyler birçok senaryoda hataları ve kondisyon sayılarını sergileyerek metotumuzun etkinliğini göstermiştir.

TABLE OF CONTENTS

LIST OF FIGURES

LIST OF TABLES

LIST OF SYMBOLS

$\lvert\cdot\rvert$	Euclidean norm on $\mathbb{R}^2$
$\lvert\lvert\cdot\rvert\rvert_\infty$	The sup-norm
$C^m(D)$	m-times continuosly differentiable functions on D
$C_p(2\pi)$	2π-periodic continuous functions
$C^{0,\alpha}$	Hölder continuous functions of order α
$C_p^{m,\alpha}(2\pi)$	m-times Hölder continuously differentiable 2π-periodic functions on $\mathbb{R}$
D	Open bounded subset of $\mathbb{R}^2$
D_s^n	n^{th} derivate operator with respect to s
$\mathbb{DL}$	Double layer potential
DL	Double layer operator
DL'	Normal derivative operator
$H_n^{(1,2)}$	Hankel functions of the first and second kind of order n
$\mathcal{H}_n(S^1)$	Surface spherical harmonics of degree n on the unit circle
$H^p[0,2\pi]$	Sobolev space of order p on the set $[0,2\pi]$
Im(z)	Imaginary part of z
i	Imaginary unit
k	Wave number
L^2	Square integrable functions
$\mathbb{N}$	Natural numbers
$\mathcal{O}$	Big-O notation
o	Little-o notation
$\mathbb{P}_n$	Polynomials of degree $\leq n$
$\mathbb{R}^n$	n-dimensional Euclidean space
Re(z)	Real part of z
S^1	Unit circle in $\mathbb{R}^2$
$\mathbb{SL}$	Single layer potential
SL	Single layer operator
supp	Support of a function

$\mathbb{T}_n$	Trigonometric polynomials of degree $\leq n$
u^i	Incident field
u^s	Scattered field
w	Angular frequency
$\mathbb{Z}^+$	The set of positive integers
Δ	The Laplacian
δ_{ij}	Kronecker delta
Φ	The fundamental solution of the Helmholtz equation in $\mathbb{R}^2$
ν	Unit normal vector
Ω_ρ	The cirle with radius ρ in $\mathbb{R}^2$
ω	Modulus of continuity
∂D	Boundary of D
∇	The gradient
$\oplus$	Direct sum

LIST OF ACRONYMS/ABBREVIATIONS

CPV	Cauchy Principle Value
BC	Boundary Condition
RC	Radiation Condition
BEM	Boundary Element Method
IL	Illuminated Region
SR	Shadow Region
DS	Deep Shadow Region
SB	Shadow Boundary
TI	Transition Region from Illuminated
TS	Transition Region from Shadow

1. INTRODUCTION

This thesis deals with the numerical solutions of the exterior Dirichlet problem for the Helmholtz equation

$$\Delta u + k^2 u = 0,$$

which describes the problem of scattering of time harmonic waves with the wave number k by bounded obstacles. Utilizing the fundamental solution and Green's identities, one can reformulate the boundary value problem as an equivalent integral equation on the boundary. The main advantage of the boundary integral methods is that the dimension of the computational domain is reduced by one, leading to a significant reduction in the size of the linear system. Furthermore, for the exterior problem, the finite element method cannot be applied using the standard techniques [38] thus the boundary element method is one of the most preferred tools in the literature. Correspondingly, boundary integral equations will be the underlying tool utilized in the thesis.

To begin with, using Green's identities, we present representation formulas for solutions of the Helmholtz equation in both bounded and unbounded domains. To reformulate our problem into an equivalent integral equation, we then introduce surface potentials and examine their jump relations and regularity properties on the boundary. Since our main concern, the direct obstacle scattering problem, is a special case of the exterior Dirichlet problem, we establish the well-posedness of the latter problem utilizing Rellich's lemma and seeking a solution in the form of a combined potentials. In the end, we derive a well-posed combined field integral equation for the scattering problem whose solution represents a physical quantity [11].

Considering numerical solutions to the integral equations of the second kind, we shall describe three fundamental methods: the Nyström method, the collocation method and the Galerkin method. The first method is based upon application of an appropriate quadrature rule for the associated integral. This consideration provides a

very efficient method (regarding computations) for the boundary integral equations of the second kind in two dimensions. The collocation method requires that the integral equation is satisfied at a finite number of points on the domain. One can consider this method as a projection method onto a finite dimensional subspace using the interpolation operator at these so-called collocation points. Note that basis selection plays an important role for the conditioning of the linear system. The last method we describe is the Galerkin method where we exploit the geometrical structure of Hilbert spaces to obtain the best approximation to the solution. Since geometry is involved, error analysis of this method is often satisfactory, however, it requires the most computational effort among all these methods. Similar to the collocation method, Galerkin method is also sensitive to the chosen basis of the approximation subspaces. Incidentally, for integral operators with weakly singular kernels, discretization is not straightforward; one should derive an appropriate quadrature formula in all mentioned methods. Finally, even though these methods are very efficient for small wave numbers, they are not robust for high frequency settings in the sense of increasing complexity [11, 28].

The main aim of the work is to develop a robust convergent algorithm for the computation of high frequency scattering, i.e. the wave number $k \gg 1$, of plane waves by convex obstacles in $\mathbb{R}^2$. In high frequency setting, the robustness of an algorithm essentially depends on the following properties [39]:

(A) The design of good, k-dependent, approximation spaces X_n so that the error

$$||v - \hat{v}|| \leq C \inf_{\hat{w} \in X_n} ||v - \hat{w}||$$

for the best approximation $\hat{v}$ is growing as slowly as possible as $k \to \infty$. Here v is the solution of the integral equation formulation of the scattering problem.

(B) The proof of sharp estimates on the dependence of the constant C on k.

(C) Efficient numerical implementation so that the computational time remains bounded as $k \to \infty$.

Incidentally, we only address items (A) and (B) in the thesis. Regarding (C), for efficient techniques concerning the evaluation of arising oscillatory integrals we refer to [11, 34–37].

Our algorithm is based on the direct boundary integral equation method incorporating k-dependent hybrid subspaces within the Galerkin approximation. In constructing the approximation spaces, we make use of the geometrical optics ansatz

$$v(\gamma(s), k) = k \, \exp(ik\gamma(s) \cdot a) \, v^{slow}(s, k) \tag{1.1}$$

for the normal derivative v of the total field, where $\gamma(s)$ is the arc-length parametrization of ∂D, the unit vector a is the direction of the incident plane wave, and $v^{slow}(\cdot, k)$ oscillates less rapidly than $v(\cdot, k)$ for large k [25]. The asymptotic analysis as $k \to \infty$ also suggests that the boundary can be decomposed into four main regions: the illuminated region, the deep shadow region and the shadow boundaries [25] (see section 4.2). Armed with this information, our method introduces a carefully chosen refined partition comprising of $4m$ regions, $m \in \mathbb{Z}^+$, over the boundary by creating transition regions between shadow boundaries and their neighbors. The slowly varying unknown $v^{slow}(\cdot, k)$ is then approximated through the Galerkin formulation in each region by both algebraic polynomials and trigonometric polynomials. The fully rigorous error analysis based on polynomial approximation is established in [26] while the case of spectral approximation can be found in [27]. Incidentally, the refined partition will account for connecting shadow boundaries to other regions in an optimal way and the case $m = 1$ corresponds to the partition having no transition regions (for an associated analysis see [28]).

If one searches an approximate solution via standard numerical techniques, e.g. usual boundary element methods approximating the solution v by polynomials, in order to maintain a prescribed level of accuracy, the degrees of freedom should increase with at least $\mathcal{O}(k)$ with increasing k [11]. This phenomena clearly obstructs the usage of these methods for high frequency settings. Our robust numerical algorithm overcomes this type of growth in computational complexity as it requires only $\mathcal{O}(k^{\varepsilon})$, $\varepsilon > 0$,

increase in degrees of freedom to preserve a given accuracy (see (A)).

In the literature, several different methods utilize hybrid boundary element methods by considering oscillatory ansatz functions. Our method is closely related to the works of [11, 28, 35, 40–42]. Some of the groundwork on the path of developing robust high frequency solvers were carried out in [40,41], wherein an ansatz similar to (4.1) was used to approximate the solution by the conventional finite element methods and the method of stationary phase, however no rigorous error analysis was given. Another approach taken in [11,35] by employing a Nyström discretization to the resulting integral equation for $v^{slow}(\cdot, k)$ gave rise to bounded computational costs for arbitrarily high frequencies. The fundamental idea was to use the method of stationary phase in which integration is localised around "critical" points. Although k-independent convergence was observed numerically, a rigorous error analysis was not given either. Moreover, [42] makes use of asymptotically derived basis functions (based on geometrical optics and geometrical theory of diffraction) while taking into account the "creeping waves" just behind the shadow boundaries and achieved quite accurate numerical results, yet this work also did not attempt a rigorous error analysis. Incidentally, using effective quadrature rules for oscillatory integrals together with ideas from the "steepest descent method" in a collocation method, [36] was able to obtain a sparse discretization matrix for the high frequency scattering problem. No stability analysis is given, nevertheless numerical experiments show that the underlying ideas produce a novel algorithm. Altogether, the superiority of our method over the ones mentioned above lies in the fact that our algorithm generates a (rigorous) convergent scheme for each fixed wave number k [26, 27].

The most closely related work to our method is presented in [28]. There it is considered to approximate $v^{slow}(\cdot, k)$ by polynomials utilizing the ansatz (4.1) in each of the four regions except the shadow region. Unlike the other methods described above, [28] established a rigorous error analysis using the asymptotic properties of the solution given in [25]. Concerning the approximation error, it is shown that degrees of freedom should increase with $\mathcal{O}(k^{1/9})$ to maintain a fixed accuracy with growing k. The notable weakness of the algorithm is that the shadow region approximation is

totally ignored (there the solution is approximated by zero), therefore the method is not convergent for fixed k. Correspondingly, it is crucial to note that our algorithm yields upto 3 digits of accuracy (in the relative L^2 norm) in the shadow region whereas the relative error in [28] is constantly 1. All in all, major advantages of our method over [28] consist of not only a superior optimized error bound, but also accurate numerical errors and better condition numbers as demonstrated by numerical experiments. Hence, our robust algorithm surpasses the one in [28] regarding both theoretical and numerical aspects.

With regards to (B), the constant C is proved to be $\mathcal{O}(k^{1/3})$ for the case of spherical geometries [28]. In addition, a more recent study shows that this constant is $\mathcal{O}(k^{1/2})$ and the coercivity constant of the integral operator contained in it can be bounded independently of k for star-shaped Lipschitz domains utilizing an alternative integral equation [30].

The thesis is organized as follows. We begin in *Chapter 2* by proving the existence and uniqueness of the exterior Dirichlet problem and transforming the problem into an equivalent integral equation.

Chapter 3 is devoted to standard numerical methods for integral equations of the second kind. There we establish convergence of these methods, provide error estimates, exhibit necessary details for their implementation and give several numerical examples.

In *Chapter 4*, we present our main high frequency scattering algorithm based on a Galerkin formulation utilizing weighted polynomial spaces adapted to the high frequency nature of the problem. Then, we support our method with a number of numerical examples comparing different scenarios. In the end, we propose an alternative robust scheme using weighted trigonometric polynomials.

2. THE HELMHOLTZ EQUATION AND DIRECT SCATTERING

Propagation of waves in a homogeneous isotropic medium is mathematically governed by the wave equation

$$\Delta U(x,t) - \frac{1}{c^2}\frac{\partial^2}{\partial t^2}U(x,t) = 0,$$

where c denotes the speed of propagation. We assume that waves are time-harmonic $U(x,t) = \mathrm{Re}\{u(x)e^{-iwt}\}$ with frequency $w > 0$, in which case, the complex-valued space dependent part u satisfies the *Helmholtz equation*

$$\Delta u + k^2 u = 0, \tag{2.1}$$

where $k = w/c > 0$ is the *wave number* [1].

The scattering of time-harmonic waves by an impenetrable bounded obstacle leads to exterior boundary value problems for the Helmholtz equation. In particular, scattering from a *sound-soft* obstacle induces a Dirichlet boundary condition whereas for a *sound-hard* obstacle we have a Neumann boundary condition [1].

In this chapter, our main concern will be the direct scattering problem:

Direct Obstacle Scattering Problem. *Given a plane wave $u^i = e^{ikx\cdot a}$ representing an incident field, find a solution*

$$u = u^i + u^s$$

to the Helmholtz equation in $\mathbb{R}^2\backslash\bar{D}$ ($D \subset \mathbb{R}^2$ is open and connected) such that scattered field u^s satisfies the Sommerfeld radiation condition (described below) and the total

field u satisfies the homogeneous boundary condition

$$u = 0 \quad on\ \partial D$$

[1].

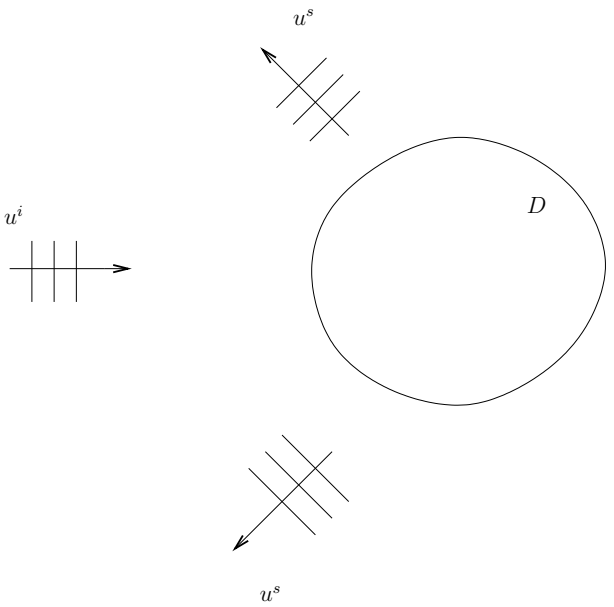

Figure 2.1. Incident field impinging upon the boundary ∂D.

Definition 2.1. *A solution u to the Helmholtz equation in $\mathbb{R}^2$ is called* radiating *if it satisfies the Sommerfeld radiation condition*

$$\frac{x}{|x|} \cdot \nabla u(x) - ik\, u(x) = o\left(\frac{1}{|x|^{1/2}}\right), \qquad |x| \to \infty,$$

uniformly in all directions $x/|x|$.

In the sequel, we will see that the Sommerfeld radiation condition characterizes the behavior of solutions to the Helmholtz equation at infinity.

The outline of this chapter is as follows. We first present Green's representation theorems for solutions of the Helmholtz equation. Then we investigate the jump relations and regularity properties of surface potentials, and finally establish the well-posedness of the exterior Dirichlet problem. In what follows, unless otherwise stated, ν will stand for the unit normal vector to ∂D directed into the exterior of D.

2.1. Green's Representation Formulas

In $\mathbb{R}^2$, the fundamental solution of the Helmholtz equation is given by [2]

$$\Phi(x,y) := \frac{i}{4} H_0^{(1)}(k|x-y|), \quad x \neq y, \tag{2.2}$$

where $H_0^{(1)}$ is the Hankel function of the first kind of order zero [3].

Theorem 2.2. *For a fixed $y \in \mathbb{R}^2$, $\Phi(\cdot, y)$ solves the Helmholtz equation in $\mathbb{R}^2 \backslash \{y\}$. Moreover, the fundamental solution (2.2) satisfies*

$$\frac{x}{|x|} \cdot \nabla_x \Phi(x,y) - ik\,\Phi(x,y) = \mathcal{O}\left(\frac{1}{|x|^{3/2}}\right), \qquad |x| \to \infty,$$

uniformly in $x/|x| \in S^1$ and $y \in D$ for every bounded subset $D \subset \mathbb{R}^2$.

Proof. The first claim follows from direct substitution and the second from the asymptotic behavior (see [3]) of Hankel functions

$$H_n^{(1,2)}(r) = \sqrt{\frac{2}{\pi r}}\, e^{\pm i(r - n\pi/2 - \pi/4)} \left(1 + \mathcal{O}\left(\frac{1}{r}\right)\right), \qquad r \to \infty. \tag{2.3}$$

□

Note that from Theorem 2.2 it can be readily seen that the fundamental solution (2.2) satisfies the Sommerfeld radiation condition.

Next, we state Green's integral identities that will be fundamental in studying the Helmholtz equation.

Theorem 2.3. (Green's identities) *Let D be a bounded domain of class C^1. Then, for $u \in C^1(\bar{D})$ and $v \in C^2(\bar{D})$ we have Green's first identity*

$$\int_D \{u\Delta v + \nabla u \cdot \nabla v\}\, dx = \int_{\partial D} u \frac{\partial v}{\partial \nu}\, ds, \tag{2.4}$$

and for $u, v \in C^2(\bar{D})$ we have Green's second identity

$$\int_D u\Delta v - v\Delta u \, dx = \int_{\partial D} u\frac{\partial v}{\partial \nu} - v\frac{\partial u}{\partial \nu} \, ds \tag{2.5}$$

[1].

Indeed, Green's identities remain valid in the case where u, v belong to $C^2(D) \cap C(\bar{D})$ as they have normal derivatives in the sense of uniform convergence throughout the boundary [4].

With the aid of Green's identities, Green's representation formula for the solutions of Helmholtz equation can be established for bounded domains [4].

Theorem 2.4. *Let D be a bounded domain of class C^2. Let $u \in C^2(D) \cap C(\bar{D})$ be a function which possesses a normal derivative on the boundary in the sense that the limit*

$$\frac{\partial u}{\partial \nu}(x) = \lim_{h \to 0^+} \nu(x) \cdot \nabla u(x - h\nu(x)), \quad x \in \partial D,$$

exists uniformly on ∂D. Assume that u is a solution to the Helmholtz equation in D. Then, we have Green's formula

$$u(x) = \int_{\partial D} \left\{ \frac{\partial u}{\partial \nu}(y)\Phi(x, y) - u(y)\frac{\partial \Phi(x, y)}{\partial \nu(y)} \right\} ds(y), \quad x \in D. \tag{2.6}$$

In order to study exterior boundary value problems, we need to investigate the asymptotic behavior of solutions of the Helmholtz equation. Therefore, we extend the Green's representation formula to unbounded domains.

Lemma 2.5. *Assume the bounded set D is the open complement of an unbounded domain of class C^2. Let $u \in C^2(\mathbb{R}^2 \backslash \bar{D}) \cap C(\mathbb{R}^2 \backslash D)$ be a radiating solution to the Helmholtz equation in $\mathbb{R}^2 \backslash \bar{D}$ which possesses a normal derivative on the boundary in*

the sense that the limit

$$\frac{\partial u}{\partial \nu}(x) = \lim_{h \to 0^+} \nu(x) \cdot \nabla u(x + h\nu(x)), \quad x \in \partial D,$$

exists uniformly on ∂D. *Then*

$$\int_{\Omega_\rho} |u|^2 ds = \mathcal{O}(1), \quad \rho \to \infty,$$

where $\Omega_\rho = \{y \in \mathbb{R}^2 : |y| = \rho\}$ [1].

Proof. For a positive real k, the equality

$$\left| \frac{\partial u}{\partial \nu} - iku \right|^2 = \left| \frac{\partial u}{\partial \nu} \right|^2 + k^2 |u|^2 + 2k \mathrm{Im} \left(u \frac{\partial \bar{u}}{\partial \nu} \right)$$

holds where ν is the unit outward normal to Ω_ρ. Then we have

$$\begin{aligned} 0 &= \lim_{\rho \to \infty} \int_{\Omega_\rho} \left| \frac{\partial u}{\partial \nu} - iku \right|^2 ds, \\ &= \lim_{\rho \to \infty} \int_{\Omega_\rho} \left\{ \left| \frac{\partial u}{\partial \nu} \right|^2 + k^2 |u|^2 + 2k \mathrm{Im} \left(u \frac{\partial \bar{u}}{\partial \nu} \right) \right\} ds, \end{aligned} \tag{2.7}$$

where the first equality follows from the Sommerfeld radiation condition. Applying Green's first identity to u and $\bar{u}$ in $D_\rho := \{y \in \mathbb{R}^2 \backslash \bar{D} : |y| < \rho\}$ yields

$$\int_{\Omega_\rho} u \frac{\partial \bar{u}}{\partial \nu} ds = \int_{\partial D} u \frac{\partial \bar{u}}{\partial \nu} ds - k^2 \int_{D_\rho} |u|^2 dx + \int_{D_\rho} |\nabla u|^2 dx.$$

Upon inserting the imaginary part of this equation into (2.7) we find that

$$\lim_{\rho \to \infty} \int_{\Omega_\rho} \left\{ \left| \frac{\partial u}{\partial \nu} \right|^2 + k^2 |u|^2 \right\} ds = -2k \mathrm{Im} \int_{\partial D} u \frac{\partial \bar{u}}{\partial \nu} ds. \tag{2.8}$$

Both terms on the left of (2.8) are nonnegative. Also, since u is continuous on ∂D and possesses normal derivative throughout ∂D, the right hand side is finite. Therefore it

must be true that each term on the left is bounded as $\rho \to \infty$. □

Theorem 2.6. *Under the assumptions of the previous theorem we have* Green's representation formula

$$u(x) = \int_{\partial D} \left\{ u(y) \frac{\partial \Phi(x,y)}{\partial \nu(y)} - \frac{\partial u}{\partial \nu}(y) \Phi(x,y) \right\} ds(y), \quad x \in \mathbb{R}^2 \backslash \bar{D} \tag{2.9}$$

[1, 4].

Proof. We have the estimate

$$\left| \int_{\Omega_\rho} \left\{ u(y) \frac{\partial \Phi(x,y)}{\partial \nu(y)} - \frac{\partial u}{\partial \nu}(y) \Phi(x,y) \right\} ds(y) \right| \leq I_1 + I_2,$$

where

$$I_1 = \left| \int_{\Omega_\rho} u(y) \left\{ \frac{\partial \Phi(x,y)}{\partial \nu(y)} - ik\Phi(x,y) \right\} ds(y) \right|,$$
$$I_2 = \left| \int_{\Omega_\rho} \Phi(x,y) \left\{ \frac{\partial u}{\partial \nu}(y) - iku(y) \right\} ds(y) \right|.$$

From the preceding lemma and Sommerfeld radiation condition for $\Phi(x,y)$, $y \in \Omega_\rho$, we see that

$$I_1 \leq \left(\int_{\Omega_\rho} |u|^2 ds \right)^{1/2} \left(\int_{\Omega_\rho} \left| \frac{\partial \Phi(x,y)}{\partial \nu(y)} - ik\Phi(x,y) \right|^2 ds(y) \right)^{1/2} \to 0, \quad \rho \to \infty.$$

Further, the radiation condition for u and asymptotics (2.3) entail

$$I_2 \leq \left(\int_{\Omega_\rho} |\Phi(x,\cdot)|^2 ds \right)^{1/2} \left(\int_{\Omega_\rho} \left| \frac{\partial u}{\partial \nu}(y) - iku(y) \right|^2 ds(y) \right)^{1/2} \to 0, \quad \rho \to \infty.$$

Therefore,

$$\lim_{\rho\to\infty}\int_{\Omega_\rho}\left\{u(y)\frac{\partial\Phi(x,y)}{\partial\nu(y)}-\frac{\partial u}{\partial\nu}(y)\Phi(x,y)\right\}ds(y)=0. \tag{2.10}$$

Now we apply Green's representation formula (2.6) in D_ρ to get

$$\begin{aligned}u(x)&=\int_{\partial D_\rho}\left\{\frac{\partial u}{\partial\nu}(y)\Phi(x,y)-u(y)\frac{\partial\Phi(x,y)}{\partial\nu(y)}\right\}ds(y),\\&=\int_{\Omega\rho}\left\{\frac{\partial u}{\partial\nu}(y)\Phi(x,y)-u(y)\frac{\partial\Phi(x,y)}{\partial\nu(y)}\right\}ds(y)\\&\quad-\int_{\partial D}\left\{\frac{\partial u}{\partial\nu}(y)\Phi(x,y)-u(y)\frac{\partial\Phi(x,y)}{\partial\nu(y)}\right\}ds(y),\end{aligned}$$

for $x\in D_\rho$. Taking the limit $\rho\to\infty$ and using (2.10) establish the proof. □

From Theorem 2.6 we can deduce that radiating solutions u to the Helmholtz equation satisfy the decay condition

$$u(x)=\mathcal{O}\left(\frac{1}{|x|^{1/2}}\right),\quad |x|\to\infty.$$

.

2.2. Surface Potentials

In this section, we introduce surface potentials and examine their jump relations and regularity properties.

Definition 2.7. *Given $\varphi\in C(\partial D)$, the integrals*

$$\mathbb{SL}(x):=\int_{\partial D}\Phi(x,y)\varphi(y)\,ds(y),\quad x\in\mathbb{R}^2\backslash\partial D,$$

and

$$\mathbb{DL}(x) := \int_{\partial D} \frac{\partial \Phi(x,y)}{\partial \nu(y)} \varphi(y)\, ds(y), \quad x \in \mathbb{R}^2 \backslash \partial D,$$

are called single layer *and* double layer potentials *with density* φ*, respectively.*

For $x \notin \partial D$, we can differentiate under the integral sign to see that both single and double layer potentials are solutions of the Helmholtz equation in D and $\mathbb{R}^2 \backslash \bar{D}$. Furthermore, from (2.6) and (2.9) we observe that any solution to the Helmholtz equation can be represented as a combination of single and double layer potentials. Since the fundamental solution $\Phi(x,y)$ is C^∞ for $x \neq y$, single and double layer potentials are in $C^\infty(D) \cap C^\infty(\mathbb{R}^2 \backslash \bar{D})$.

In the rest of the section, we investigate the behavior of these potentials for points on the boundary. For the following theorems, we assume ∂D is of class C^2.

Theorem 2.8. *Let G be a closed domain in $\mathbb{R}^2$ containing ∂D in its interior. Suppose the function K is defined and continuous for all $x \in G$, $y \in \partial D$, $x \neq y$, and assume there exist positive constants C and $\alpha \in (0,1]$ such that for all $x \in G$, $y \in \partial D$ with $x \neq y$, we have*

$$|K(x,y)| \leq C|x-y|^{\alpha-1}. \tag{2.11}$$

Suppose further that there exists $m \in \mathbb{N}$ such that

$$|K(x_1,y) - K(x_2,y)| \leq C \sum_{j=1}^{m} |x_1 - y|^{\alpha-1-j} |x_1 - x_2|^j \tag{2.12}$$

for all $x_1, x_2 \in G$, $y \in \partial D$ with $2|x_1 - x_2| \leq |x_1 - y|$. Then the potential v defined by

$$v(x) := \int_{\partial D} K(x,y)\varphi(y) ds(y), \quad x \in G,$$

with $\varphi \in C(\partial D)$ belongs to the Hölder space $C^{0,\beta}(G)$ for all $\beta \in (0,\alpha]$ if $0 < \alpha < 1$,

and for all $\beta \in (0,1)$ *if* $\alpha = 1$.

Proof. For a proof in three dimensions see [4], and this two dimensional version follows similarly. □

Theorem 2.9. *The single layer potential* $\mathbb{SL}$ *with continuous density* φ *is Hölder continuous in* $\mathbb{R}^2$ (*see Appendix B*) *and*

$$||\mathbb{SL}||_{\alpha,\mathbb{R}^2} \leq C||\varphi||_{\infty,\partial D}$$

for $0 < \alpha < 1$ *and some constant* C_α *depending on* ∂D *and* α.

Proof. The statement follows from the fact that fundamental solution $\Phi(x,y)$ satisfies Theorem 2.8 for appropriate values of α and m. □

For the next theorem about $\mathbb{DL}$, it suffices to carry out the proof in the case $k = 0$ with the fundamental solution $\Phi_0(x,y) := \frac{1}{2\pi}\log\frac{1}{|x-y|}$ of the Laplace equation since

$$K(x,y) := \frac{\partial\Phi(x,y)}{\partial\nu(y)} - \frac{\partial\Phi_0(x,y)}{\partial\nu(y)}$$

satisfies conditions (2.11) and (2.12) with $\alpha = 1$ and $m = 1$.

Theorem 2.10. *The double layer potential* $\mathbb{DL}$ *with continuous density* φ *can be continuously extended from from* D *to* $\bar{D}$ *and* $\mathbb{R}^2\backslash\bar{D}$ *to* $\mathbb{R}^2\backslash D$ *with boundary values*

$$\mathbb{DL}_\pm(x) = \int_{\partial D} \varphi(y)\,\frac{\partial\Phi(x,y)}{\partial\nu(y)}\,ds(y) \pm \frac{1}{2}\,\varphi(x), \quad x \in \partial D, \tag{2.13}$$

where $\mathbb{DL}_\pm(x) := \lim_{h\to 0^+} \mathbb{DL}(x \pm h\nu(x))$ *and the integral exists as an improper integral* [5].

Proof. By Theorem C.1 we have

$$\left|\frac{\partial\Phi_0(x,y)}{\partial\nu(y)}\right| = \frac{|\{x-y\}\cdot\nu(y)|}{2\pi|x-y|^2} \leq \frac{L|x-y|^2}{2\pi|x-y|^2} = \frac{L}{2\pi}, \quad x \neq y.$$

Then, the integral in (2.13) has a weakly singular kernel (see definition A.0.1) and thus exists for $x \in \partial D$ as an improper integral.

For the double layer potential with constant density $\varphi = 1$ we have

$$\int_{\partial D} \frac{\partial\Phi_0(x,y)}{\partial\nu(y)} ds(y) = \begin{cases} -1, & x \in D, \\ -1/2, & x \in \partial D, \\ 0, & x \in \mathbb{R}^2\backslash\bar{D}. \end{cases} \tag{2.14}$$

This follows for $x \in D$ from Green's formula (2.6) applied to $u = 1$ in D and for $x \in \mathbb{R}^2\backslash\bar{D}$ from Green's first identity (2.4) with $v = \Phi_0(x,\cdot)$ and $u = 1$. For $x \in \partial D$, we exclude x from integration by circumscribing it with a circle Ω_r of radius r and centered at x, then again apply (2.4) with $v = \Phi_0(x,\cdot)$ and $u = 1$ on $\Omega_r \cap D$, and take the limit as $r \to 0$.

Now, we introduce the concept of parallel surfaces

$$\partial D_h := \{z = x + h\nu(x) : x \in \partial D\}, \quad h \in [-h_0, h_0] \text{ for some } h_0 > 0.$$

If h_0 is chosen sufficiently small, then parallel surfaces are well-defined, and in a sufficiently small neighborhood U of ∂D we can represent each $z \in U$ uniquely in the form $z = x + h\nu(x)$ for some $x \in \partial D$ [5]. Then we can write the double layer potential $\mathbb{DL}$ with density φ as

$$\mathbb{DL}(z) = \varphi(x)w(z) + v(z), \qquad z = x + h\nu(x) \in U\backslash\partial D, \tag{2.15}$$

where

$$w(z) := \int_{\partial D} \frac{\partial \Phi_0(x,y)}{\partial \nu(y)} ds(y) \quad \& \quad v(z) := \int_{\partial D} \{\varphi(y) - \varphi(x)\} \frac{\partial \Phi_0(z,y)}{\partial \nu(y)} ds(y). \quad (2.16)$$

We observe that for $x \in \partial D$ the second integral in (2.16) exists as an improper integral and represents a continuous function on the boundary. Therefore, with the aid of (2.14) and (2.15), in order to establish the theorem it is enough to show that

$$\lim_{h \to 0^+} v(x + h\nu(x)) = v(x), \quad x \in \partial D,$$

uniformly on ∂D. For a (technical) justification of this limit we refer to [5]. □

We begin to examine the regularity properties of single and double layer potentials. Proofs can be found in [4].

Theorem 2.11. *Let $\varphi \in C(\partial D)$. Then for the single layer potential $\mathbb{SL}$ with density φ we have*

$$\frac{\partial \mathbb{SL}_{\pm}}{\partial \nu}(x) = \int_{\partial D} \varphi(y) \, \frac{\partial \Phi(x,y)}{\partial \nu(x)} \, ds(y) \mp \frac{1}{2} \varphi(x) \quad x \in \partial D,$$

where $\partial \mathbb{SL}_{\pm}/\partial \nu(x) := \lim_{h \to 0^+} \nu(x) \cdot \nabla \mathbb{SL}(x \pm h\nu(x))$ is to be understood in the sense of uniform convergence on ∂D and the integral exists as an improper integral [4] .

Theorem 2.12. *The double layer potential v with continuous density φ satisfies*

$$\lim_{h \to 0^+} \nu(x) \cdot \{\nabla \mathbb{DL}(x + h\nu(x)) - \nabla \mathbb{DL}(x - h\nu(x))\} = 0$$

uniformly for all $x \in \partial D$ [4] .

In the following theorem, we formulate the regularity properties of single and double layer potentials in terms of Hölder continuity.

Theorem 2.13. *Let $\alpha \in (0,1)$. The first derivatives of the single layer potential $\mathbb{SL}$ with density $\varphi \in C^{0,\alpha}(\partial D)$ can be Hölder continuously extended from D to $\bar{D}$ and from*

$\mathbb{R}^2\backslash\bar{D}$ *to* $\mathbb{R}^2\backslash D$ *with limiting values*

$$\nabla\mathbb{SL}_{\pm}(x) = \int_{\partial D} \varphi(y)\, \nabla_x \Phi(x,y)\, ds(y) \mp \frac{1}{2}\, \varphi(x)\, \nu(x), \quad x \in \partial D,$$

where $\nabla\mathbb{SL}_{\pm}(x) := \lim_{h\to 0^+} \nabla\mathbb{SL}(x \pm h\nu(x))$. *Moreover, the first derivatives of the double layer potential* $\mathbb{DL}$ *with density* $\varphi \in C^{1,\alpha}(\partial D)$ *can be Hölder continuously extended from* D *to* $\bar{D}$ *and from* $\mathbb{R}^2\backslash\bar{D}$ *to* $\mathbb{R}^2\backslash D$ [4].

To study the direct values of surface potentials, it is convenient to define the single and double layer operators SL, DL and the normal derivative operator DL'

$$\begin{aligned}
(\mathrm{SL}\,\varphi)(x) &:= 2\int_{\partial D} \Phi(x,y)\, \varphi(y)\, ds(y), \quad x \in \partial D,\\
(\mathrm{DL}\,\varphi)(x) &:= 2\int_{\partial D} \frac{\partial\Phi(x,y)}{\partial\nu(y)}\, \varphi(y)\, ds(y), \quad x \in \partial D,\\
(\mathrm{DL}'\,\varphi)(x) &:= 2\int_{\partial D} \frac{\partial\Phi(x,y)}{\partial\nu(x)}\, \varphi(y)\, ds(y), \quad x \in \partial D,
\end{aligned}$$

and then analyze their mapping properties.

Theorem 2.14. *The operators* SL, DL *and* DL' *are bounded from* $C(\partial D)$ *into* $C^{0,\alpha}(\partial D)$, *and the operators* SL *and* DL *are also bounded from* $C^{0,\alpha}(\partial D)$ *into* $C^{1,\alpha}(\partial D)$.

Proof. The statements about SL follow from Theorems 2.9 and 2.13. For the rest of claims see [4]. □

As a consequence of Theorems 2.14 and B.1, the operators SL, DL, and DL' are compact from $C(\partial D)$ into $C(\partial D)$.

2.3. Direct Obstacle Scattering

Scattering of time-harmonic waves by an obstacle gives rise to exterior boundary value problems for the Helmholtz equation, e.g. exterior Dirichlet and Neumann problems. For a detailed analysis of the exterior Neumann problem we refer to [1]. Here,

we prove the well-posedness of the exterior Dirichlet problem. In this endeavor, our main machinery will be boundary integral equations. Most of the work in this section is based on [4] and [1].

Exterior Dirichlet Problem. *Given $f \in C(\partial D)$, find a radiating solution $u \in C^2(\mathbb{R}^2\backslash\bar{D}) \cap C(\mathbb{R}^2\backslash D)$ to the Helmholtz equation in $\mathbb{R}^2\backslash\bar{D}$ which satisfies the boundary condition*

$$u = f \quad on\ \partial D.$$

Observe that the direct obstacle scattering problem stated at the begining of this chapter is a special case of the exterior Dirichlet problem. Therefore, this boundary value problem will be our primary interest. To prove well-posedness, we first present some auxiliary results.

Any two times continuously differentiable solution to the Helmholtz equation in a domain is analytic since the fundamental solution is analytic for $x \neq y$ [1]. Therefore, we deduce that a solution of the Helmholtz equation that vanishes in an open subset of its domain of definition must vanish everywhere [6].

Lemma 2.15. (Rellich) *Assume the bounded set D is the open complement of an unbounded domain and let $u \in C^2(\mathbb{R}^2\backslash\bar{D})$ be a solution to the Helmholtz equation satisfying*

$$\lim_{\rho\to\infty} \int_{\Omega_\rho} |u|^2 \, ds = 0. \tag{2.17}$$

Then $u = 0$ in $\mathbb{R}^2\backslash\bar{D}$ [7].

Proof. Let $\{\psi_n^m \ : \ 1 \leq m \leq N(2,n)\}$ be an orthonormal basis for surface spherical harmonics of degree n, $\mathcal{H}_n(S^1)$ with $\dim\mathcal{H}_n(S^1) =: N(2,n)$ [8]. Then for sufficiently large

$|x|$, we have an expansion with respect to spherical harmonics

$$u(x) = \sum_{n=0}^{\infty} \sum_{m=1}^{N(2,n)} f_n^m(k|x|)\psi_n^m(\omega), \quad x = |x|\omega,\ \omega \in S^1,$$

where the coefficients are given by

$$f_n^m(t) = \int_{S^1} u(k^{-1}t\omega)\overline{\psi_n^m(\omega)}d\omega.$$

Further,

$$\begin{aligned}\int_{\Omega_\rho} |u(x)|^2 ds &= \int_{S^1} |u(\rho\omega)|^2 \rho d\omega \\ &= \rho \int_{S^1} \left(\sum_{n=0}^{\infty} \sum_{m=1}^{N(2,n)} f_n^m(k\rho)\psi_n^m(\omega) \right) \left(\sum_{n'=0}^{\infty} \sum_{m'=1}^{N(2,n')} \overline{f_{n'}^{m'}(k\rho)\psi_{n'}^{m'}(\omega)} \right) \\ &= \rho \sum_{n=0}^{\infty} \sum_{m=1}^{N(2,n)} |f_n^m(k\rho)|^2.\end{aligned}$$

Here and above we used the relation $\int_{S^1} \psi_{n'}^{m'} \overline{\psi_n^m} d\omega = \delta_{mm'}\delta_{nn'}$ [8]. Then from (2.17) we deduce that, for each n and m

$$\rho |f_n^m(k\rho)|^2 \to 0, \quad \text{as } \rho \to \infty.$$

Since u satisfies the Helmholtz equation, by a separation of variables argument, we see that f_n^m is a solution of Bessel's equation, and therefore it can be written as

$$f_n^m(t) = a_n^m H_n^{(1)}(t) + b_n^m H_n^{(2)}(t) \tag{2.18}$$

for appropriate constants a_n^m and b_n^m [9]. Using the asymptotic behavior (2.3) of Hankel functions, simple calculations yield

$$\rho |f_n^m(k\rho)|^2 = \frac{2}{\pi k} |a_n^m e^{2i(k\rho - n\pi/2 - \pi/4)} + b_n^m|^2 + \mathcal{O}\left(\frac{1}{\rho}\right). \tag{2.19}$$

Since $\lim_{\rho\to\infty} \rho|f_n^m(k\rho)|^2 = 0$, we must have $a_n^m = b_n^m = 0$ for all n and m. Thus, $u = 0$ outside a sufficiently large circle, and hence using the preceding remark gives $u = 0$ in $\mathbb{R}^2\backslash\bar{D}$. □

With the help of Rellich's lemma, as can be readily seen from identity (2.8), we obtain the following theorem.

Theorem 2.16. *Let D be as in the previous lemma and suppose that ∂D is of class C^2. If $u \in C^2(\mathbb{R}^2\backslash\bar{D}) \cap C(\mathbb{R}^2\backslash D)$ is a radiating solution to the Helmholtz equation which has a normal derivative in the sense of uniform convergence and if*

$$\operatorname{Im} \int_{\partial D} u \frac{\partial \bar{u}}{\partial \nu}\, ds \geq 0,$$

then $u = 0$ in $\mathbb{R}^2\backslash\bar{D}$ [1] .

We are now ready to tackle the well-posedness of the exterior Dirichlet problem.

Theorem 2.17. (Uniqueness) *The exterior Dirichlet problem has at most one solution* [1].

Proof. We have to show that solutions to the homogeneous boundary value problem $u = 0$ on ∂D vanish identically in $\mathbb{R}^2\backslash\bar{D}$. If u has a normal derivative (see the remark right after Theorem 2.19) in the sense of uniform convergence, then Theorem 2.16 yields $u = 0$ in $\mathbb{R}^2\backslash\bar{D}$. (For a proof under the weaker regularity assumption that $f \in C(\partial D)$, we refer to [1].) □

Theorem 2.18. (Existence) *The exterior Dirichlet problem has a unique solution and the solution depends continuously on the boundary data in the maximum norm* [1].

Proof. We seek a solution of the exterior Dirichlet problem in the form of a combined

single and double layer potential

$$u(x) = \int_{\partial D} \left\{ \frac{\partial \Phi(x,y)}{\partial \nu(y)} - i\eta \Phi(x,y) \right\} \varphi(y)\, ds(y), \quad x \in \mathbb{R}^2 \backslash \partial D \tag{2.20}$$

with the density $\varphi \in C(\partial D)$ and a real parameter $\eta \neq 0$. By using jump relations for the double layer potential, Theorem 2.10, and the continuity of the single layer potential, Theorem 2.9, we see that u given by (2.20) solves the exterior Dirichlet problem in $\mathbb{R}^2 \backslash \bar{D}$ provided that the density φ is a solution of the boundary integral equation

$$\varphi + DL\varphi - i\eta SL\varphi = 2f. \tag{2.21}$$

It suffices to show that the homogeneous form of (2.21) has only the trivial solution since the injectivity of the operator $\mathcal{M} := (I + DL - i\eta SL) : C(\partial D) \to C(\partial D)$ implies the bijectivity of $\mathcal{M}$ and that its inverse operator $\mathcal{M}^{-1} : C(\partial D) \to C(\partial D)$ is bounded via the Fredholm alternative (Theorem A.1).

Let $\varphi \in C(\partial D)$ be a solution of the homogeneous form of (2.21) . Then u satisfies the homogeneous boundary condition $u_+ = 0$ on ∂D from which we get $u = 0$ in $\mathbb{R}^2 \backslash \bar{D}$ by uniqueness. Using jump relations, Theorems 2.9 through 2.12, we have

$$\begin{aligned} u_+ - u_- &= DL_+ - DL_- - i\eta(SL_+ - SL_-), \\ -u_- &= \varphi, \quad \text{on } \partial D, \end{aligned}$$

and

$$\begin{aligned} \frac{\partial u_+}{\partial \nu} - \frac{\partial u_-}{\partial \nu} &= \frac{\partial DL_+}{\partial \nu} - \frac{\partial DL_-}{\partial \nu} - i\eta \left(\frac{\partial SL_+}{\partial \nu} - \frac{\partial SL_-}{\partial \nu} \right), \\ -\frac{\partial u_-}{\partial \nu} &= i\eta\varphi, \quad \text{on } \partial D. \end{aligned}$$

Now applying Green's first identity and using these identities yield

$$\int_{\partial D} \bar{u}_- \frac{\partial u_-}{\partial \nu} ds = \int_D \bar{u}\Delta u + |\nabla u|^2 dx = \int_D |\nabla u|^2 - k^2|u|^2 dx,$$
$$i\eta \int_{\partial D} |\varphi|^2 ds = \int_D |\nabla u|^2 - k^2|u|^2 dx.$$

Taking the imaginary part of the last equation gives $\varphi = 0$ on ∂D. Finally, the continuous dependence is a direct consequence of Fredholm alternative. □

Note that for $\eta = 0$, the integral equation (2.21) has more than one solution if k is an interior Neumann eigenvalue, i.e. irregular wave number for which there exists nontrivial solutions to the homogeneous interior Neumann problem. This is due to the facts that, the adjoint integral operator $I + DL'$ corresponds to interior Neumann problem and the nullspace of $(I + DL)$ consists of solutions of homogeneous form of this problem, and thus $\dim \mathrm{Null}(I + DL) = \dim \mathrm{Null}(I + DL') \neq 0$ provided k is an eigenvalue [4]. To remedy non-uniqueness, this elegant combined field approach was introduced in [10].

In order to use Green's representation formula for the solution of the exterior Dirichlet problem, we need the normal derivative of the solution. However, the continuity of the solution, in general, does not guarantee existence of the normal derivative. Thus, we need a stronger regularity condition on the boundary data.

Theorem 2.19. *The solution to the exterior Dirichlet problem belongs to* $C^{1,\alpha}(\mathbb{R}^2\backslash D)$ *provided boundary values are in* $C^{1,\alpha}(\partial D)$ [1].

Proof. Injectivity of $\mathcal{M} : C(\partial D) \to C(\partial D)$ implies the injectivity of $\mathcal{M} : C^{1,\alpha}(\partial D) \to C^{1,\alpha}(\partial D)$. By Theorems 2.14 and B.1 , $SL, DL : C^{1,\alpha}(\partial D) \to C^{1,\alpha}(\partial D)$ are compact, therefore $\mathcal{M} : C^{1,\alpha}(\partial D) \to C^{1,\alpha}(\partial D)$ is bijective and has a bounded inverse by Fredholm alternative. Hence for $f \in C^{1,\alpha}(\partial D)$ we get that the solution φ of (2.21) lies in $C^{1,\alpha}(\partial D)$. Finally, using Theorem 2.13, we observe that $u \in C^{1,\alpha}(\mathbb{R}^2\backslash D)$. □

From the preceding theorem, we deduce that the normal derivative $\partial u/\partial \nu$ of the solution u exists and belongs to $C^{0,\alpha}(\partial D)$ if $f \in C^{1,\alpha}(\partial D)$.

Returning to the direct obstacle scattering problem, we assume that incident field u^i is a plane wave

$$u^i(x) = e^{ikx\cdot a} \tag{2.22}$$

with the direction a ($|a| = 1$).

Theorem 2.20. *For the scattering of an entire field u^i (a solution of the Helmholtz equation in $\mathbb{R}^2$) from a sound-soft obstacle D we have*

$$u(x) = u^i(x) - \int_{\partial D} \Phi(x,y)\, \frac{\partial u}{\partial \nu}(y)\, ds(y), \quad x \in \mathbb{R}^2 \backslash \bar{D} \tag{2.23}$$

[1].

Proof. Using analyticity of u^i and $u = u^i + u^s = 0$ on ∂D, from Theorem 2.19 we observe that the scattered field $u^s \in C^{1,\alpha}(\mathbb{R}^2 \backslash D)$. Hence, we can apply Green's representation formula (2.9) to obtain

$$u^s(x) = \int_{\partial D} \left\{ u^s(y) \frac{\partial \Phi(x,y)}{\partial \nu(y)} - \frac{\partial u^s}{\partial \nu}(y) \Phi(x,y) \right\} ds(y), \quad x \in \mathbb{R}^2 \backslash \bar{D}.$$

Also, Green's first identity (2.4) applied to u^i and $\Phi(x,\cdot)$ for $x \in \mathbb{R}^2 \backslash \bar{D}$ in D yields

$$0 = \int_{\partial D} \left\{ u^i(y) \frac{\partial \Phi(x,y)}{\partial \nu(y)} - \frac{\partial u^i}{\partial \nu}(y) \Phi(x,y) \right\} ds(y), \quad x \in \mathbb{R}^2 \backslash \bar{D}.$$

Adding these two equations and using the Dirichlet boundary condition $u = u^i + u^s = 0$ prove the theorem. □

Corollary 2.21. *For the scattering of an entire field u^i, we have the well-posed com-*

bined field integral equation

$$\frac{\partial u}{\partial \nu}(x) + 2\int_{\partial D}\left\{\frac{\partial \Phi(x,y)}{\partial \nu(x)} - i\eta\Phi(x,y)\right\}\frac{\partial u}{\partial \nu}(y)\,ds(y) = 2\left\{\frac{\partial u^i}{\partial \nu}(x) - i\eta u^i(x)\right\},\ x \in \partial D, \tag{2.24}$$

where $\eta \in \mathbb{R} \setminus \{0\}$.

Proof. Letting $x \to \partial D$ in the previous theorem, and using continuity of SL and the boundary condition $u = 0$ we find

$$-i\eta SL\frac{\partial u}{\partial \nu} = -2i\eta u^i, \quad \text{on } \partial D. \tag{2.25}$$

Moreover, using theorem 2.19, we can differentiate both sides of (2.23) to get

$$\frac{\partial u}{\partial \nu}(x) + \int_{\partial D}\frac{\partial \Phi(x,y)}{\partial \nu(x)}\frac{\partial u}{\partial \nu}(y)\,ds(y) = \frac{\partial u^i}{\partial \nu}(x), \quad x \in \mathbb{R}^2 \setminus \bar{D}.$$

Again letting $x \to \partial D$ and using jump relations for DL', Theorem 2.11, we see that

$$\frac{\partial u}{\partial \nu} + DL'\frac{\partial u}{\partial \nu} = 2\frac{\partial u^i}{\partial \nu}, \quad \text{on } \partial D. \tag{2.26}$$

Hence, combining (2.25) and (2.26) yields the combined field integral equation

$$(I + DL' - i\eta SL)\frac{\partial u}{\partial \nu} = 2\left\{\frac{\partial u^i}{\partial \nu} - i\eta u^i\right\}.$$

Existence and uniqueness of a solution to (2.24) follow from the fact that the compact operators $DL' - i\eta SL$ and $DL - i\eta SL$ are adjoint in the dual system $\langle C(\partial D), C(\partial D)\rangle$ [4]. □

In brief, we reformulated the direct scattering problem in the form of the well-posed combined field boundary integral equation (2.24). The unknown of this integral equation represents a physical quantity whereas the density φ in (2.21) does not [11].

Thus, it is preferable to work with (2.24). Observe that if we know the solution of this integral equation then we will have the total field u of the direct scattering problem with the aid of Theorem 2.20.

3. NUMERICAL METHODS FOR INTEGRAL EQUATIONS OF THE SECOND KIND

In the previous chapter, we derived the combined field integral equation representations (2.21) and (2.24) for the direct scattering problem. Correspondingly, this chapter is devoted to numerical methods for the approximate solution of integral equations of the second kind. We shall describe three fundamental methods: the Nyström method, the collocation method and the Galerkin method [5, 12–14].

3.1. Preliminaries

In this section we present auxiliary results on interpolation and approximation theory.

Concerning interpolation on $[a,b] \subset \mathbb{R}$ with piecewise linear continuous functions, we divide $[a,b]$ into n subintervals using $n+1$ equispaced nodes. Further, denote by X_n the subspace of continuous functions on $[a,b]$ whose restrictions to each of the subintervals are linear and $P_n : C[a,b] \to X_n$ the interpolation operator that interpolates any $u \in C[a,b]$ at these nodes.

Theorem 3.1. *For piecewise linear interpolation we have*

$$||P_n u - u||_\infty \leq \begin{cases} \omega(u,h), & u \in C[a,b], \\ \frac{h^2}{8}||u''||_\infty, & u \in C^2[a,b], \end{cases} \tag{3.1}$$

where

$$\omega(u,h) := \sup_{\substack{t,s \in [a,b] \\ |t-s| \leq h}} |u(t) - u(s)|$$

is the modulus of continuity of u, and $h = (b-a)/n$ is the stepsize. Furthermore, $||P_n||_\infty = 1$ [12, 13].

We now consider trigonometric interpolation for 2π-periodic continuous functions, $C_p(2\pi)$. For $n \geq 1$, define the space of trigonometric polynomials of degree $\leq n$ by $\mathbb{T}_n := \text{span}\{1, \cos t, \sin t, .., \cos nt, \sin nt\}$. Let $t_j := j\pi/n$, $j = 0, ..., 2n-1$, be an equidistant subdivision of the interval $[0, 2\pi]$ and $P_n : C_p(2\pi) \to \mathbb{T}_n$ be the trigonometric interpolation operator at these grid points.

Theorem 3.2. *Given the values $y_0, ..., y_{2n-1}$, there exists a unique trigonometric polynomial of the form*

$$v_n(t) = \frac{a_0}{2} + \sum_{k=1}^{n-1} \{a_k \cos kt + b_k \sin kt\} + \frac{a_n}{2} \cos nt \tag{3.2}$$

with the interpolation property $v_n(t_j) = y_j$, $j = 0, ..., 2n-1$, where the coefficients are given by

$$a_k = \frac{1}{n} \sum_{j=0}^{2n-1} y_j \cos kt_j, \quad k = 0, ..., n,$$
$$b_k = \frac{1}{n} \sum_{j=0}^{2n-1} y_j \sin kt_j, \quad k = 1, ..., n-1$$

[12].

We claim that the Lagrange basis for trigonometric interpolation has the form

$$L_j(t) = \frac{1}{2n} \left\{ 1 + 2 \sum_{k=1}^{n-1} \cos k(t - t_j) + \cos n(t - t_j) \right\} \tag{3.3}$$

for $t \in [0, 2\pi]$ and $j = 0, ..., 2n-1$. To see this, we write $v_n(t)$ in the complex form

$$v_n(t) = \frac{\gamma_{-n}}{2} e^{-int} + \sum_{k=-n+1}^{n-1} \gamma_k e^{ikt} + \frac{\gamma_n}{2} e^{int} =: \sum_{-n \leq k \leq n}'' \gamma_k e^{ikt}$$

with $\gamma_0 = a_0/2, \gamma_{\pm k} = \frac{1}{2}(a_k \mp i b_k)$ for $k = 1, ..., n-1$ and $\gamma_n = \gamma_{-n} = a_n/2$ where $\sum''$ means that the first and last terms are halved. Then the interpolation property

$v_n(t_j) = y_j$ can be rewritten as

$$\sum_{k}'' \gamma_k e^{ikt_j} = y_j, \quad j = 0, ..., 2n-1.$$

Further we deduce that

$$\sum_{j=0}^{2n-1} y_j e^{-imt_j} = \sum_{k}'' \gamma_k \underbrace{\sum_{j=0}^{2n-1} e^{i(k-m)t_j}}_{2n\delta_{km}} = 2n\gamma_m, \quad m = -n, ...n,$$

or

$$\gamma_m = \frac{1}{2n} \sum_{j=0}^{2n-1} y_j e^{-imt_j}, \quad m = -n, ...n.$$

To derive the Lagrange basis, we take $y_j = \delta_{jk}$ and get the coefficients of Lagrange basis as

$$\gamma_m = \frac{1}{2n} \sum_{k=0}^{2n-1} \delta_{jk} e^{-imt_k} = \frac{1}{2n} e^{-imt_j}, \quad \text{for} \;\; m = -n, ..., n,$$

and therefore

$$L_j(t) = \sum_{m}'' \frac{e^{-imt_j}}{2n} e^{imt} = \frac{1}{2n} \sum_{m}'' e^{im(t-t_j)}, \quad j = 0, ..., 2n-1,$$

which is exactly the form (3.3).

It is essential to note that the trigonometric interpolation operator satisfies [15]

$$||P_n||_\infty = \mathcal{O}(\log n), \quad \text{as } n \to \infty. \tag{3.4}$$

The following theorem of Dunham Jackson provides an error estimate for the best approximation of 2π-periodic m-times Hölder continuously differentiable functions with

respect to trigonometric polynomials, $\mathbb{T}_n$.

Theorem 3.3. (Jackson) *Assume that* $u \in C_p^{m,\alpha}(2\pi)$ (*see Appendix B*) *for some* $m \in \mathbb{N} \cup \{0\}$ *and* $0 < \alpha \leq 1$. *Then*

$$\inf_{p \in \mathbb{T}_n} ||u - p||_\infty \leq \frac{c}{n^{m+\alpha}} ||u||_{m,\alpha}$$

for some positive constant c *that does not depend on* u [16].

The next statement readily follows from the norm (3.4) and Jackson's theorem.

Corollary 3.4. *Let* $m \in \mathbb{N} \cup \{0\}$ *and* $0 < \alpha \leq 1$. *Then for trigonometric interpolation the inequality*

$$||P_n u - u||_\infty \leq C \frac{\log n}{n^{m+\alpha}} ||u||_{m,\alpha}$$

holds for all $u \in C_p^{m,\alpha}(2\pi)$ *and some constant* $C > 0$.

Finally, we carry out trigonometric interpolation in the Sobolev spaces (see Appendix B).

Theorem 3.5. *Let* $p > \frac{1}{2}$. *Then for trignometric interpolation we have*

$$||P_n u - u||_{H^q} \leq \frac{C}{n^{p-q}} ||u||_{H^p}, \quad 0 \leq q \leq p, \tag{3.5}$$

for all $u \in H^p[0, 2\pi]$ *and some positive constant* C *depending on* p *and* q [5, 17].

3.2. Operator Approximations

As we shall see, the numerical methods that will be described in this chapter are based upon results of this section, in particular the Nyström method.

Considering the approximate solution of an operator equation

$$\varphi - A\varphi = f$$

of the second kind, we replace it by an approximate equation

$$\varphi_n - A_n\varphi_n = f_n$$

with approximating sequences $A_n \to A$ and $f_n \to f$ as $n \to \infty$. In this section we will briefly present convergence results and error analysis for such approximation schemes.

In the case of norm convergence of the sequence $A_n \to A$ $(n \to \infty)$ we have the following theorem.

Theorem 3.6. *Let $A : X \to X$ be a compact operator on a Banach space X such that $I - A$ is injective. Assume that the sequence $A_n : X \to X$ of bounded linear operators is norm convergent, i.e. $||A_n - A|| \to 0$, $n \to \infty$. Then, for sufficiently large n, the inverse operators $(I - A_n)^{-1} : X \to X$ exist and are uniformly bounded. For the solutions of the equations*

$$\varphi - A\varphi = f \quad \textit{and} \quad \varphi_n - A_n\varphi_n = f_n$$

we have the error estimate

$$||\varphi_n - \varphi|| \leq C\{||(A_n - A)\varphi|| + ||f_n - f||\} \tag{3.6}$$

for some constant C [5].

To establish a similar result when (A_n) is pointwise convergent, i.e. $A_n\varphi \to A\varphi$, $n \to \infty$, for all φ, we need the uniform boundedness principle and the concept of collectively compact operators.

Theorem 3.7. (Principle of Uniform Boundedness) *Suppose the sequence $A_n : X \to Y$*

of bounded linear operators mapping a Banach space X into a normed space Y is pointwise bounded, i.e. for each $\varphi \in X$ there exists a constant $C_\varphi > 0$ depending on φ such that $||A_n\varphi|| \leq C_\varphi$, for all $n \in \mathbb{N}$. Then the sequence (A_n) is uniformly bounded [5, 13].

A set $\mathbb{A} = \{A : X \to Y\}$ of linear operators from a normed space X into a normed space Y is called *collectively compact* if for each bounded set $U \subset X$ the image set $\mathbb{A}(U) = \{A\varphi : \varphi \in U, A \in \mathbb{A}\}$ is relatively compact. Moreover, the sequence (A_n) is called *collectively compact* when the corresponding set is. We observe that each operator in a collectively compact set is compact.

The next lemma can be established using the definition of collective compactness.

Lemma 3.8. *Let X be a Banach space and let $A_n : X \to X$ be a collectively compact sequence. Assume that $B_n : X \to X$ is a pointwise convergent sequence with limit B. Then we have*

$$||(B_n - B)A_n|| \to 0, \quad n \to \infty$$

[12].

Use of this lemma results in the following theorem that concerns the case of a collectively compact and pointwise convergent sequence (A_n).

Theorem 3.9. *Let $A : X \to X$ is compact linear operator such that $I - A$ is injective. Assume that the sequence $A_n : X \to X$ of linear operators is collectively compact and pointwise convergent $A_n\varphi \to A\varphi$, $n \to \infty$, for all $\varphi \in X$. Then, for sufficiently large n, the inverse operators $(I - A_n)^{-1} : X \to X$ exist and are uniformly bounded. For the solutions of the equations*

$$\varphi - A\varphi = f \quad \textit{and} \quad \varphi_n - A_n\varphi_n = f_n$$

we have the error estimate

$$||\varphi_n - \varphi|| \leq C\{||(A_n - A)\varphi|| + ||f_n - f||\} \tag{3.7}$$

for some constant $C > 0$ [5].

Proof. By Fredholm alternative, $(I - A)^{-1}$ exists and is bounded. Defining $M_n := I + (I - A)^{-1}A_n$ we get

$$\begin{aligned} M_n(I - A_n) &= I + (I - A)^{-1}A_n - A_n - (I - A)^{-1}A_n^2 \\ &= I - (I - A)^{-1}(A_n - A)A_n =: I - L_n. \end{aligned}$$

Since A_n is collectively compact and pointwise convergent, we use the previous lemma to conclude that $||L_n|| \to 0$, $n \to \infty$. Then, for large n we have $||L_n|| < 1$ so that the Neumann series theorem (A.2) entails that the inverse operators $(I - L_n)^{-1}$ exist and are uniformly bounded. Injectivity of the composition $M_n(I - A_n) = I - L_n$ implies that $I - A_n$ is injective therefore the compactness of A_n yields the existence of inverse operators $(I - A_n)^{-1}$. Also, because M_n is pointwise convergent, by uniform boundedness principle it is uniformly bounded. Hence $(I - A_n)^{-1} = (I - L_n)^{-1}M_n$ are uniformly bounded. Finally, the error estimate (3.7) follows from

$$(I - A_n)(\varphi_n - \varphi) = (A_n - A)\varphi + f_n - f.$$

□

3.3. The Nyström Method

Basic numerical integration techniques consist of interpolatory quadratures and composite rules. For a classical reference which includes both analysis and implementation issues see [18].

Here we consider numerical quadrature rules of the form

$$I_n(g) := \sum_{j=1}^{n} w_{n,j} g(x_{n,j})$$

for approximating the integrals

$$I(g) := \int_D g(x)dx$$

with quadrature points $x_{n,1}, ..., x_{n,n} \in D$ and real quadrature weights $w_{n,1}, ..., w_{n,n}$. We assume that $D \subset \mathbb{R}^m$ is compact and $g \in C(D)$. To simplify notation, we omit the subscript n and write $x_j \equiv x_{n,j}$, $w_j \equiv w_{n,j}$.

Definition 3.10. *A sequence (I_n) of quadrature rules is called convergent provided that $I_n(g) \to I(g)$, $n \to \infty$, for all $g \in C(D)$.*

Nyström's method is a straightforward scheme that approximates integral operators by numerical integration operators. We choose a convergent sequence (I_n) of quadratures rules for the integral $I(g)$ and apply the quadrature formula to $g = K(x, \cdot)\varphi$ to approximate the integral operator

$$(A\varphi)(x) := \int_D K(x, y)\varphi(y)dy, \quad x \in D,$$

by a sequence of numerical integration operators

$$(A_n\varphi)(x) := \sum_{j=1}^{n} w_j K(x, x_j)\varphi(x_j), \quad x \in D, \tag{3.8}$$

where $K \in C(D \times D)$. Thus we approximate the solution to the integral equation of the second kind

$$\varphi - A\varphi = f$$

by the solution of

$$\varphi_n - A_n\varphi_n = f.$$

Next, we state a straightforward but important theorem about the Nyström method.

Theorem 3.11. (Nyström) *Let φ_n be a solution of*

$$\varphi_n(x) - \sum_{j=1}^{n} w_j K(x, x_j)\varphi_n(x_j) = f(x), \quad x \in D. \tag{3.9}$$

Then $\varphi_k^{(n)} := \varphi_n(x_k)$, $k = 1, ..., n$, at the quadrature points satisfy the linear system

$$\varphi_k^{(n)} - \sum_{j=1}^{n} w_j K(x_k, x_j)\varphi_j^{(n)} = f(x_k), \quad k = 1, ..., n. \tag{3.10}$$

Conversely, let $\varphi_k^{(n)}$, $k = 1, ..., n$, be a solution of the system (3.10)*. Then the function*

$$\varphi_n(x) := f(x) + \sum_{j=1}^{n} w_j K(x, x_j)\varphi_j^{(n)}, \quad x \in D \tag{3.11}$$

solves equation (3.9) [19].

Thus Nyström method reduces to solving the linear system (3.10). Convergence analysis of the method will be through the following result [5].

Theorem 3.12. *The sequence (A_n) defined by* (3.8) *is collectively compact and pointwise convergent, i.e. $A_n\varphi \to A\varphi, n \to \infty$, for all $\varphi \in C(D)$, provided that the quadrature formulas (I_n) are convergent.*

Proof. Since the quadrature formulas (I_n) are convergent, by principle of uniform

boundedness there exists a constant C such that

$$||I_n||_\infty = \sum_{j=1}^{n} |w_{n,j}| \leq C$$

for all $n \in \mathbb{N}$. With this bound, we have the estimates

$$||A_n\varphi||_\infty \leq C||\varphi||_\infty \max_{x,y\in D} |K(x,y)| \tag{3.12}$$

$$|(A_n\varphi)(x_1) - (A_n\varphi)(x_2)| \leq C||\varphi||_\infty \max_{y\in D} |K(x_1,y) - K(x_2,y)| \tag{3.13}$$

for all $x_1, x_2 \in D$. To prove collective compactness, we take a bounded subset $G \subset C(D)$. Then the set $\{A_n\varphi : \varphi \in G, n \in \mathbb{N}\}$ is bounded and equicontinuous respectively from (3.12) and (3.13) since K is uniformly continuous on $D \times D$. Therefore by Arzela-Ascoli theorem, Theorem A.3, (A_n) is collectively compact.

For a fixed $\varphi \in C(D)$, the sequence $(A_n\varphi)$ is pointwise convergent, $(A_n\varphi)(x) \to (A\varphi)(x)$, $n \to \infty$ for all $x \in D$, since the quadrature is assumed to be convergent. Also from (3.13), $(A_n\varphi)$ is equicontinuous. Since a pointwise convergent equicontinuous sequence on a compact set is uniformly convergent, we have $||A_n\varphi - A\varphi||_\infty \to 0$, $n \to \infty$, i.e. (A_n) is pointwise convergent on $C(D)$. □

With the aid of Theorems 3.9 and 3.12, we have the following convergence result.

Corollary 3.13. (Convergence) *The Nyström method with a convergent sequence of quadrature formulas is uniformly convergent for a uniquely solvable integral equation of the second kind with a continuous kernel and a continuous right hand side.*

Error analysis of the method follows from Theorem 3.9 as the error estimate (3.7)

entails

$$||\varphi_n - \varphi||_\infty \leq C\,||(A - A_n)\varphi||_\infty$$
$$= C \max_{x\in D}\left|\int_D K(x,y)\varphi(y)dy - \sum_{j=1}^{n} w_j K(x,x_j)\varphi(x_j)\right|.$$

Therefore, under suitable regularity assumptions on the kernel and exact solution, the convergence order of this method will be the same as that of the quadrature formulas. Thus, for the one dimensional case on $[a,b]$ with $h=(b-a)/n$, we will have $\mathcal{O}(h^2)$ and $\mathcal{O}(h^4)$ in use of trapezoidal and composite Simpson's rule respectively. For analytic boundary curves we will have an exponential order [5].

Regarding stability, condition numbers for the Nyström linear system (3.10) are uniformly bounded [5, 14].

Weakly Singular Kernels:

The fundamental solution of the Helmholtz equation in $\mathbb{R}^2$ contains a logarithmic singularity. Therefore the boundary integral equation approach (discussed in chapter 2) to two-dimensional boundary value problems via a periodic parametrization of the boundary curve leads to logarithmic singularities in integrals. For their proper numerical treatment, we split off the logarithmic singularity via the weakly singular operator

$$(A\varphi)(t) := \int_0^{2\pi} \log\left(4\sin^2\frac{t-s}{2}\right) K(t,s)\,\varphi(s)\,ds, \quad 0\leq t\leq 2\pi, \tag{3.14}$$

where the kernel K is continuous and 2π-periodic with respect to both variables. In order to approximate the solution of the integral equation with this operator, we first have to construct a numerical quadrature for the improper integral

$$(I^s g)(t) := \int_0^{2\pi} \log\left(4\sin^2\frac{t-s}{2}\right) g(s)\,ds.$$

Indeed, replacing the function g with its trigonometric interpolation polynomial and using the Lagrange basis $L_j(t)$ (see (3.3)) yield

$$(I_n^s g)(t) := \sum_{j=0}^{2n-1} R_j^{(n)}(t) g(t_j) \tag{3.15}$$

with $t_j = \pi j/n$ where the quadrature weights are given by

$$R_j^{(n)}(t) = \int_0^{2\pi} \log\left(4\sin^2\frac{t-s}{2}\right) L_j(s)\, ds, \quad j = 0, ..., 2n-1.$$

To derive a formula for these quadrature weights, we need the following technical lemma.

Lemma 3.14.

$$\int_0^{2\pi} \log\left(4\sin^2\frac{t-s}{2}\right) e^{ims}\, ds = \begin{cases} 0, & m = 0, \\ -2\pi\frac{e^{imt}}{|m|}, & m = \pm 1, \pm 2... \end{cases}$$

for $t \in [0, 2\pi]$ [5].

Proof. The integral

$$\begin{aligned} \int_0^{2\pi} \cot\frac{t}{2}\, dt &= \lim_{\epsilon\to 0^+} \int_\epsilon^{2\pi-\epsilon} \cot\frac{t}{2}\, dt \\ &= \lim_{\epsilon\to 0^+} \log\left(4\sin^2\frac{t}{2}\right)|_\epsilon^{2\pi-\epsilon} \\ &= \lim_{\epsilon\to 0^+} \log\left(\frac{\sin^2\frac{2\pi-\epsilon}{2}}{\sin^2\frac{\epsilon}{2}}\right) = 0 \end{aligned}$$

exists as a Cauchy principal value (CPV). Now, integrating the geometric series

$$\begin{aligned} 1 + 2\sum_{k=1}^{m-1} e^{ikt} + e^{imt} &= \frac{(e^{imt}-1)(-e^{it}-1)}{1-e^{it}}, \\ &= (e^{imt}-1)\frac{(e^{it/2}+e^{-it/2})}{(e^{it/2}-e^{-it/2})} = i(1-e^{imt})\cot\frac{t}{2}, \quad 0 < t < 2\pi, \end{aligned}$$

we obtain

$$\int_0^{2\pi} e^{imt} \cot \frac{t}{2}\, dt = 2\pi i, \quad m = 1, 2, ..., \tag{3.16}$$

in the sense of CPV. Moreover, integrating the identity

$$\frac{d}{dt}\left\{[e^{imt} - 1] \log\left(4 \sin^2 \frac{t}{2}\right)\right\} = ime^{imt} \log\left(4 \sin^2 \frac{t}{2}\right) + [e^{imt} - 1] \cot \frac{t}{2}$$

implies

$$0 = im \int_0^{2\pi} e^{imt} \log\left(4 \sin^2 \frac{t}{2}\right) dt + \int_0^{2\pi} e^{imt} \cot \frac{t}{2}\, dt,$$

and therefore using (3.16) we get

$$\int_0^{2\pi} e^{imt} \log\left(4 \sin^2 \frac{t}{2}\right) dt = -\frac{1}{im} \int_0^{2\pi} e^{imt} \cot \frac{t}{2}\, dt = -\frac{2\pi}{m}$$

for $m = 1, 2, \ldots$. For $m = -1, -2, ...$, one can proceed analogously. For the case $m = 0$, it is not difficult to show that

$$I := \int_0^{2\pi} \log\left(4 \sin^2 \frac{t}{2}\right) dt = 0$$

as

$$2I = \int_0^{2\pi} \log\left(4 \sin^2 \frac{t}{2}\right) dt + \int_0^{2\pi} \log\left(4 \cos^2 \frac{t}{2}\right) dt = I.$$

Now, the result follows by a simple change of variables. □

Recall from (3.3) that the complex form of the Lagrange basis is

$$L_j(t) = \frac{1}{2n} \sum_{-n \le m \le n}'' e^{im(t - t_j)},$$

where $t_j = \pi j/n$, $j = 0, ..., 2n-1$. Then using the preceding lemma we get

$$\begin{aligned} R_j^{(n)}(t) &= \frac{1}{2n}\sum_m{}'' e^{-imt_j}\int_0^{2\pi}\log(4\sin^2\frac{t-s}{2})\,e^{ims}\,ds \\ &= -\frac{2\pi}{2n}\sum_{m\neq 0}{}''\frac{1}{|m|}e^{im(t-t_j)} \\ &= -\frac{2\pi}{n}\left[\sum_{m=1}^{n-1}\frac{1}{m}\cos m(t-t_j)+\frac{1}{2n}\cos n(t-t_j)\right] \end{aligned}$$

for $j = 0, ..., 2n-1$. Also for the weights we have the circular relation

$$R_j^{(n)}(t_k) = R_{|j-k|}^{(n)}, \quad j,k = 0, ..., 2n-1 \tag{3.17}$$

with

$$R_j^{(n)} = -\frac{2\pi}{n}\left\{\sum_{m=1}^{n-1}\cos(mt_j)+\frac{(-1)^j}{2n}\right\}, \quad j = 0, ..., 2n-1,$$

which simplifies evaluation of the weights, therefore computational cost of assembling the linear system can be reduced substantially.

It can be shown that the sequence

$$(A_n\varphi)(t) := \sum_{j=0}^{2n-1} R_j^{(n)}(t)K(t,t_j)\varphi(t_j)$$

is collectively compact and pointwise convergent to the integral operator (3.14) with logarithmic singularity, and thus the error analysis based on Theorem 3.9 is again applicable [5].

3.3.1. Numerical Examples

Example 3.15. First we consider an application of the Nyström method to the integral equation

$$\varphi(x) - \frac{1}{2}\int_0^1 (x+1)e^{-xy}\varphi(y)dy = e^{-x} - \frac{1}{2} + \frac{1}{2}e^{-(x+1)}, \tag{3.18}$$

for $x \in [0,1]$. The equation has the solution $\varphi(x) = e^{-x}$ [5]. As seen from the table expected convergence rates $\mathcal{O}(h^2)$ and $\mathcal{O}(h^4)$ are exhibited.

Table 3.1. Nyström method for equation (3.18).

	n	$\|\|\varphi_n - \varphi\|\|_\infty$
Trapezoidal rule	4	1.54E-02
	8	3.88E-03
	16	9.71E-04
	32	2.42E-04
Simpson's Rule	4	2.14E-04
	8	1.36E-05
	16	8.57E-07
	32	5.36E-08

Example 3.16. Consider the integral equation

$$\phi(t) + \frac{ab}{\pi}\int_0^{2\pi} \frac{\phi(s)ds}{a^2 + b^2 - (a^2 - b^2)\cos(t+s)} = g(t), \quad 0 \le t \le 2\pi \tag{3.19}$$

with $a \ge b > 0$, the right-hand side $g(t) = e^{\cos t}\cos(\sin t) + e^{c\cos t}\cos(c\sin t)$ and the exact solution $\phi(t) = e^{\cos t}\cos(\sin t)$ where $c = (a-b)/(a+b)$ and $t \in [0, 2\pi]$ [5].

Table 3.2. Nyström method for equation (3.19).

	$2n$	$\|\|\phi_n - \phi\|\|_\infty$
$a = 1$ & $b = 0.5$	4	1.53E-01
	8	2.81E-03
	16	4.40E-07
$a = 1$ & $b = 0.1$	16	1.25E-01
	32	5.08E-03
	64	8.26E-06
	128	2.18E-11

Example 3.17. The next example we consider is the scattering of plane waves. We recall that the scattering of the incoming wave field $u^i(x)$ from a sound-soft obstacle D leads to the exterior Dirichlet problem for the scattered field $u^s(x)$:

$$\begin{cases} \Delta u^i(x) + k^2 u^i(x) = 0, \quad x \in \mathbb{R}^2, \\ \Delta u^s(x) + k^2 u^s(x) = 0, \quad x \in \mathbb{R}^2 \backslash \bar{D}, \\ BC:\ u^s = -u^i, \quad on\ \partial D, \\ RC:\ \lim\limits_{|x|\to\infty} |x|^{1/2} \left(\dfrac{x}{|x|} \cdot \nabla u^s(x) - iku^s(x) \right) = 0. \end{cases} \tag{3.20}$$

In chapter 2, we reformulated this problem using the boundary integral equation (2.21) for an unknown density $\varphi(x)$ on ∂D

$$\varphi(x) + 2\int_{\partial D} \left\{ \frac{\partial \Phi(x,y)}{\partial \nu(y)} - i\eta \Phi(x,y) \right\} \varphi(y)\, ds(y) = -2u^i(x), \quad x \in \partial D,$$

where $\Phi(x,y)$ is the fundamental solution of the Helmholtz equation in $\mathbb{R}^2$ and the incident plane wave is given in (2.22). Once we obtain $\varphi(x)$, the scattered field $u^s(x)$ at any $x \in \mathbb{R}^2 \backslash \bar{D}$ can be evaluated through the combined potential (2.20).

To employ a concrete example, first, we have to describe the necessary parametrization of this integral equation. Assume that the boundary curve ∂D possesses a regular analytic and 2π-periodic parametric representation of the form $x(t) = (x_1(t), x_2(t))$, $t \in [0, 2\pi]$, in counterclockwise orientation satisfying $|x'(t)|^2 > 0$ for all t. Setting $\psi(t) := \varphi(x(t))$, $g(t) := -2u^i(x(t))$ and using $H_1^{(1)} = -H_0^{(1)'}$, the integral equation reads

$$\psi(t) - \int_0^{2\pi} \{L(t,s) + i\eta M(t,s)\}\, \psi(s)\, ds = g(t), \quad 0 \le t \le 2\pi,$$

where kernels are given by

$$L(t,s) := \frac{ik}{2} H_1^{(1)}(k|x(s)-x(t)|) \frac{x(s)-x(t)}{|x(s)-x(t)|} \cdot \nu(x(s)) |x'(s)|, \qquad t \neq s,$$
$$M(t,s) := \frac{i}{2} H_0^{(1)}(k|x(s)-x(t)|) |x'(s)|, \qquad t \neq s,$$

and unit normal vector is $\nu(x(s)) := (x_2'(s), -x_1'(s))/|x'(s)|$. For proper numerical treatment of logarithmic singularities at $t = s$, following [1], we split the kernels into

$$L(t,s) = L_1(t,s) \log\left(4\sin^2\frac{t-s}{2}\right) + L_2(t,s),$$
$$M(t,s) = M_1(t,s) \log\left(4\sin^2\frac{t-s}{2}\right) + M_2(t,s),$$

where

$$L_1(t,s) := -\frac{k}{2\pi} J_1(k|x(s)-x(t)|) \frac{x(s)-x(t)}{|x(s)-x(t)|} \cdot \nu(x(s)) |x'(s)|,$$
$$L_2(t,s) := L(t,s) - L_1(t,s) \log\left(4\sin^2\frac{t-s}{2}\right),$$
$$M_1(t,s) := -\frac{1}{2\pi} J_0(k|x(s)-x(t)|) |x'(s)|,$$
$$M_2(t,s) := M(t,s) - M_1(t,s) \log\left(4\sin^2\frac{t-s}{2}\right)$$

for $t \neq s$. The kernels L_1, L_2, M_1, and M_2 turn out to be analytic (see below) and we note that in here, it is essential to split the logarithmic singularities in a way that kernels preserve their 2π-periodicity.

Now, we derive the diagonal terms of the kernels L, L_1, L_2, M_1, M_2. Define $n(x(s)) := (x_2'(s), -x_1'(s))$. First we utilize L'Hopital's rule to get

$$\lim_{s\to t\pm} \frac{x(s)-x(t)}{|x(s)-x(t)|} \cdot \nu(x(s)) = \pm \frac{x'(t)}{|x'(t)|} \cdot \nu(x(t)) = 0, \tag{3.21}$$

and

$$\begin{aligned}\lim_{s\to t}\frac{x(s)-x(t)}{|x(s)-x(t)|^2}\cdot\nu(x(s))\,|x'(s)| &= \lim_{s\to t}\frac{x(s)-x(t)}{|x(s)-x(t)|^2}\cdot n(x(s))\\ &= \lim_{s\to t}\frac{n(x(s))'\cdot(x(s)-x(t))+n(x(s))\cdot x'(s)}{2|x(s)-x(t)|\frac{x(s)-x(t)}{|x(s)-x(t)|}\cdot x'(s)}\\ &= \frac{1}{2}\lim_{s\to t}\frac{\frac{x(s)-x(t)}{s-t}\cdot n(x(s))'}{\frac{x(s)-x(t)}{s-t}\cdot x'(s)} = -\frac{1}{2}\frac{x''(t)}{|x'(t)|^2}\cdot n(x(t)),\end{aligned} \tag{3.22}$$

and further

$$\begin{aligned}\lim_{s\to t}\frac{k^2|x(s)-x(t)|^2}{16\sin^2\frac{t-s}{2}} &= \frac{k^2}{16}\lim_{s\to t}\frac{2(x(s)-x(t))\cdot x'(s)}{-\sin\frac{t-s}{2}\cos\frac{t-s}{2}}\\ &= \frac{k^2}{4}\lim_{s\to t}\frac{\frac{x(t)-x(s)}{t-s}\cdot x'(s)}{\frac{\sin(t-s)}{t-s}} = \frac{k^2}{4}|x'(t)|^2.\end{aligned} \tag{3.23}$$

Define the Euclidean distance as $r(t,s) := |x(t)-x(s)|$. Then by the expansions of Bessel and Neumann functions

$$\begin{aligned}J_1(t) &= \sum_{p=0}^{\infty}\frac{(-1)^p}{p!(p+1)!}\left(\frac{t}{2}\right)^{1+2p},\\ Y_1(t) &= \frac{2}{\pi}\left\{\log\frac{t}{2}+C\right\}J_1(t)-\frac{2}{\pi t}-\frac{1}{\pi}\sum_{p=0}^{\infty}\frac{(-1)^p\{\xi(1+p)+\xi(p)\}}{p!(1+p)!}\left(\frac{t}{2}\right)^{1+2p}\end{aligned}$$

where

$$\xi(p) := \sum_{m=1}^{p}\frac{1}{m},\quad p=1,2,...,\text{ with}\quad \xi(0):=0,$$

and

$$C := \lim_{p\to\infty}\left\{\sum_{m=1}^{p}\frac{1}{m}-\log p\right\}$$

is the Euler's constant, we have

$$\begin{aligned}\frac{ik}{2}H_1^{(1)}(kr) &= \left(\frac{ik}{2} - \frac{k}{2\pi}\log\left(\frac{k^2r^2}{4}\right) - \frac{kC}{\pi}\right)\sum_{p=0}^{\infty}\frac{(-1)^p}{p!(1+p)!}\left(\frac{kr}{2}\right)^{1+2p} \\ &\quad + \frac{k}{2\pi}\sum_{p=0}^{\infty}\frac{(-1)^p\{\xi(1+p)+\xi(p)\}}{p!(1+p)!}\left(\frac{kr}{2}\right)^{1+2p} + \frac{1}{\pi r} \\ &= \frac{1}{\pi r}\left[1 + \sum_{p=0}^{\infty}\frac{(-1)^p}{p!(1+p)!}\left(\frac{kr}{2}\right)^{2+2p}\right. \\ &\qquad \left.\times\left\{\xi(1+p)+\xi(p)+i\pi - 2C - \log\left(\frac{k^2r^2}{4}\right)\right\}\right].\end{aligned}$$

From the last identity and definitions of kernels L_2 and L, we see that

$$\begin{aligned}L_2(t,s) &= \frac{1}{\pi}\frac{(x(s)-x(t))}{r^2}\cdot n(x(s)) \\ &\quad\times\left[1 + \sum_{p=0}^{\infty}\frac{(-1)^p}{p!(1+p)!}\left(\frac{kr}{2}\right)^{2+2p}\right. \\ &\qquad\left.\times\left\{\xi(1+p)+\xi(p)+i\pi - 2C - \log\left(\frac{k^2r^2}{16\sin^2\frac{t-s}{2}}\right)\right\}\right] \qquad (3.24)\end{aligned}$$

Hence, recalling $|x'(t)|^2 > 0$ and using the limits (3.22), (3.23) and the definition of $\xi(p)$, from (3.24) we get

$$L_2(t,t) := \lim_{s\to t} L_2(t,s) = -\frac{1}{2\pi}\frac{x''(t)}{|x'(t)|^2}\cdot n(x(t)).$$

Also definitions of J_1, L_1 and the limit (3.21) yield

$$\lim_{s\to t} L_1(t,s)\log\left(4\sin^2\frac{t-s}{2}\right) = 0,$$

thus the definition of L_2 implies that

$$L(t,t) = L_2(t,t).$$

As for the diagonal of L_1, using (3.21) and $J_1(0) = 0$ we get

$$L_1(t,t) := \lim_{s\to t} L_1(t,s) = \lim_{s\to t} -\frac{k}{2\pi}\, J_1(k\,|x(s)-x(t)|)\,\frac{x(s)-x(t)}{|x(s)-x(t)|}\cdot \nu(x(s))\,|x'(s)| = 0.$$

Concerning M, as is clear

$$M(t,t) := \lim_{s\to t} M(t,s) = -\infty,$$

however, since J_0 is analytic on $\mathbb{R}$ with $J_0(0) = 1$, we have

$$M_1(t,t) := \lim_{s\to t} M_1(t,s) = -\frac{1}{2\pi}\left(\lim_{s\to t} J_0(k\,|x(s)-x(t)|)\right)\left(\lim_{s\to t}|x'(s)|\right) = -\frac{1}{2\pi}\,|x'(t)|.$$

Also, after extraction of singularity

$$M_2(t,s) = \left\{\frac{i}{2}J_0(kr) - \frac{C}{\pi}J_0(kr) - \frac{1}{2\pi}\log\left(\frac{k^2r^2}{16\sin^2\frac{t-s}{2}}\right)J_0(kr) + \frac{1}{\pi}\sum_{p=0}^{\infty}\frac{(-1)^p\xi(p)}{p!^2}\left(\frac{kr}{2}\right)^{2p}\right\}|x'(s)|. \tag{3.25}$$

Using $J_0(0) = 1$, definition of $\xi(p)$ and the limit (3.23), from (3.25) we find

$$M_2(t,t) := \lim_{s\to t} M_2(t,s) = \left\{\frac{i}{2} - \frac{C}{\pi} - \frac{1}{2\pi}\log\left(\frac{k^2}{4}|x'(t)|^2\right)\right\}|x'(t)|.$$

Hence, we have to numerically solve an integral equation of the form

$$\psi(t) - \int_0^{2\pi} K(t,s)\psi(s)\,ds = g(t), \quad 0 \le t \le 2\pi, \tag{3.26}$$

where

$$K(t,s) = K_1(t,s)\log\left(4\sin^2\frac{t-s}{2}\right) + K_2(t,s),$$
$$K_1(t,s) = L_1(t,s) + i\eta M_1(t,s),$$
$$K_2(t,s) = L_2(t,s) + i\eta M_2(t,s).$$

with analytic functions K_1 and K_2 and with an analytic right hand side g. Regarding numerical discretization of the integral, for the singular part the quadrature formula (3.15) is used as derived earlier. For the smooth part we utilize the trapezoidal rule

$$\int_0^{2\pi} u(t)dt \approx \sum_{j=0}^{2n-1} u(t_j)\int_0^{2\pi} L_j(t)dt = \frac{\pi}{n}\sum_{j=0}^{2n-1} u(t_j) \tag{3.27}$$

for a function $u \in C_p(2\pi)$. Then, in the Nyström method, our integral equation is replaced by the approximation equation

$$\psi^{(n)}(t) - \sum_{j=0}^{2n-1}\left\{R_j^{(n)}(t)K_1(t,t_j) + \frac{\pi}{n}K_2(t,t_j)\right\}\psi^{(n)}(t_j) = g(t), \quad 0 \le t \le 2\pi, \tag{3.28}$$

by applying the quadrature rule (3.15) to $K_1(t,\cdot)\psi$ and trapezoidal rule (3.27) to $K_2(t,\cdot)\psi$. Then, the solution of (3.28) reduces to solving a finite dimensional linear system

$$\psi^{(n)}(t_i) - \sum_{j=0}^{2n-1}\left\{R_{|i-j|}^{(n)}K_1(t_i,t_j) + \frac{\pi}{n}K_2(t_i,t_j)\right\}\psi^{(n)}(t_j) = g(t_i),$$

for $i = 0, ..., 2n-1$, where we use the relation (3.17) for the weights.

To exemplify this procedure, consider the scattering of plane waves by a non-convex kite-shaped scatterer described by the parametric representation

$$x(t) = (\cos t + 0.65\cos 2t - 0.65, 1.5\sin t), \quad t \in [0, 2\pi].$$

We choose the direction of planes waves as $a = (1, 0)$ and the coupling parameter as $\eta = k$ [20]. Since the exact solution for this setting is unknown, we select a very fine grid to compute the relative error.

Table 3.3. Nyström method for equation (3.26).

	$2n$	$\|\|\psi_n - \psi_{512}\|\|_\infty / \|\|\psi_{512}\|\|_\infty$
$k = 5$	32	2.33E-02
	64	5.63E-06
	128	2.81E-09
$k = 20$	64	3.63E-01
	128	1.22E-02
	256	2.34E-12
$k = 50$	64	5.94E-01
	128	3.98E-01
	256	6.46E-02

3.4. Projection Methods

To investigate the collocation and Galerkin methods, we first need to present the general theory of projection methods.

To this end, considering the operator equation of the second kind

$$\varphi - A\varphi = f, \tag{3.29}$$

where A is a bounded linear operator on a Banach space X, we choose a sequence of subspaces $X_n \subset X$ with $\dim X_n = n$, and let $P_n : X \to X_n$ be projection operators (bounded linear operators with $P_n\varphi = \varphi$ for all $\varphi \in X_n$) [21]. The projection method approximates the above equation by the projected equation

$$\varphi_n - P_n A\varphi_n = P_n f, \tag{3.30}$$

where $\varphi_n \in X_n$. The method is called *convergent* provided that for sufficiently large n the approximating equation (3.30) has a unique solution $\varphi_n \in X_n$ and these solutions converge to the unique solution φ, $n \to \infty$.

Here, we assume that the subspaces X_n have the denseness property

$$\lim_{n\to\infty} \inf_{\psi\in X_n} ||\psi - \varphi|| = 0, \quad \text{for all } \varphi \in X. \tag{3.31}$$

This, in general, is required in order to guarantee convergence.

We now proceed to establish the general convergence and error analysis results for the projection method.

Theorem 3.18. (Convergence) *Let $A : X \to X$ be a compact linear operator such that $I - A$ is injective. Assume that the projection operators $P_n : X \to X_n$ satisfy $||P_nA - A|| \to 0$, $n \to \infty$. Then, for sufficiently large n, the approximate equation* (3.30) *is uniquely solvable for all $f \in X$ and the error estimate*

$$||\varphi_n - \varphi|| \leq C||P_n\varphi - \varphi|| \tag{3.32}$$

holds for some positive constant C [5].

Proof. We apply Theorem 3.6 with $A_n = P_nA$ to get unique solvability of (3.29), and error estimate follows from manipulating (3.29) and (3.30). □

The following useful result follows easily from Lemma 3.8 with the aid of the previous theorem.

Corollary 3.19. *Let $A : X \to X$ be a compact linear operator such that $I - A$ is injective. Assume that the projections $P_n : X \to X_n$ converge pointwise; $P_n\varphi \to \varphi$, $n \to \infty$, for all $\varphi \in X$. Then, for sufficiently large n, the approximate equation* (3.30) *is uniquely solvable for all $f \in X$ and the error estimate* (3.32) *holds.*

Observe that the equation (3.30) is only semi-discrete. Thus, in practice, we will use the fully-discrete equation

$$\widehat{\varphi}_n - P_n A_n \widehat{\varphi}_n = P_n f_n, \tag{3.33}$$

where A_n and f_n are some approximations of A and f, respectively. Sufficient conditions for unique solvability of this equation are given in the next theorem.

Theorem 3.20. (Convergence: fully-discrete case) *Under the assumptions of Theorem 3.18 on A and P_n, further suppose that $(P_n A_n - P_n A)\phi \to 0$, $n \to \infty$, for all $\phi \in X$ and $||P_n A_n - P_n A||_{X_n \to X_n} \to 0$, $n \to \infty$. Then, for sufficiently large n, the fully-discrete equation* (3.33) *is uniquely solvable and we have*

$$||\widehat{\varphi}_n - \varphi|| \leq C\{||P_n\varphi - \varphi|| + ||P_n(A_n - A)\varphi|| + ||P_n(f_n - f)||\} \tag{3.34}$$

for some positive constant C [5].

Proof. By assumption $||P_n A_n - P_n A||_{X_n \to X_n} \to 0$, $n \to \infty$, with the help of Theorem 3.6 we establish the existence and uniform boundedness of the inverse operators $(I - P_n A_n)^{-1} : X_n \to X_n$ for sufficiently large n. Then from error estimate (3.6) of the same theorem for semi- and fully-discrete equations we see that

$$||\widehat{\varphi}_n - \varphi_n|| \leq C\{||(P_n A_n - P_n A)\varphi_n|| + ||P_n(f_n - f)||\}$$

for some constant $C > 0$. Now, using the error estimate (3.32) repeatedly and the uniform boundedness principle yield

$$\begin{aligned}
||\widehat{\varphi}_n - \varphi|| &\leq C\{||(P_n A_n - P_n A)\varphi_n|| + ||P_n(f_n - f)|| + ||P_n\varphi - \varphi||\} \\
&\leq C\{(||P_n A_n - P_n A|| + 1)||P_n\varphi - \varphi|| + ||P_n(A_n - A)\varphi|| + ||P_n(f_n - f)||\} \\
&\leq C\{||P_n\varphi - \varphi|| + ||P_n(A_n - A)\varphi|| + ||P_n(f_n - f)||\}
\end{aligned}$$

for some generic positive constant C changing from line to line. □

3.4.1. The Collocation Method

The collocation method for approximately solving the equation of the second kind (3.29) searches an approximate solution in a finite dimensional subspace by requiring that this equation is satisfied only at a finite number of so called collocation points. We assume that $A : C(D) \to C(D)$ is a bounded linear operator and let $X_n \subset C(D)$ be a sequence of finite dimensional subspaces that are *unisolvent* with respect to chosen collocation points $x_1, x_2, ..., x_n \in D$, i.e., each function from X_n that vanishes at $x_1, x_2, ..., x_n$ vanishes identically. Then the collocation method approximates the solution of the equation of the second kind by $\varphi_n \in X_n$ such that

$$\varphi_n(x_j) - (A\varphi_n)(x_j) = f(x_j), \quad j = 1, ..., n. \tag{3.35}$$

The collocation method can be interpreted as a projection method with the projection operator $P_n : C(D) \to X_n$ which assigns a function $f \in C(D)$ to its interpolating function $P_n f \in X_n$. Since the interpolating function is uniquely determined by its values at the interpolation points we see that (3.35) is also equivalent to

$$\varphi_n - P_n A\varphi_n = P_n f. \tag{3.36}$$

We now consider the application of specific projection operators within the collocation method. Let P_n be the piecewise linear interpolation operator on $C[a, b]$ discussed in section 3.1. Then, using the error estimate (3.1) and the norm $||P_n||_\infty = 1$, by uniform boundedness principle we have the pointwise convergence $P_n\psi \to \psi$, $n \to \infty$, for all $\psi \in C[a, b]$. Hence, by Corollary 3.19 we immediately have the following theorem.

Theorem 3.21. (Linear Splines) *The collocation method with piecewise linear interpolation converges for integral equations of the second kind with continuous or weakly singular kernels* [5, 13].

In the case that the exact solution $\varphi \in C^2[a,b]$, from error estimates (3.1) and (3.32) we see that $||\varphi_n - \varphi||_\infty = \mathcal{O}(h^2)$. Moreover, fully discrete approximation will be still of order $\mathcal{O}(h^2) = ||\widehat{\varphi}_n - \varphi||_\infty$ provided the kernel and right hand side are twice continuously differentiable [12].

Theorem 3.22. (Trigonometric Polynomials) *The collocation method with trigonometric interpolation converges for integral equations of the second kind provided f and K are 2π-periodic continuously differentiable* [5].

Proof. Since the kernel K is 2π-periodic continuously differentiable, the operator A maps $C_p(2\pi)$ into the continuously differentiable 2π-periodic functions, $C_p^1(2\pi)$. Recall that for $q > 1/2$ the embedding $H^q[0,2\pi] \hookrightarrow C_p(2\pi)$ is compact (Theorem B.2). Then we have

$$\begin{aligned}
||P_nA\varphi - A\varphi||_\infty &\le C||P_nA\varphi - A\varphi||_{H^q} \\
&\le Cn^{q-1}||A\varphi||_{H^1} \qquad \text{(Theorem 3.5)} \\
&\le Cn^{q-1}\left(||A\varphi||_{L^2}^2 + ||(A\varphi)'||_{L^2}^2\right)^{1/2} \\
&\le Cn^{q-1}(||A\varphi||_{L^2} + ||(A\varphi)'||_{L^2}) \\
&\le Cn^{q-1}(||A\varphi||_\infty + ||(A\varphi)'||_\infty) \\
&\le Cn^{q-1}||\varphi||_\infty \qquad \text{(K is continuously differentiable)}
\end{aligned}$$

for all $\varphi \in C_p(2\pi)$ with $1/2 < q < 1$ and C is a generic positive constant depending on q. From the last estimate we see that

$$||P_nA - A||_\infty \le Cn^{q-1}, \quad 1/2 < q < 1,$$

and applying Theorem 3.18 establishes the proof. □

Weakly Singular Kernels:

We apply the collocation method to equations of the second kind with weakly singular kernels. To this end, we specifically consider the operator

$$(A\varphi)(t) := \int_0^{2\pi} \log\left(4\sin^2\frac{t-s}{2}\right) K(t,s)\varphi(s)ds, \quad 0 \le t \le 2\pi, \tag{3.37}$$

with a 2π-periodic infinitely differentiable kernel K.

Theorem 3.23. *The collocation method with trigonometric polynomials converges for integral equations of the second kind with a logarithmic singularity of the form* (3.37) *provided the kernel* $K \in C_p^\infty(2\pi)$ *and right-hand side* $f \in C_p^1(2\pi)$ [5].

Proof. Since the logarithmic singularity is integrable, $A\varphi \in C_p(2\pi)$ for any $\varphi \in C_p(2\pi)$. Then by Sobolev embedding (Theorem B.2) and interpolation in Sobolev spaces (Theorem 3.5) we have

$$\begin{aligned} ||P_nA\varphi - A\varphi||_\infty &\le C||P_nA\varphi - A\varphi||_{H^q} \\ &\le Cn^{q-1}||A\varphi||_{H^1} \\ &\le Cn^{q-1}||\varphi||_{L^2} \le Cn^{q-1}||\varphi||_\infty \end{aligned}$$

for all $\varphi \in C_p(2\pi)$ and all $1/2 < q < 1$ with some constant generic constant $C > 0$. In the third inequality, we use the fact that the operator A given by (3.37) is bounded from $H^p[0, 2\pi]$ into $H^{p+1}[0, 2\pi]$, $\forall p \ge 0$ (see [5, Theorem 12.15]) Hence the proof can now be completed as in the preceding theorem. □

Regarding numerical implementation, if we choose the Lagrange basis of $X_n = \mathbb{T}_n$ and write $\varphi_n = \sum_{k=0}^{2n-1} \gamma_k L_k$, then for (3.37) we see that (3.35) is equivalent to the linear system

$$\gamma_j - \sum_{k=0}^{2n-1} \gamma_k \int_0^{2\pi} \log\left(4\sin^2\frac{t_j-s}{2}\right) K(t_j,s)L_k(s)ds = f(t_j), \quad j = 0, ..., 2n-1, \tag{3.38}$$

since $L_k(t_j) = \delta_{kj}$ and $t_j = j\pi/n$, $j = 0, ..., 2n-1$. To evaluate matrix elements, we replace $K(t_j, \cdot)$ by its trigonometric interpolation and get

$$\int_0^{2\pi} \log\left(4\sin^2\frac{t_j - s}{2}\right) K(t_j, s)L_k(s)ds \approx \sum_{m=0}^{2n-1} E_{k-j,m-j}K(t_j, t_m) \tag{3.39}$$

where

$$E_{k,m} := \int_0^{2\pi} \log\left(4\sin^2\frac{s}{2}\right) L_k(s)L_m(s)ds, \quad k, m = 0, ..., 2n-1$$

with $E_{k,m} = E_{-k,m} = E_{k,-m}$. Observe that the weights in (3.39) can be evaluated as

$$E_{k,m} = \sum_{j=0}^{4n-1} R_j^{(2n)} L_k(t_j^{(2n)})L_m(t_j^{(2n)}), \quad k, m = 0, ..., 2n-1,$$

since the quadrature rule (3.15) with the number of interpolation points $2n$ doubled to $4n$ integrates trigonometric polynomials of degree $\leq 2n$ exactly.

With the aid of the quadrature rule (3.39), the system (3.38) corresponds to solving the fully-discrete equation (3.33) with

$$(A_n\varphi)(t) := \int_0^{2\pi} \log\left(4\sin^2\frac{t - s}{2}\right) \sum_{m=0}^{2n-1} K(t, t_m)L_m(s)\varphi(s)ds, \quad 0 \leq t \leq 2\pi.$$

Now, we observe that the kernel $K_n(t) := \sum_{m=0}^{2n-1} K(t, t_m)L_m(s)$ in A_n satisfies for $p \geq 2$

$$||P_nK - K||_\infty = ||K_n - K||_\infty \leq C||K_n - K||_{H^1} \leq Cn^{1-p}||K||_{H^p}.$$

by Theorems B.2 and 3.5. Therefore since K is assumed to be infinitely differentiable, $||K_n - K||_\infty = \mathcal{O}(n^{-m})$ holds for each $m \in \mathbb{N}$ from which we conclude $||A_n - A||_\infty = \mathcal{O}(n^{-m})$. Furthermore, recall that $||P_n||_\infty = \mathcal{O}(\log(n))$ as $n \to \infty$, thus $||P_n(A_n - A)||_\infty \to 0$, $n \to \infty$. Hence Theorem 3.20 and its error estimate (3.34) apply. When the exact solution φ is infinitely differentiable, from that estimate via theorems B.2

and 3.5 we deduce that the error in the fully-discrete equation is $||\widehat{\varphi}_n - \varphi||_\infty = \mathcal{O}(n^{-m})$ [5]. Finally, if both the kernel K and the exact solution φ are analytic, the order of convergence will be exponential [5].

Contrary to the Nyström method, condition numbers for the linear systems associated with the collocation method are not uniformly bounded and depend on the choice of the basis for the approximating subspaces, see [5] or [14]. Therefore, bases should be chosen carefully preventing the method suffer from instabilities.

3.4.2. Numerical Examples for the Collocation Method

Example 3.24. We exercise the collocation method with linear splines to the integral equation (3.18).

Table 3.4. Collocation method for equation (3.18).

	n	$\|\|\varphi_n - \varphi\|\|_\infty$
Linear Splines	4	8.33E-03
	8	2.07E-03
	16	5.19E-04
	32	1.29E-04

Example 3.25. The collocation method with trigonometric polynomials is applied to the integral equation (3.19).

Table 3.5. Collocation method for equation (3.19).

	2n	$\|\|\phi_n - \phi\|\|_\infty$
$a = 1$ & $b = 0.5$	4	1.07E-01
	8	2.31E-03
	16	4.37E-07
$a = 1$ & $b = 0.1$	16	1.25E-01
	32	5.08E-03
	64	8.26E-06
	128	2.18E-11

Example 3.26. For an another example, recall the combined field integral equation (2.24) corresponding to exterior Dirichlet problem (3.20) for the unknown density

$v(x) := \partial u/\partial\nu(x)$

$$v(x) + 2\int_{\partial D}\left\{\frac{\partial\Phi(x,y)}{\partial\nu(x)} - i\eta\Phi(x,y)\right\} v(y)\, ds(y) = 2\left\{\frac{\partial u^i}{\partial\nu}(x) - i\eta u^i(x)\right\}$$

for $x \in \partial D$. Once $v(x)$ is obtained, we can find the scattered field for the exterior problem by Theorem 2.20 as

$$u^s(x) = -\int_{\partial D}\Phi(x,y)v(y)ds(y), \quad \textit{for } x \in \mathbb{R}^2\backslash\bar{D}.$$

Now assume that ∂D has a regular analytic and 2π-periodic representation $x(t) = (x_1(t), x_2(t))$ with $|x'(t)| > 0$. Set $\tilde{\psi}(t) := v(x(t))$ and $\tilde{g}(t) := 2\left\{\frac{\partial u^i}{\partial\nu}(x(t)) - i\eta u^i(x(t))\right\}$. Then, straightforward calculations gives the parametrization

$$\tilde{\psi}(t) - \int_0^{2\pi}\left\{\tilde{L}(t,s) + i\eta M(t,s)\right\}\tilde{\psi}(s)ds = \tilde{g}(t), \quad 0 \le t \le 2\pi, \tag{3.40}$$

where

$$\begin{aligned}
\tilde{L}(t,s) &:= \frac{ik}{2}\, H_1^{(1)}(k|x(t)-x(s)|)\frac{x(t)-x(s)}{|x(t)-x(s)|}\cdot\nu(x(t))\,|x'(s)|, \qquad t \neq s,\\
M(t,s) &:= \frac{i}{2}H_0^{(1)}(k|x(t)-x(s)|)|x'(s)|, \qquad t \neq s,
\end{aligned}$$

and $\nu(x(t)) := (x_2'(t), -x_1'(t))/|x'(t)|$. Again we split the kernels into,

$$\begin{aligned}
\tilde{L}(t,s) &= \tilde{L}_1(t,s)\log\left(4\sin^2\frac{t-s}{2}\right) + \tilde{L}_2(t,s),\\
M(t,s) &= M_1(t,s)\log\left(4\sin^2\frac{t-s}{2}\right) + M_2(t,s),
\end{aligned}$$

where

$$\tilde{L}_1(t,s) := -\frac{k}{2\pi} J_1(k|x(t)-x(s)|)\frac{x(t)-x(s)}{|x(t)-x(s)|}\cdot\nu(x(t))\,|x'(s)|,$$
$$\tilde{L}_2(t,s) := \tilde{L}(t,s) - \tilde{L}_1(t,s)\log\left(4\sin^2\frac{t-s}{2}\right),$$
$$M_1(t,s) := -\frac{1}{2\pi}J_0(k|x(t)-x(s)|)|x'(s)|,$$
$$M_2(t,s) := M(t,s) - M_1(t,s)\log\left(4\sin^2\frac{t-s}{2}\right).$$

Utilizing techniques as in example (3.17), it is not difficult to derive

$$\tilde{L}_1(t,t) = 0,$$
$$\tilde{L}(t,t) = \tilde{L}_2(t,t) = -\frac{1}{2\pi}\frac{x''(t)}{|x'(t)|}\cdot\nu(x(t)),$$
$$M_2(t,t) = \left\{\frac{i}{2} - \frac{C}{\pi} - \frac{1}{2\pi}\log\left(\frac{k^2}{4}|x'(t)|^2\right)\right\}|x'(t)|.$$

Setting

$$\tilde{K}_1(t,s) := \tilde{L}_1(t,s) + i\eta M_1(t,s),$$
$$\tilde{K}_2(t,s) := \tilde{L}_2(t,s) + i\eta M_2(t,s),$$
$$\tilde{K}(t,s) := \tilde{K}_1(t,s)\log\left(4\sin^2\frac{t-s}{2}\right) + \tilde{K}_2(t,s),$$

transforms the integral equation (3.40) into

$$\tilde{\psi}(t) - \int_0^{2\pi}\tilde{K}(t,s)\tilde{\psi}(s)\,ds = \tilde{g}(t), \quad 0\le t\le 2\pi. \tag{3.41}$$

We choose the approximating space $\mathbb{T}_n$, trigonometric polynomials, with the Lagrange basis L_k, $k = 0, ..., 2n-1$, and grid points as $t_j = \pi j/n$, $j = 0, ..., 2n-1$. Then the approximate solution ψ_n generated by the method satisfies

$$\tilde{\psi}_n(t_j) - \int_0^{2\pi}\left\{\log\left(4\sin^2\frac{t_j-s}{2}\right)\tilde{K}_1(t_j,s) + \tilde{K}_2(t_j,s)\right\}\tilde{\psi}_n(s)ds = \tilde{g}(t_j).$$

Writing the linear combination $\tilde{\psi}_n(t) = \sum_{k=0}^{2n-1} \gamma_k L_k(t)$ yields the linear system

$$\gamma_j - \sum_{k=0}^{2n-1} \gamma_k \int_0^{2\pi} \left\{ \log\left(4\sin^2\frac{t_j - s}{2}\right) \tilde{K}_1(t_j, s) + \tilde{K}_2(t_j, s) \right\} L_k(s)ds = \tilde{g}(t_j),$$

for $j = 0, ...2n-1$. For the singular integral we replace $\tilde{K}_1(t_j, \cdot)$ by its interpolating polynomial and then use the quadrature formula (3.39). The smooth part is evaluated by replacing $\tilde{K}_2(t_j, \cdot)$ by its interpolating polynomial and then using the formula

$$\int_0^{2\pi} L_m(s)L_k(s)ds = \frac{\pi}{n}\delta_{mk} - (-1)^{m-k}\frac{\pi}{4n^2}, \quad m, k = 0, ..., 2n-1. \tag{3.42}$$

We consider the scattering of planes waves from the unit circle with the parametrization $x(t) = (\cos(t), \sin(t))$, $t \in [0, 2\pi]$, with the direction $a = (1, 0)$. In this case, the exact density can be found by Fourier analysis as given in Proposition C.2. Also, we take $\eta = k$.

Table 3.6. Collocation method for equation (3.41).

	$2n$	$\|\|\tilde{\psi}_n - \tilde{\psi}\|\|_\infty$
$k = 5$	16	4.18E-02
	32	3.19E-08
	64	3.47E-14
$k = 20$	32	11.71
	64	3.23E-05
	128	5.88E-13
$k = 50$	32	78.14
	64	80.92
	128	4.34E-04

3.4.3. The Galerkin Method

We consider solving general operator equations of the form

$$A\varphi = f \tag{3.43}$$

with a bijective bounded linear operator A mapping a Hilbert space X into its dual space X' with respect to the dual pairing induced by the inner product $\langle \cdot, \cdot \rangle$ and $f \in X'$. An equivalent way of solving this equation is its variational formulation: Find $\varphi \in X$ such that

$$\langle A\varphi, \psi \rangle = \langle f, \psi \rangle, \quad \text{for all } \psi \in X. \tag{3.44}$$

To ensure the existence and uniqueness of the solutions to this variational problem we need a further assumption on the operator A.

Definition 3.27. *A bounded linear operator $A : X \to X'$ is called coercive provided there exists a constant $c > 0$ such that*

$$|\langle A\psi, \psi \rangle| \geq c||\psi||_X^2, \quad \textit{for all } \psi \in X. \tag{3.45}$$

Theorem 3.28. (Lax-Milgram) *Let $A : X \to X'$ be a coercive bounded linear operator satisfying*

$$|\langle A\psi, \psi \rangle| \geq c_e||\psi||_X^2, \quad ||A\psi||_{X'} \leq c_b||\psi||_X \quad \textit{for all } \psi \in X.$$

Then for any $f \in X'$ there exists a unique solution φ of (3.44) *satisfying*

$$||\varphi||_X \leq \frac{1}{c_e}||f||_{X'}$$

[22].

To obtain a numerical scheme, we consider a sequence of finite dimensional subspaces $X_n \subset X$ with $\dim X_n = n$. Galerkin's method approximates the solution of the variational problem (3.44) with $\varphi_n \in X_n$ requiring

$$\langle A\varphi_n, \psi\rangle = \langle f, \psi\rangle, \quad \text{for all } \psi \in X_n. \tag{3.46}$$

For a coercive operator, convergence of the approximate solution $\varphi_n \to \varphi$, $n \to \infty$, in X follows immediately from the denseness property (3.31) of the subspaces X_n and Cea's lemma.

Theorem 3.29. (Cea's lemma) *Under the assumptions of the previous theorem, the finite dimensional Galerkin approximation* (3.46) *has a unique solution* $\varphi_n \in X_n$ *satisfying*

$$||\varphi_n||_X \leq \frac{1}{c_e}||f||_{X'}$$
$$||\varphi - \varphi_n||_X \leq \frac{c_b}{c_e} \inf_{\psi \in X_n} ||\varphi - \psi||_X$$

[23].

Proof. A consequence of Lax-Milgram lemma with the aid of Galerkin orthogonality

$$\langle A(\varphi - \varphi_n), \psi\rangle = 0, \quad \psi \in X_n.$$

□

We now proceed to apply Galerkin's method to integral equations of the second kind. Let X be a Hilbert space with the inner product $\langle \cdot, \cdot \rangle$ and $I - A : X \to X$ be an injective bounded operator. Also let $X_n \subset X$ be subspaces with $\dim X_n = n$ and $P_n : X \to X_n$ be the orthogonal projection operator mapping each element into its unique best approximation with respect to X_n. Consider the integral equation of the

second kind (3.29). Then $\varphi_n \in X_n$ is a solution of the projected equation

$$\varphi_n - P_n A\varphi_n = P_n f$$

if and only if

$$\langle (I - A)\varphi_n, \psi\rangle = \langle f, \psi\rangle, \quad \forall \psi \in X_n. \tag{3.47}$$

The equation (3.47) is called the Galerkin equation. If we choose a basis $\{v_1, ..., v_n\}$ for X_n and write φ_n as a linear combination $\varphi_n = \sum_{j=1}^{n} \alpha_j v_j$ then we find that Galerkin equation is equivalent to the linear system

$$\sum_{j=1}^{n} \alpha_j \{\langle v_j, v_k\rangle - \langle Av_j, v_k\rangle\} = \langle f, v_k\rangle, \quad k = 1, ..., n.$$

for the coefficients $\alpha_1, ..., \alpha_n$.

By definition of orthogonal projection and denseness assumption (3.31) we have the pointwise convergence $P_n\varphi \to \varphi$, $n \to \infty$, $\forall \varphi \in X$. Therefore, applying Corollary 3.19 gives the following convergence theorem.

Theorem 3.30. *Let $A : X \to X$ be a compact linear operator such that $I - A$ is injective. Then the Galerkin method converges for integral equations of the second kind* [5].

Let us demonstrate examples of Galerkin's method in some appropriate spaces. Firstly, let $X = L^2[a, b]$, X_n be the subspace of piecewise linear functions and P_n be the orthogonal projection of $L^2[a, b]$ onto X_n. We first show pointwise convergence $P_n\varphi \to \varphi$ for all $\varphi \in C[a, b]$. Since continuous functions on $[a, b]$ is dense in $L^2[a, b]$ we would conclude that $P_n\varphi \to \varphi$ for all $\varphi \in L^2[a, b]$, i.e. Galerkin method with piecewise linear interpolation converges in $L^2[a, b]$. If $S_n\varphi$ denotes the function in X_n

that interpolates φ, then

$$||\varphi - P_n\varphi||_{L^2} \leq ||\varphi - S_n\varphi||_{L^2} \leq C||\varphi - S_n\varphi||_\infty \leq C\omega(x, h)$$

where the last inequality follows from Theorem 3.1 and $C > 0$. This shows that $P_n\varphi \to \varphi$, $n \to \infty$ for all $\varphi \in C[a, b]$ since φ is continuous on $[a, b]$ if and only if $\lim_{h\to 0} \omega(\varphi, h) = 0$. Therefore, we have convergence of Galerkin's method in $L^2[a, b]$. For the case $\varphi \in C^2[a, b]$ by Theorem 3.1 and the error estimate (3.32) we conclude that $||\varphi - \varphi_n||_{L^2} = \mathcal{O}(h^2)$.

Now we consider integral equation of the second kind with kernel K and right-hand side being 2π-periodic functions. In this case, let $X = L^2[0, 2\pi]$ and X_n be the subspace of trigonometric polynomials of degree $\leq n$. For each $\varphi \in L^2[0, 2\pi]$, we know that its Fourier series converges to φ in L^2 norm and the orthogonal projection $P_n\varphi$ of φ to X_n is given through truncation of this series. Thus the denseness assumption (3.31) is clearly satisfied and therefore by Corollary 3.19 we have convergence of Galerkin's method. For the speed of convergence we use trigonometric interpolation formula (3.5) and deduce that

$$||\varphi - \varphi_n||_{L^2} \leq C_1||\varphi - P_n\varphi||_{L^2} \leq \frac{C_2}{n^q}||\varphi||_{H^q},$$

for some positive constants C_1 and C_2 whenever $q > 1/2$ and $\varphi \in H^q[0, 2\pi]$. Hence $||\varphi - \varphi_n||_{L^2} = \mathcal{O}(n^{-q})$ if $\varphi \in H^q[0, 2\pi]$.

Another motivation can be obtaining uniform convergence of φ_n to φ. We take $X = C_p(2\pi)$ and consider $P_n : C_p(2\pi) \to \mathbb{T}_n$ as the trigonometric interpolation operator. Unfortunately, pointwise convergence $P_n\varphi \to \varphi$, for all $\varphi \in C_p(2\pi)$ is no longer true due to uniform boundedness principle with the norm $||P_n||_\infty = \mathcal{O}(\log n)$ as (see $n \to \infty$ (3.4)) since there exists $\varphi \in C_p(2\pi)$ such that $P_n\varphi$ does not converge to φ in

$C_p(2\pi)$. Therefore we must directly show that

$$||P_nA - A||_\infty = \max_{t\in[0,2\pi]} \left| \int_0^{2\pi} K_n(t,s) - K(t,s)ds \right|$$

converges to zero to apply Theorem 3.18. Here $K_n(\cdot, s) = P_nK(\cdot, s)$ for each fixed s. Under the assumption $K(\cdot, s) \in C_p^{m,\alpha}(2\pi)$ for some $m \in \mathbb{N} \cup \{0\}$ and $0 < \alpha \leq 1$ from Corollary 3.4 we have

$$||P_nA - A||_\infty \leq C\frac{\log n}{n^{m+\alpha}}$$

for some constant $C > 0$, and thus we obtain a complete convergence for Galerkin method on $C_p(2\pi)$; in other words uniform convergence of φ_n to the exact solution φ.

Condition numbers for the Galerkin linear system significantly depend on the chosen basis; poor choice of basis may lead to instabilities [14]. The linear system is well-behaved provided an orthonormal basis is used in the implementation [13].

For a further discussion on fully-discrete Galerkin method see [13].

3.4.4. Numerical Examples for the Galerkin Method

Example 3.31. We apply the Galerkin method to the integral equation (3.18) by choosing the finite dimensional approximating space as piecewise linear functions.

Table 3.7. Galerkin method for equation (3.18).

	n	$\|\|\varphi_n - \varphi\|\|_\infty$
Linear Splines	4	4.90E-03
	8	1.26E-03
	16	3.20E-04
	32	8.07E-05

Example 3.32. In this example, Galerkin method with trigonometric polynomials is applied to the integral equation (3.19).

Table 3.8. Galerkin method for equation (3.19).

	$2n$	$\|\|\phi_n - \phi\|\|_\infty$
$a = 1$ & $b = 0.5$	4	2.18E-01
	8	9.94E-03
	16	3.05E-06
$a = 1$ & $b = 0.1$	16	1.25E-01
	32	5.08E-03
	64	8.27E-06
	128	2.19E-11

Example 3.33. We exercise the Galerkin method with trigonometric polynomials to the integral equation (3.41)

$$\tilde{\psi}(t) - \int_0^{2\pi} \tilde{K}(t,s)\tilde{\psi}(s)\, ds = \tilde{g}(t), \quad 0 \le t \le 2\pi,$$

to obtain a numerical solution for the scattering from the unit circle. Let the space of trigonometric polynomials $\mathbb{T}_n$ be the approximation space with the approximate solution $\tilde{\psi}_n$. Also $t_j = \pi j/n$ and $L_j(t)$, $j = 0, ..., 2n-1$, denotes the Lagrange basis. First requiring the equality of the scalar products with respect to this basis

$$\int_0^{2\pi} \tilde{\psi}_n(t)\overline{L_j(t)}dt - \int_0^{2\pi}\int_0^{2\pi} \tilde{K}(t,s)\tilde{\psi}_n(s)\overline{L_j(t)}dsdt = \int_0^{2\pi} \tilde{g}(t)\overline{L_j(t)}dt$$

and then expressing the approximate solution as a linear combination $\tilde{\psi}_n = \sum_{k=0}^{2n-1} \gamma_k L_k$ yield the Galerkin linear system

$$\sum_{k=0}^{2n-1} \gamma_k \left\{ \int_0^{2\pi} L_k(t)\overline{L_j(t)}dt - \int_0^{2\pi}\int_0^{2\pi} \tilde{K}(t,s)L_k(s)\overline{L_j(t)}dsdt \right\} = \int_0^{2\pi} \tilde{g}(t)\overline{L_j(t)}dt, \quad j = 0, ..., 2n-1.$$

For the double integral with logarithmic singularity, we use the quadrature rule (3.39) followed by the trapezoidal rule (3.27) taking doubled interpolation points as quadrature points. The rest can be evaluated with formula (3.42) and repeated trapezoidal rule.

Table 3.9. Galerkin method for equation (3.41).

	$2n$	$\|\|\tilde{\psi}_n - \tilde{\psi}\|\|_\infty$
$k = 5$	16	1.58E-01
	32	7.41E-07
	64	5.21E-14
$k = 20$	32	12.00
	64	5.27E-04
	128	4.63E-13
$k = 50$	32	78.62
	64	60.17
	128	4.46e-03

As long as the numerical quadrature formulas are available, the other methods cannot compete in efficieny with the Nyström method since Nyström's method requires the least computational effort for evaluating the matrix elements. Furthermore, the Galerkin method is less efficient than the collocation method because it requires double integration for the matrix elements while its error analysis is often more satisfactory.

In the case of three space dimensions, *boundary element method* (BEM), a combination of one of the three fundamental methods described earlier with certain subdivision of boundary surface into finite number of segments, is one of the most important numerical approximation methods. For a detailed description and a review of corresponding literature of BEM see [13]. Furthermore, *multi-grid* methods developed as a means to solve discretization of elliptic boundary value problems can also be applied to integral equations of second kind [24].

4. HIGH-FREQUENCY SCATTERING

4.1. Introduction

In this chapter, we deal with the direct obstacle scattering problem in the high-frequency regime, i.e. the wave number $k \gg 1$. With the aim of computing the scattering of plane waves by smooth convex obstacles $D \subset \mathbb{R}^2$, here we devise an algorithm based on the direct boundary integral equation method incorporating k-dependent hybrid subspaces within the Galerkin approximation. In constructing the approximation spaces, we make use of the geometrical optics ansatz

$$v(\gamma(s), k) = k \, \exp(ik\gamma(s) \cdot a) \, v^{slow}(s, k) \tag{4.1}$$

for the normal derivative v of the total field, where $\gamma(s)$ is the arc-length parametrization of ∂D, the unit vector a is the direction of the incident plane wave, and $v^{slow}(\cdot, k)$ oscillates less rapidly than $v(\cdot, k)$ for large k [25]. The asymptotic analysis as $k \to \infty$ also suggests that the boundary can be decomposed into four main regions: the illuminated region, the deep shadow region and the shadow boundaries [25] (for precise definitions see the next section). Armed with this information, our method introduces a carefully chosen refined partition comprising of $4m$ regions, $m \in \mathbb{Z}^+$, over the boundary by creating transition regions between shadow boundaries and their neighbors. The slowly varying unknown $v^{slow}(\cdot, k)$ is then approximated through the Galerkin formulation in each region by both algebraic polynomials and trigonometric polynomials. The fully rigorous error analysis based on polynomial approximation is established in [26] while the case of spectral approximation can be found in [27]. Incidentally, the refined partition will account for connecting shadow boundaries to other regions in an optimized way and the case $m = 1$ corresponds to the partition having no transition regions (a related analysis can be found in [28]).

If one searches an approximate solution via standard numerical techniques, e.g. usual boundary element methods approximating the solution v by polynomials, in

order to maintain a prescribed level of accuracy, the degrees of freedom should increase with linearly with increasing k [11]. This phenomena clearly obstructs the usage of these methods for high frequency scattering problems. Our robust numerical algorithm overcomes this type of growth in computational complexity as it requires only $\mathcal{O}(k^{\varepsilon})$, $\varepsilon > 0$, increase in the degrees of freedom to preserve a given accuracy.

The most closely related work to our method is presented in [28]. There it is considered to approximate $v^{slow}(\cdot, k)$ by polynomials utilizing the ansatz (4.1) in each of the four regions except the shadow region. Unlike the other methods [11,35,36,40–42], [28] establishes a rigorous error analysis using the asymptotic properties of the solution [25]. Concerning the approximation error, it is shown that the degrees of freedom should increase with $\mathcal{O}(k^{1/9})$ to maintain a fixed error bound with growing k. The notable weakness of the algorithm is that the shadow region approximation is totally ignored (the solution is approximated by zero there), therefore the method is not convergent for fixed k. Correspondingly, it is crucial to note that our algorithm yields upto 3 digits of accuracy (in the relative L^2 norm) in the shadow region whereas the relative error in [28] is constantly 1. All in all, major advantages of our method over [28] consist of not only a superior optimized error bound, but also accurate numerical errors and better condition numbers as demonstrated by numerical experiments (see sections 4.2.1 and 4.3.1). Hence, our robust algorithm surpasses the one in [28] regarding both theoretical and numerical aspects.

The chapter is organized as follows. Our main robust scheme including theoretical properties is presented in the next section. Then, we discuss necessary implementation issues, and with a number of examples we demonstrate the efficiency of our algorithm based on polynomial approximation. In the end, we provide a robust alternative scheme using spectral approximation with supporting numerical examples.

4.2. Main Galerkin Scheme

Recall the problem (3.20) of scattering of the incident plane waves $u^i(x)$ by the obstacle $D \subset \mathbb{R}^2$. In this chapter D is assumed to be a smooth convex domain.

The convenient boundary integral equation reformulation was for the unknown $v(x) = \partial u/\partial\nu(x)$, $x \in \partial D$, satisfying the integral equation (2.24)

$$(I + DL' - i\eta SL)v = 2\left\{\frac{\partial u^i}{\partial \nu} - i\eta u^i\right\}.$$

More abstractly, we write this equation as

$$\mathcal{A}_k v = f_k, \tag{4.2}$$

where $\mathcal{A}_k := I + DL' - i\eta SL$, $f_k := 2\{\partial u^i/\partial\nu - i\eta u^i\}$ and $\eta \in \mathbb{R}\backslash\{0\}$. The coupling parameter $\eta = k$ as before. In chapter 2, we proved that $\mathcal{A}_k : C(\partial D) \to C(\partial D)$ is bijective and has a bounded inverse when ∂D is C^2. Actually, equation (4.2) is uniquely solvable in $L^2(\partial D)$ for a general Lipschitz domain [29].

To begin with, suppose a 2π-periodic parametrization $\gamma(s)$ of the boundary ∂D that is proportional to arc-length is given. Then, using the same symbols, equation (4.2) can be rewritten as

$$\mathcal{A}_k v(s) = f_k(s), \quad s \in [0, 2\pi].$$

Hence the variational formulation is to find $v \in L^2$ such that

$$\langle \mathcal{A}_k v, w\rangle = \langle f_k, w\rangle, \quad \text{for all } \ w \in L^2. \tag{4.3}$$

The following construction is mainly based on [26]. First note that as the plane wave is impinging upon the boundary, tangency points T_1 and T_2 divide the boundary into an "illuminated region" (IL), a "shadow region" (SR) and "shadow boundaries"

(SB). Mathematically,

$$IL = \{x \in \partial D : a \cdot \nu(x) < 0\},$$
$$SR = \{x \in \partial D : a \cdot \nu(x) > 0\},$$
$$SB = \{x \in \partial D : a \cdot \nu(x) = 0\}.$$

Then, we choose the parametrization $\gamma : [0, 2\pi] \to \partial D$ such that $\gamma(0)$ lies in the deep shadow region and the tangency points $T_1 = \gamma(t_1)$, $T_2 = \gamma(t_2)$ ($t_i \in [0, 2\pi)$, $i = 1, 2$ are the preimages). Next, we select three overlapping closed subintervals $\Lambda_j \subset (0, 2\pi)$, $j = 1, 2, 3$ so that tangency point T_j lies only in $\gamma(\Lambda_j)$, $j = 1, 2$, and $\gamma(\Lambda_3)$ is contained in the illuminated region. Finally, we set $\Lambda_4 := [0, 2\pi] \setminus \cup_{j=1}^{3} \Lambda_j$ so that the shadow region contains $\gamma(\Lambda_4)$.

The above setting corresponds to the case $m = 1$ (total 4 regions: $\{\Lambda_j : j = 1, ..., 4\}$) of the subsequent $4m$ partitioning, $m \in \mathbb{Z}^+$. For $m \geq 2$, we consider the regions $\{\Lambda_j : j = 1, ..., 4\}$ are constucted as nonoverlapping and the complement of $\cup_{j=1}^{4} \Lambda_j$ is then called transition regions, Figure 4.1. In order to cover these regions, we introduce a number of $4m - 4$ closed subintervals $\{\Lambda_j \subset (0, 2\pi) : j = 5, ..., 4m\}$ such that each transition region contains $m - 1$ subregions. Note that each transtion region overlaps with its two neighbors.

To introduce a corresponding partition of unity $\{\chi_j : j = 1, ..., 4m\}$ we choose $\chi_j \in L^\infty$ (see section 4.2.1) satisfying

$$\text{supp}\chi_j = \Lambda_j, \quad 0 \leq \chi_j(s) \leq 1, \quad \left(\sum_{j=1}^{4m} \chi_j\right)(s) = 1, \quad s \in [0, 2\pi]. \tag{4.4}$$

In numerical experiments, we utilize a smooth partition of unity, and to achieve robustness sizes of Λ_j will be adapted as k increases. Note also that although we use $\{\Lambda_1, ..., \Lambda_{4m}\}$ to denote the regions, in what follows, we will use the notation Λ^{IL}, Λ^{DS}, Λ^{SB}, Λ^{TI} and Λ^{TS} for the associated regions for convenience.

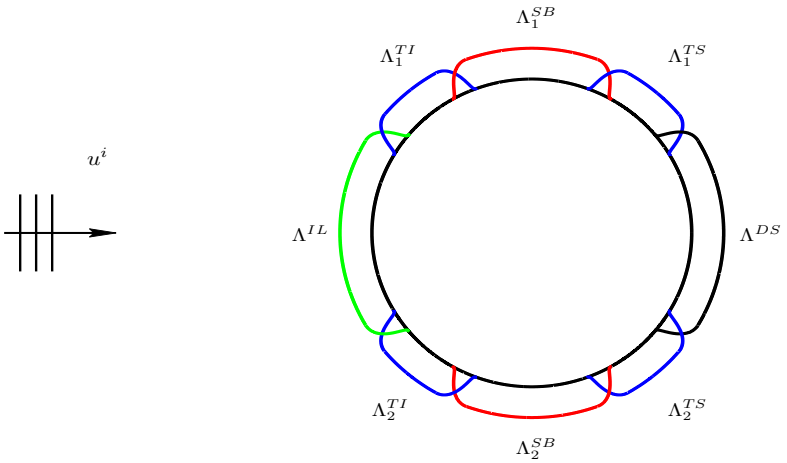

Figure 4.1. A smooth partition of unity for $m = 2$.

With the help of the ansatz (4.1), the Galerkin scheme assumes that the solution v of the integral equation $\mathcal{A}_k v = f_k$ satisfies

$$\chi_j(s)v(s) = k\ \chi_j(s)\ \exp\left(ik\gamma(s)\cdot a\right) v_j^{slow}(s,k), \quad s \in [0, 2\pi] \tag{4.5}$$

with unknowns $v_j^{slow}(s,k)$ varying more slowly than $v(s,k)$ which will be approximated. Here, $v_j^{slow}(s,k)$ is the restriction of $v^{slow}(s,k)$ on Λ_j, $j = 1, ..., 4m$.

With these settings, we construct the Galerkin scheme based upon polynomial approximation as follows. Let $\mathbb{P}_d$ denote algebraic polynomials of degree $\leq d$, $d \in \mathbb{Z}^+$. Then for each region, $j = 1, ..., 4m$, we choose integers $d_j \geq 0$ and set the finite dimensional approximation subspaces $U_j^k \subset L^2$

$$U_j^k := \text{span}\{k\,\chi_j(s)\,e^{ik\gamma(s)\cdot a}\,s^p : p = 0, ..., d_j\}. \tag{4.6}$$

Then the underlying Galerkin approximation space is

$$U_{\mathbf{d}}^k := \oplus_{j=1}^{4m} U_j^k, \qquad \text{with the dimension} \qquad \#\mathbf{d} = d_1 + ... + d_{4m} + 4m.$$

Hence, the solution v of the variational problem (4.3) is approximated by $\hat{v} \in U_{\mathbf{d}}^k$ such

that

$$\langle \mathcal{A}_k \hat{v}, \hat{w} \rangle = \langle f_k, \hat{w} \rangle, \quad \text{for all } \hat{w} \in U_{\mathbf{d}}^k. \tag{4.7}$$

For coercive problems, a standard application of the Cea's lemma, Theorem 3.29, ensures the well-posedness of both variational form (4.3) and its Galerkin approximation (4.7). Further there holds the error estimate

$$||v - \hat{v}||_{L^2} \leq \frac{\beta_k}{\alpha_k} \inf_{\hat{w} \in U_k^{\mathbf{d}}} ||v - \hat{w}||_{L^2} \tag{4.8}$$

with $v \in L^2$ and $\hat{v} \in U_k^{\mathbf{d}}$ are solutions of (4.3) and (4.7) respectively. Here β_k,α_k are the continuity and coercivity constants for the operator $\mathcal{A}_k$, respectively. Incidentally, for circular or spherical domains, coercivity and continuity of $\mathcal{A}_k$ are proved in [28, Section 4]. Also, the constant β_k/α_k depends on the integral equation and is shown to be $\mathcal{O}(k^{1/3})$ [28] . A more recent study shows that this constant is $\mathcal{O}(k^{1/2})$ for all Lipschitz star-shaped domains considering an alternative integral equation [30].

To apply the error estimate (4.8), we use (4.4) and (4.5) to write

$$v(s) = \sum_{j=1}^{4m} \chi_j(s) v(s) = k \sum_{j=1}^{4m} \chi_j(s)\, e^{ik\gamma(s)\cdot a}\, v_j^{slow}(s,k).$$

Then through the error estimate (4.8) and properties of partition of unity (4.4) we readily have the following corollary.

Corollary 4.1. *If β_k and α_k are the continuity and coercivity constants of the operator $\mathcal{A}_k$, then*

$$||v - \hat{v}||_{L^2} \leq \left(\frac{\beta_k}{\alpha_k}\right) k \left\{ \sum_{j=1}^{4m} ||e^{ik\gamma(\cdot)\cdot a}||_{L^\infty} \inf_{p \in \mathbb{P}_{d_j}} ||v_j^{slow}(\cdot,k) - p||_{L^2(\Lambda_j)} \right\}.$$

As discussed above, the constant (β_k/α_k) is shown to be of order $k^{1/3}$ and

$\exp(ik\gamma(\cdot)\cdot a)$ is a complex exponential therefore its modulus is 1. Hence, the only term we need to estimate is the best approximation error term in each region Λ_j. To this end, we state a useful proposition without a proof.

Proposition 4.2. *Given an interval $I=(a,b)$ and $n\in\mathbb{N}\cup\{0\}$, there exist C_n such that, for all nonnegative integers $n\leq d+1$*

$$\inf_{p\in\mathbb{P}_d}||f-p||_{L^2(I)}\leq C_n d^{-n}|f|_{n,I}$$

holds for all suitable functions f where the seminorm $|f|_{n,I}$ is given by

$$|f|_{n,I}:=\left[\int_a^b |f^{(n)}(s)|^2(s-a)^n(b-s)^n ds\right]^{1/2}$$

[31].

With this proposition, for each subregion, we observe that

$$\inf_{p\in\mathbb{P}_{d_j}}||v_j^{slow}(\cdot,k)-p||_{L^2(\Lambda_j)}\leq C_n d^{-n}|v_j^{slow}(\cdot,k)|_{n,\Lambda_j}. \tag{4.9}$$

Therefore, estimates for the derivatives of $v^{slow}(s,k)$ are needed. To achieve this, we make use of the following result which can be derived from the appreciated asymptotic expansion of $v^{slow}(s,k)$ in [25].

Theorem 4.3. *For all $n\in\mathbb{N}\cup\{0\}$ there exist constants $C_n>0$ independent of k and s such that for sufficiently large k,*

$$|D_s^n v^{slow}(s,k)|\leq C_n\begin{cases}1, & n=0,1,\\ 1+\sum_{j=2}^n k^{(j-1)/3}(1+k^{1/3}|w(s)|)^{-j-2}, & n\geq 2,\end{cases} \tag{4.10}$$

where $w(s)=(s-t_1)(t_2-s)$ [28].

Before giving the estimation for the error term, to obtain a robust approximation we define the intervals depending on k. Let $0\leq\varepsilon_m<\varepsilon_{m-1}<....<\varepsilon_1\leq 1/3$ for

some $m \in \mathbb{Z}^+$. Then, following [26], for sufficiently large k and some positive constants c_1, c_2, c_3, c_4 we set

- the illuminated region: $\Lambda^{IL} := [t_1 + c_1\ k^{-1/3+\varepsilon_1}, t_2 - c_2\ k^{-1/3+\varepsilon_1}]$
- the deep shadow region: $\Lambda^{DS} := [t_2 - 2\pi + c_2\, k^{-1/3+\varepsilon_1}, t_1 - c_1\, k^{-1/3+\varepsilon_1}]$
- the shadow boundaries:
  $\Lambda_1^{SB} := [t_1 - c_3\ k^{-1/3+\varepsilon_m}, t_1 + c_3\, k^{-1/3+\varepsilon_m}]$,
  $\Lambda_2^{SB} := [t_2 - c_3\,, k^{-1/3+\varepsilon_m}, t_2 + c_3\, k^{-1/3+\varepsilon_m}]$
- the transition regions from illuminated to shadow boundaries:
  $\Lambda_i^{TI} := [t_1 + c_4\, k^{-1/3+\varepsilon_{i+1}}, t_1 + c_4\, k^{-1/3+\varepsilon_i}]$, for $i = 1, ..., m-1$,
  $\Lambda_{i+m-1}^{TI} := [t_2 - c_4\, k^{-1/3+\varepsilon_i}, t_2 - c_4\, k^{-1/3+\varepsilon_{i+1}}]$, for $i = 1, ..., m-1$
- the transition regions from deep shadow to shadow boundaries:
  $\Lambda_i^{TS} := [t_1 - c_4\, k^{-1/3+\varepsilon_i}, t_1 - c_4\, k^{-1/3+\varepsilon_{i+1}}]$, for $i = 1, ..., m-1$,
  $\Lambda_{i+m-1}^{TS} := [t_2 + c_4\, k^{-1/3+\varepsilon_{i+1}}, t_2 + c_4\, k^{-1/3+\varepsilon_i}]$, for $i = 1, ..., m-1$

such that, ultimately, we have a total number of $4m$ subregions on the boundary. Notice that the shadow boundaries are formed in $\mathcal{O}(k^{-1/3})$ widths based on the analysis in [25].

This construction will enable us to handle the shadow boundaries by allowing these regions to shrink with increasing k. Also, observe that sizes of illuminated and deep shadow regions are getting larger as k increases. Thus, transition regions allow us to connect shadow boundaries to other regions in an optimal way. This k-dependent setting is crucial in achieving robustness of the numerical method. After rearranging ε_i's in an appropriate way, using equation (4.9), Corollary 4.1, Proposition 4.2 and Theorem 4.3 we finally conclude the following error estimate [26, 27].

Theorem 4.4. *Suppose that d is the maximum of degrees of polynomials to approximate $v_j^{slow}(\cdot, k)$'s. For $n \geq 2$ with $n \leq d+1$, there holds the error estimate*

$$k^{-1}||v - \hat{v}||_{L^2} \leq C_n k^{-1/6} \left(\frac{k^{1/(6m+3)}}{d} \right)^n \tag{4.11}$$

for some constant $C_n > 0$ independent of k.

From the error estimate (4.11), we deduce that in order to maintain a fixed accuracy as $k \to \infty$, d has to increase very mildly provided m is chosen sufficiently large, i.e. $d \sim k^{\varepsilon}$, for any $\epsilon > 0$.

Since the solution v depends on k, rather than controlling the error term $||v-\hat{v}||_{L^2}$ it would be more plausible to control the relative error $||v-\hat{v}||_{L^2}/||v||_{L^2}$. For smooth convex obstacles, it is well-known that via Kirckhoff approximation, [25], $v \approx 0$ on the shadow side and $v \approx 2\ \partial u^i/\partial\nu$ on the lit side. Therefore, in the illuminated region $||v||_{L^2}$ grows proportional to $||\partial u^i/\partial\nu||_{L^2} = \mathcal{O}(k)$ as $k \to \infty$ thus the form $k^{-1}||v-\hat{v}||_{L^2}$ eliminates the k-dependency in the error. However, this form obviously does not capture the deep shadow errors correctly therefore the relative error will be a more reliable measure in numerical experiments.

4.2.1. Numerical Implementation

In this section we discuss the implementation issues and exhibit errors in different scenarios.

Smooth partition unity is constructed in terms of the bump function

$$\chi(x) = \frac{1}{2}\left[\varphi(x) + 1 - \varphi(1-x)\right],$$

where

$$\varphi(x) = \begin{cases} 1, & x \le 0, \\ \exp\left(\dfrac{2\exp\left(-\dfrac{1}{x}\right)}{x-1}\right), & 0 < x < 1, \\ 0, & 1 \le x, \end{cases}$$

which provides a smooth transition between the constant functions 1 and 0 [11].

Considering the affine maps on an interval $[a, b]$

- $\phi_l : [a, b] \to [0, 1] : x \to \dfrac{x - a}{b - a}$
- $\phi_r : [a, b] \to [0, 1] : x \to \dfrac{x - b}{a - b}$

we define the 'left looking' semi-bump function on $[a, b]$, namely $\varphi_l : [a, b] \to \mathbb{R}$ by

$$\varphi_l(x) := \varphi(\phi_l(x; a, b))$$

and the 'right looking' semi-bump function on $[a, b]$, namely $\varphi_r : [a, b] \to \mathbb{R}$ by

$$\varphi_r(x) := \varphi(\phi_r(x; a, b)).$$

Then on an interval $[\alpha, \beta] \subset [0, 2\pi]$ containing a proper subset $[\alpha', \beta']$ we use the left looking semi-bump function $\chi_{\alpha\alpha'} = \varphi(\phi_l(x; \alpha, \alpha'))$ on $[\alpha, \alpha']$ and the right looking semi-bump function $\chi_{\beta'\beta} = \varphi(\phi_r(x; \beta', \beta))$ on $[\beta', \beta]$ so that the cut-off function on $[\alpha, \beta]$ becomes

$$\chi_{\alpha\beta} = \chi_{\alpha\alpha'}\chi_{\beta'\beta}.$$

Note that the subintervals $[\alpha, \alpha']$ and $[\beta', \beta]$ will correspond to the overlapping parts between approximation regions.

When basis functions (4.6) are used in numerical experiments, the norms of the columns of the Galerkin matrix vary significantly in magnitude due the growth of polynomials resulting in a highly ill-conditioned matrix. Therefore, to obtain a similar scale between basis functions (for numerical stability), we consider the finite dimensional ap-

proximation subspaces U_j^k (4.6) with normalized basis functions:

$$U_j^k = \text{span}\{B_{pj}(s,k)/||B_{pj}(s,k)||_{L^2} : p = 0, ..., d_j\},$$

where $B_{pj}(s,k) := k\,\chi_j(s)\,e^{ik\gamma(s)\cdot a}\,s^p$. Even further, on each interval $[\alpha,\beta]$ we shift the basis functions by $\frac{\alpha+\beta}{2}$ before evaluating. A diagonal preconditioner whose diagonal entries comprise of maximum norms of columns of the Galerkin matrix is applied to the linear system. For numerical discretization of integrals we utilize combinations of quadrature rules (3.39) and (3.27) with sufficiently high quadrature points.

Throughout this chapter, we test our method for the unit circle taking the direction of incidence as $a = (1, 0)$.

Example 4.5. For this example, we take $m = 1$ so that the corresponding 4 regions are

- *the shadow boundaries:*
  $\Lambda_1^{SB} = \big[t_1 - \pi\,k^{-1/3+\varepsilon},\, t_1 + 7\pi/15\,k^{-1/3+\varepsilon}\big]$,
  $\Lambda_2^{SB} = \big[t_2 - 7\pi/15\,k^{-1/3+\varepsilon},\, t_2 + \pi\,k^{-1/3+\varepsilon}\big]$
- *the illuminated region:* $\Lambda^{IL} = \big[t_1 + \pi/5\,k^{-1/3+\varepsilon},\, t_2 - \pi/5\,k^{-1/3+\varepsilon}\big]$,
- *the deep shadow region:* $\Lambda^{DS} = \big[0, t_1 - 2\pi/3\,k^{-1/3+\varepsilon}] \cup [t_2 + 2\pi/3\,k^{-1/3+\varepsilon}, 2\pi\big]$,

with $t_1 = \pi/2$, $t_2 = 3\pi/2$ and $\varepsilon = 1/9$. Contrary to [28], we also approximate the solution in the deep shadow by polynomials. As we will compare shadow region errors (see the next example), the generic quadruple of degrees of freedom is taken as $\mathbf{d} = (d, d, d, 2d + 1)$ yielding $\#\mathbf{d} = 5d + 5$ where the last item corresponds to the deep shadow region. In experiments, we set d as multiples of 4 upto 20. Numerical results are presented in the figure below for $k = 50, 100, 200, 400$ and 800. Note that x-axes correspond to the total degrees of freedom.

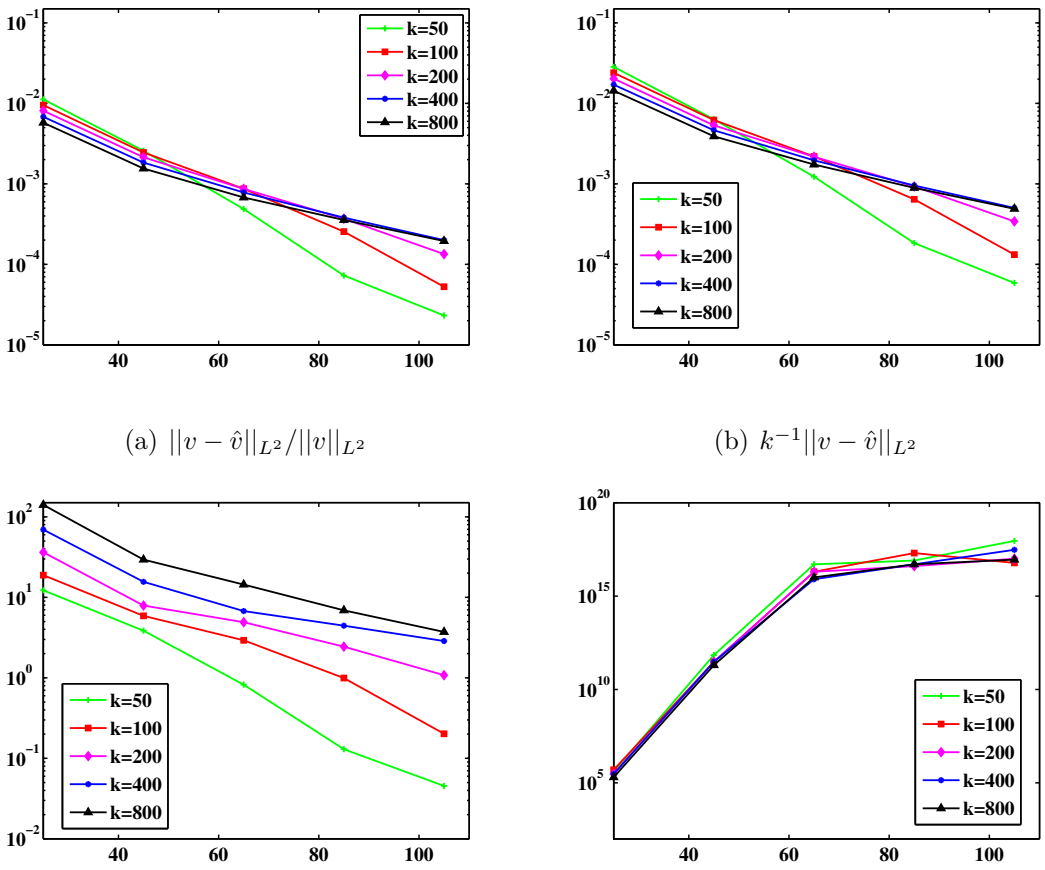

(a) $||v-\hat{v}||_{L^2}/||v||_{L^2}$ (b) $k^{-1}||v-\hat{v}||_{L^2}$

(c) Relative errors on Λ^{DS} (d) Condition numbers

Figure 4.2. Results using 4 regions with normalized basis functions.

Example 4.6. It is important to observe the deep shadow errors in the previous example achieve only 10^{-1} (at best) accuracy although we used doubled degrees of freedom compared to other regions, Figure 4.3 (c). This consideration leads to the idea that the accuracy in the shadow region does not only depend on the degrees of freedom but also on the structure of the partition of unity. In this connection, under the same construction we split the deep shadow region into two overlapping pieces by setting:

- *deep shadow regions:*

  $\Lambda_1^{DS} := [0, t_1 - 2\pi/3\, k^{-1/3+\varepsilon}] \cup [t_2 + 8\pi/7\, k^{-1/3+\varepsilon}, 2\pi]$

  $\Lambda_2^{DS} := [t_2 + 2\pi/3\, k^{-1/3+\varepsilon}, 2\pi] \cup [0, t_1 - 8\pi/7\, k^{-1/3+\varepsilon}].$

Also, the quintuple of degrees of freedom is taken as $\mathbf{d} = (d, d, d, d, d)$ giving $\#\mathbf{d} = 5d + 5$. Thus the total dimension on the shadow region $\Lambda_1^{DS} \cup \Lambda_2^{DS}$ is $2d + 2$ as in the

previous example.

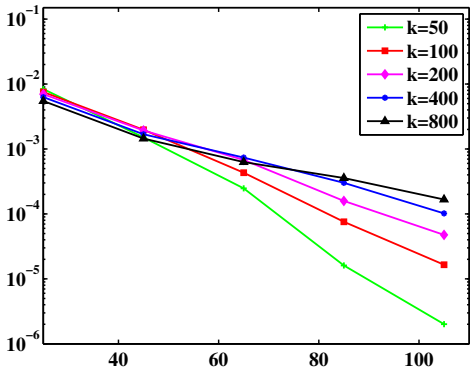

(a) $||v - \hat{v}||_{L^2}/||v||_{L^2}$

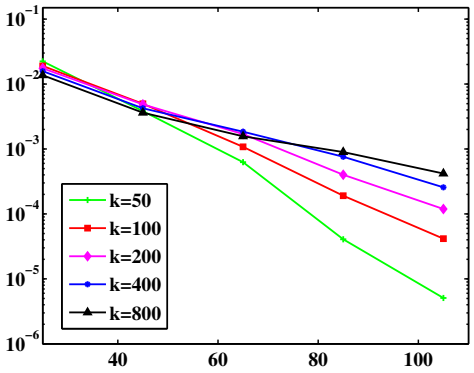

(b) $k^{-1}||v - \hat{v}||_{L^2}$

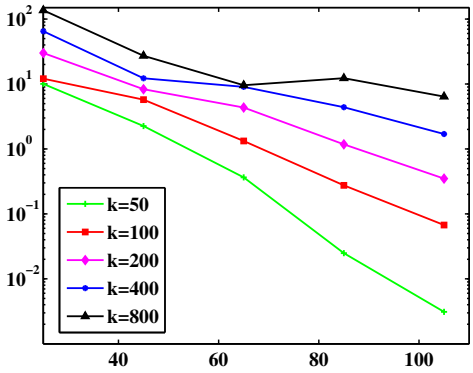

(c) Relative errors on $\Lambda_1^{DS} \cup \Lambda_2^{DS}$

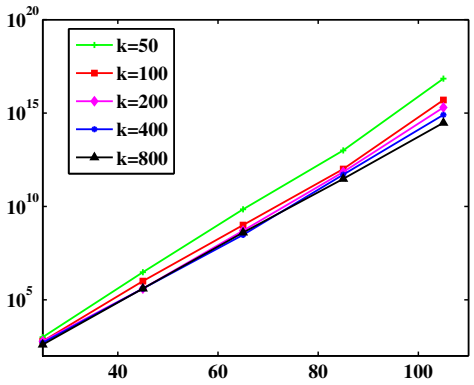

(d) Condition numbers

Figure 4.3. Results using 5 regions with normalized basis functions.

Note that separating shadow region into two gives slightly better accuracy (for moderate values of k) in the shadow errors even though the dimension remains the same. This behavior might be explained as each grazing ray gives rise to a surface diffracted ray ("creeping wave") which begins at the points of tangency, and travels on the boundary along a geodesic [32]. Thus, splitting the shadow region accounts for a better realization of behaviors of these diffracted rays (see also example 4.12). Indeed, the alternative approach utilized in the next example clarifies this discussion thoroughly.

Example 4.7. Strengthening the partition of unity, we take $m = 2$, total 8 regions over the boundary of the unit circle, and set $\varepsilon_1 = 1/5$, $\varepsilon_2 = 1/15$ with

- *the illuminated region:* $\Lambda^{IL} := [t_1 + \pi/2\, k^{-1/3+\varepsilon_1}, t_2 - \pi/2\, k^{-1/3+\varepsilon_1}]$
- *the deep shadow region:* $\Lambda^{DS} := [0, t_1 - 3\pi/5\, k^{-1/3+\varepsilon_1}] \cup [t_2 + 3\pi/5\, k^{-1/3+\varepsilon_1}, 2\pi]$
- *the shadow boundaries:*

  $\Lambda_1^{SB} := [t_1 - 14\pi/15\, k^{-1/3+\varepsilon_2}, t_1 + 7\pi/15\, k^{-1/3+\varepsilon_2}]$,

  $\Lambda_2^{SB} := [t_2 - 7\pi/15\, k^{-1/3+\varepsilon_2}, t_2 + 14\pi/15\, k^{-1/3+\varepsilon_2}]$
- *the transition regions from illuminated to shadow boundaries:*

  $\Lambda_1^{TI} := [t_1 + 2\pi/15\, k^{-1/3+\varepsilon_2}, t_1 + 7\pi/10\, k^{-1/3+\varepsilon_1}]$,

  $\Lambda_2^{TI} := [t_2 - 7\pi/10\, k^{-1/3+\varepsilon_1}, t_2 - 2\pi/15\, k^{-1/3+\varepsilon_2}]$,
- *the transition regions from deep shadow to shadow boundaries:*

  $\Lambda_1^{TS} := [t_1 - 4\pi/5\, k^{-1/3+\varepsilon_1}, t_1 - 3\pi/5\, k^{-1/3+\varepsilon_2}]$,

  $\Lambda_2^{TS} := [t_2 + 3\pi/5\, k^{-1/3+\varepsilon_2}, t_2 + 4\pi/5\, k^{-1/3+\varepsilon_1}]$.

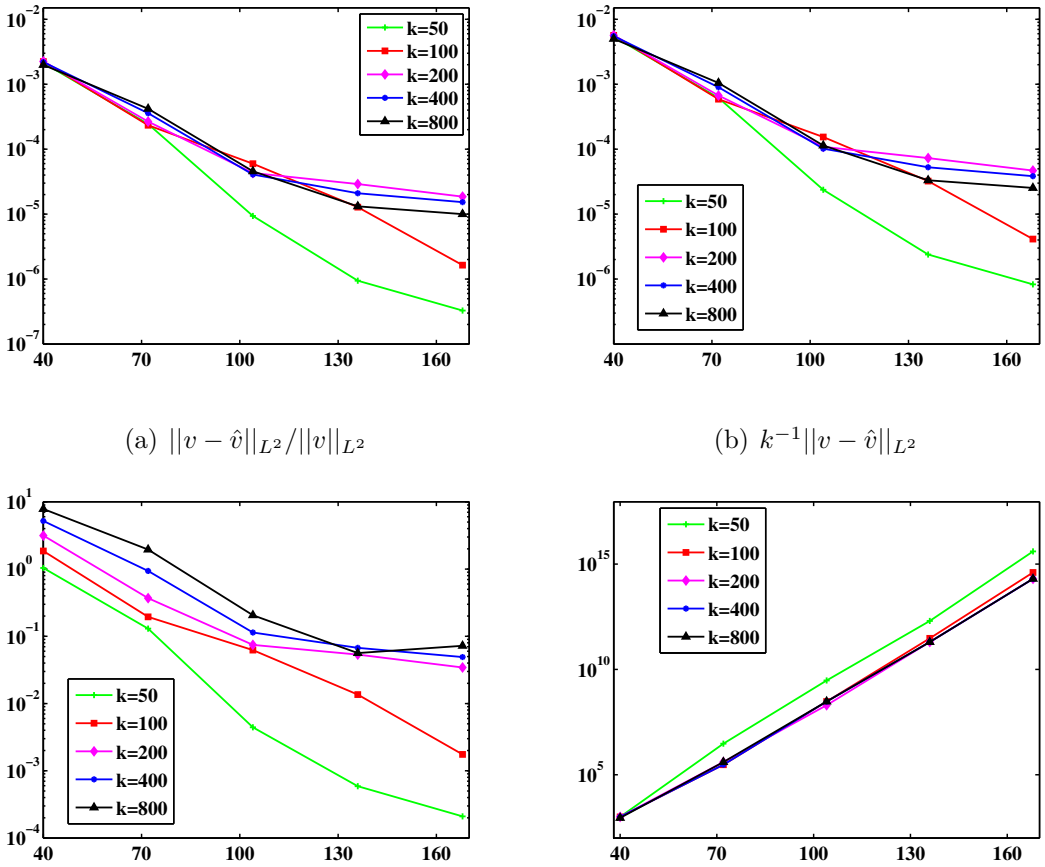

(a) $||v - \hat{v}||_{L^2}/||v||_{L^2}$ (b) $k^{-1}||v - \hat{v}||_{L^2}$

(c) Relative errors on $\Lambda_1^{TS} \cup \Lambda_2^{TS} \cup \Lambda^{DS}$ (d) Condition numbers

Figure 4.4. Results using 8 regions with normalized basis functions.

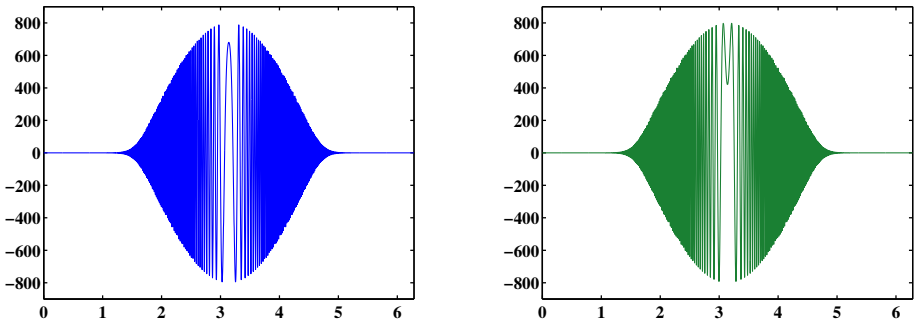

(a) Real part of $v(\cdot, 400)$

(b) Imaginary part of $v(\cdot, 400)$

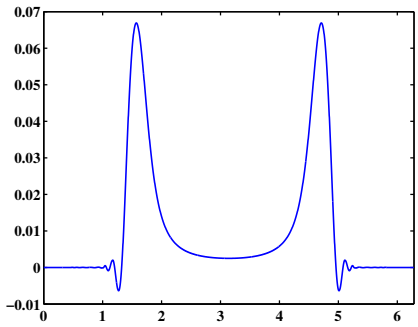

(c) Real part of $v^{slow}(\cdot, 400)$

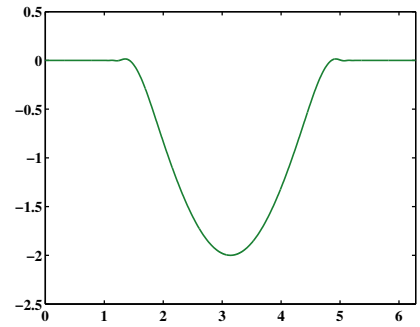

(d) Imaginary part of $v^{slow}(\cdot, 400)$

Figure 4.5. Computed approximations for $v(\cdot, 400)$ & $v^{slow}(\cdot, 400)$.

Comparing Figures 4.3 and 4.4 for similar degrees of freedom, we observe that resulting condition numbers and errors are slightly better. More importantly, approximation errors in the shadow region errors are substantially (at least one digit) improved due to the structured partitioning.

It is crucial to note that the robustness of the algorithm depends heavily on the choice of the constants used in constructing the regions.

Example 4.8. Next, we apply the algorithm of [28] (where it is proven that to fix the accuracy of this method, the degrees of freedom should be increased in proportion to $k^{1/9}$). To this end, the solution v (Proposition C.2) is approximated by zero in the shadow region and the basis

$$\{k\,\chi_j(s)\,e^{ik\gamma(s)\cdot a}\,s^p : p = 0, ..., d_j\}, \qquad j = 1, 2, 3, \tag{4.12}$$

is used on the 3 overlapping regions

- *the shadow boundaries:*
  $\Lambda_1^{SB} = \left[t_1 - 7\pi/5\, k^{-1/3+\delta},\, t_1 + 7\pi/15\, k^{-1/3+\varepsilon}\right]$,
  $\Lambda_2^{SB} = \left[t_2 - 7\pi/15\, k^{-1/3+\varepsilon},\, t_2 + 7\pi/5\, k^{-1/3+\delta}\right]$
- *the illuminated region:* $\Lambda^{IL} = \left[t_1 + \pi/5\, k^{-1/3+\varepsilon},\, t_2 - \pi/5\, k^{-1/3+\varepsilon}\right]$,

where $\varepsilon = 1/9$ and $\delta = 0$ [28].

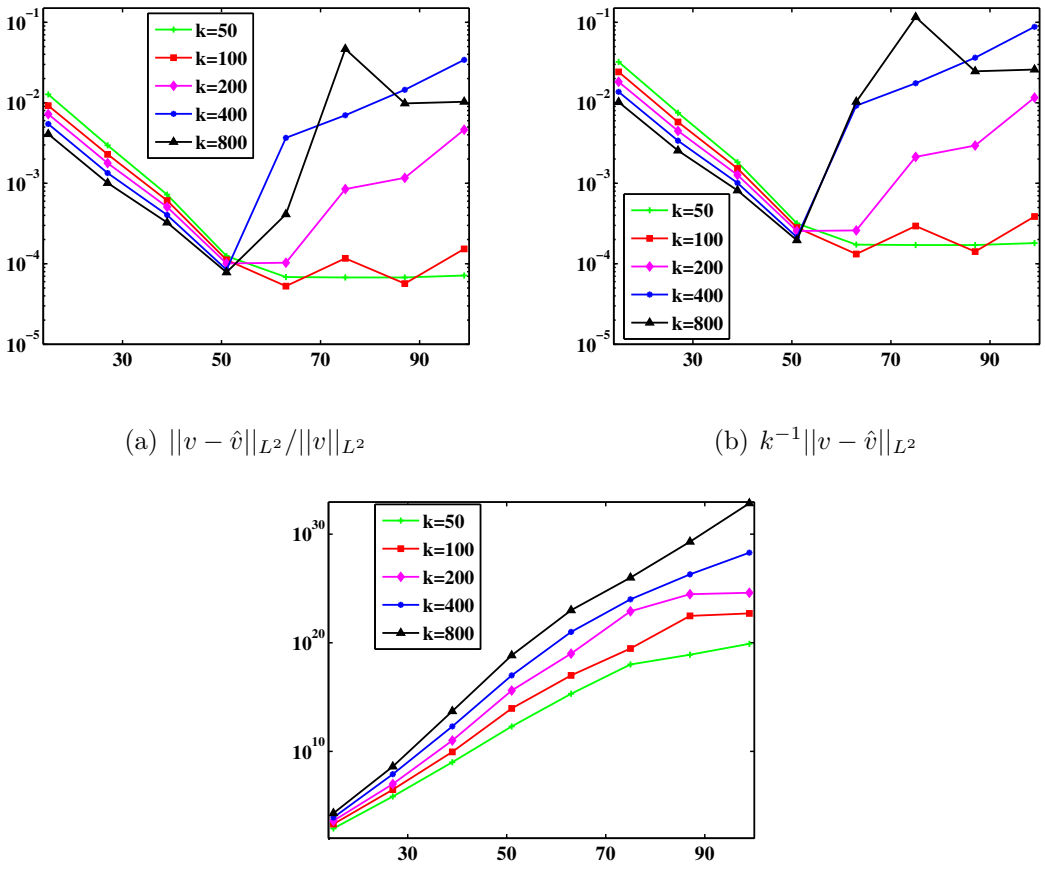

(a) $||v - \hat{v}||_{L^2}/||v||_{L^2}$

(b) $k^{-1}||v - \hat{v}||_{L^2}$

(c) Condition numbers

Figure 4.6. Results using the construction in [28].

From Figure 4.6, it can be observed that the condition numbers are extremely high with growing d, therefore the approximation utilizing $\#\mathbf{d} \geq 51$ is considerably inaccurate. As we compare Figure 4.4 with Figure 4.7 for a fixed k and similar degrees of freedom (e.g. compare $\#\mathbf{d} = 75$ with $\#\mathbf{d} = 72$ of example 4.7), we see that condition

numbers are approximately squared due to the weak structured partition of unity. Also, comparison indicates that in some cases, our algorithm (e.g. $m = 2$) achieves one/two digit better accuracy than [28].

Example 4.9. Under the same setting of the previous example, to get better numerical results, we exercise normalized versions of the basis (4.12) considered in [28].

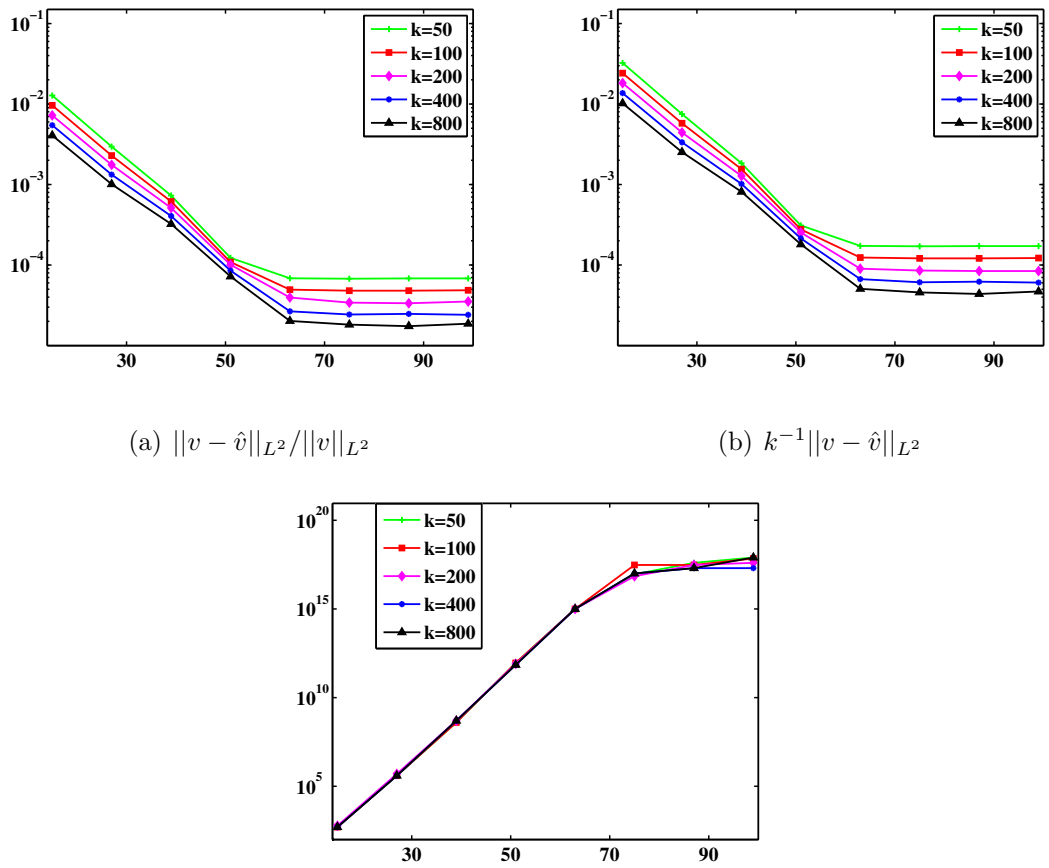

(a) $||v - \hat{v}||_{L^2}/||v||_{L^2}$ (b) $k^{-1}||v - \hat{v}||_{L^2}$

(c) Condition numbers

Figure 4.7. Results using 3 regions with normalized basis functions.

From the previous figure we observe that for a fixed k the error decreases quickly until it stagnates. Also, notice that condition numbers are better behaved than the previous example although they are still larger than condition numbers produced by our algorithm (see Figures 4.7, 4.6, 4.4). Therefore, even this modified version can not beat our algorithm regarding entailed errors and condition numbers.

While comparing our algorithm with the algorithm of [28], one should keep in

mind that our setting is a fully convergent scheme whereas the other is not.

4.3. Yet An Alternative Convergent Scheme

From the empirical results of the previous section, we deduce that condition numbers of the Galerkin linear system become larger with increasing k and increasing degrees of freedom, and eventually exceed the limit of computational framework. Undoubtedly, (clever) choice of the basis functions plays a crucial role in the structure of the linear system. In this connection, we next propose a different approach for choosing the approximation spaces.

Due to the robust theoretical and computational properties of the refined partition, we utilize $4m$ partitioning of the boundary. Denoting by $\mathbb{T}_d$ the trigonometric polynomials of degree $\leq d$, for $d \in \mathbb{Z}^+$ and armed with the corresponding partition of unity, the ansatz (4.1) and chosen even integers $d_j \geq 0$, $j = 1, ..., 4m$, for each region $[\alpha, \beta] \subset [0, 2\pi]$ we define the finite dimensional approximation subspaces $Y_j^k \subset L^2$ as

$$Y_j^k := \text{span}\left\{ k\,\chi_j(s)\, e^{ik\gamma(s)\cdot a} \exp\left(ip\,\pi\left(2\,\frac{s-\alpha}{\beta-\alpha}\right)\right) \,:\, p = -\frac{d_j}{2}, ..., \frac{d_j}{2}\right\}. \tag{4.13}$$

The form of the argument of the exponential in (4.13) is a necessary implication of the following best approximation theorem.

Theorem 4.10. *Let $d \in \mathbb{N}$, and assume that the periodic function f of period $\beta - \alpha$ possesses $(n-1)^{th}$ absolutely continuous derivative and a derivative $f^{(n)}$ of order n belongs to $L^2[\alpha, \beta]$ for some nonnegative integer $n < d$. Then,*

$$\inf_{p \in \mathbb{T}_{d-1}} ||f - p||_{L^2} \lesssim_n \left(\frac{\beta-\alpha}{d}\right)^n \tilde{\omega}\left(f^{(n)}, \frac{\beta-\alpha}{2\pi d}\right)_{L^2},$$

where the integral modulus of smoothness

$$\tilde{\omega}(f,t)_{L^2} = \sup_{|h|\leq t} \left\{ \int_{\alpha}^{\beta} |f(x+h) - f(x)|^2 dx \right\}^{1/2}$$

[33].

Using this theorem and derivative estimates (4.10) for $v^{slow}(\cdot, k)$ with the definition of regions in an analogous version of Corollary (4.1) will yield the error bounds for this setting. This is the subject of ongoing work [27].

4.3.1. Numerical Experiments

Example 4.11. Our setting for this example is as follows. Since the transition regions in the shadow do not improve upon the theoretical error bound [27], here we use 6 regions over the boundary of the unit circle:

- *the illuminated region:* $\Lambda^{IL} := [t_1 + \pi/2\, k^{-1/3+\varepsilon_1}, t_2 - \pi/2\, k^{-1/3+\varepsilon_1}]$
- *the deep shadow region:* $\Lambda^{DS} := [0, t_1 - 3\pi/5\, k^{-1/3+\varepsilon_2}] \cup [t_2 + 3\pi/5\, k^{-1/3+\varepsilon_2}, 2\pi]$
- *the shadow boundaries:*
  $\Lambda_1^{SB} := [t_1 - 14\pi/15\, k^{-1/3+\varepsilon_2}, t_1 + 7\pi/15\, k^{-1/3+\varepsilon_2}]$,
  $\Lambda_2^{SB} := [t_2 - 7\pi/15\, k^{-1/3+\varepsilon_2}, t_2 + 14\pi/15\, k^{-1/3+\varepsilon_2}]$
- *the transition regions from illuminated to shadow boundaries:*
  $\Lambda_1^{TI} := [t_1 + 2\pi/15\, k^{-1/3+\varepsilon_2}, t_1 + 7\pi/10\, k^{-1/3+\varepsilon_1}]$,
  $\Lambda_2^{TI} := [t_2 - 7\pi/10\, k^{-1/3+\varepsilon_1}, t_2 - 2\pi/15\, k^{-1/3+\varepsilon_2}]$,

where $\varepsilon_1 = 1/5$, $\varepsilon_2 = 1/15$ and $t_1 = \pi/2$, $t_2 = 3\pi/2$. Notice that here we do not utilize transition regions from deep shadow region to shadow boundaries and unlike before the deep shadow region is constructed using ε_2.

As we shall compare the shadow region errors later on, here the generic sextuple of degrees of freedom is taken as $\mathbf{d} = (d, d, d, d, d, 2d+1)$ where the last item corresponds

to the deep shadow region yielding $\#\mathbf{d} = 7d + 7$. In our experiments, we take d as multiples of 4 upto 32.

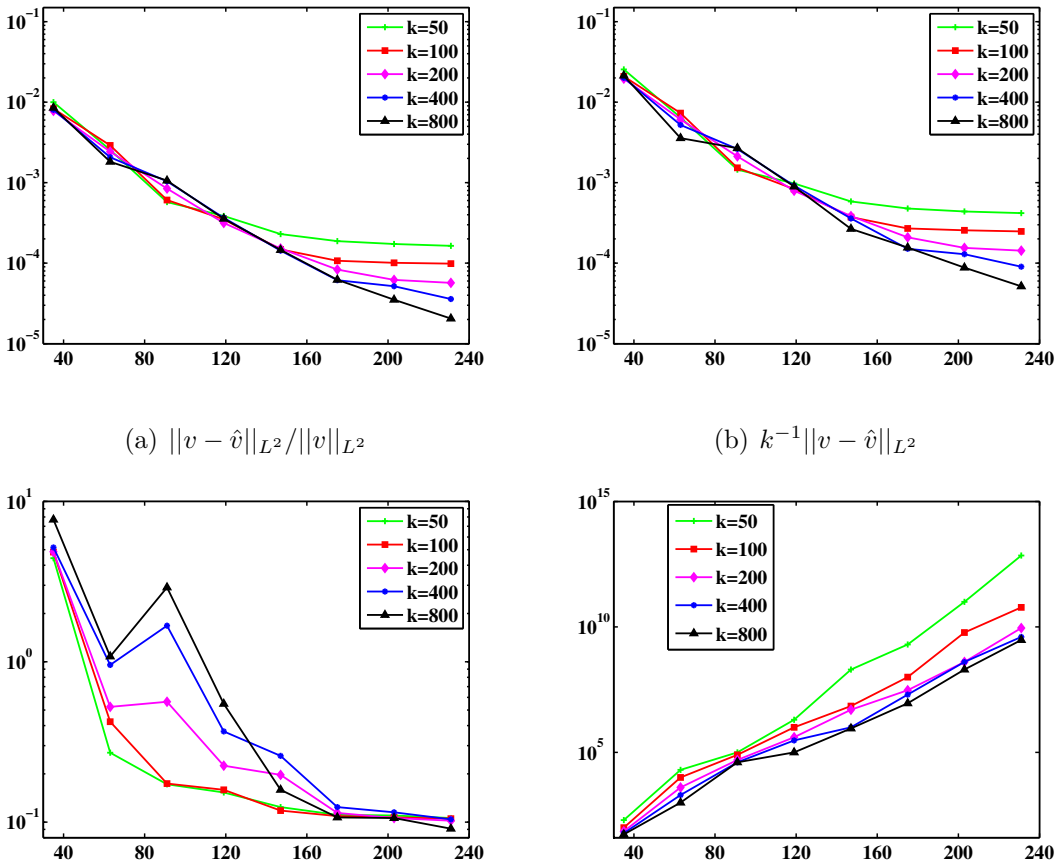

(a) $||v - \hat{v}||_{L^2}/||v||_{L^2}$

(b) $k^{-1}||v - \hat{v}||_{L^2}$

(c) Relative errors on Λ^{DS}

(d) Condition numbers

Figure 4.8. Results using 6 regions with exponentials.

The first important consequence of this example is that employing spectral approximation entails smaller condition numbers (reduced to square roots approximately) than polynomial approximation as expected (see Figures 4.8 and 4.4). Thus we can further increase the degrees of freedom without a significant loss of accuracy. Also note that the polynomial approximation error achieves better accuracy compared to this example, however, we will retain this accuracy also in spectral approximation in the following examples.

Example 4.12. Under the same setting of the previous example, as in example 4.6, using the old trick we split the deep shadow region:

- *deep shadow regions:*

  $\Lambda_1^{DS} := [0, t_1 - 3\pi/5\, k^{-1/3+\varepsilon_2}] \cup [t_2 + 2\pi/3\, k^{-1/3+\varepsilon_1}, 2\pi]$

  $\Lambda_2^{DS} := [t_2 + 3\pi/5\, k^{-1/3+\varepsilon_2}, 2\pi] \cup [0, t_1 - 2\pi/3\, k^{-1/3+\varepsilon_1}].$

The generic sextuple of degrees of freedom is taken as $\mathbf{d} = (d, d, d, d, d, d, d)$ so that $\#\mathbf{d} = 7d + 7$.

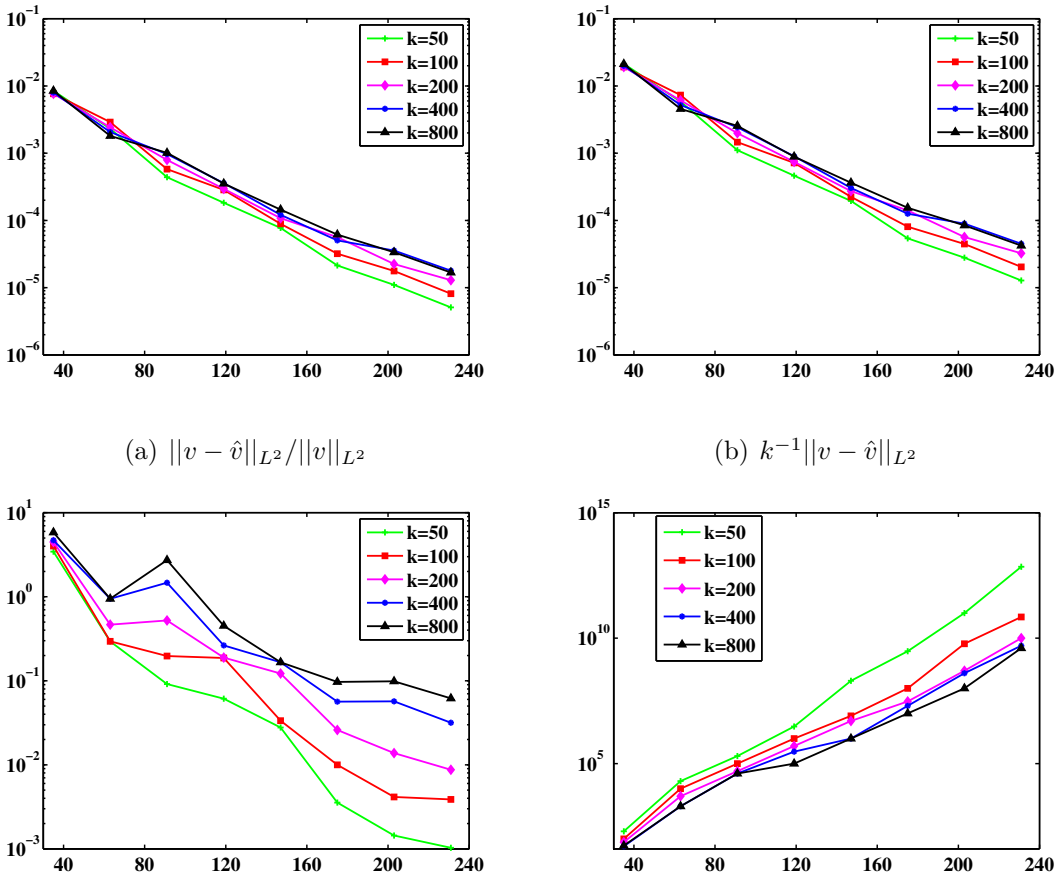

(a) $||v - \hat{v}||_{L^2}/||v||_{L^2}$ (b) $k^{-1}||v - \hat{v}||_{L^2}$

(c) Relative errors on $\Lambda_1^{DS} \cup \Lambda_2^{DS}$ (d) Condition numbers

Figure 4.9. Results using 7 regions with exponentials.

Comparing Figures 4.9 and 4.8, we see that both global and shadow region errors are significantly improved supporting the aforementioned argument about capturing the behaivor of creeping waves. The modification engenders upto 3 digits accurate shadow region errors although the dimension remains the same.

Example 4.13. In this example, using the same partition of unity of the previous

example we consider slightly different approximation spaces

$$\text{span}\left\{k\,\chi_j(s)\,e^{ik\gamma(s)\cdot a}\cos\left(p\,\pi\left(\frac{s-\alpha}{\beta-\alpha}\right)\right)\,:\,p=0,...,d_j\right\},$$

utilizing cosines instead of exponentials.

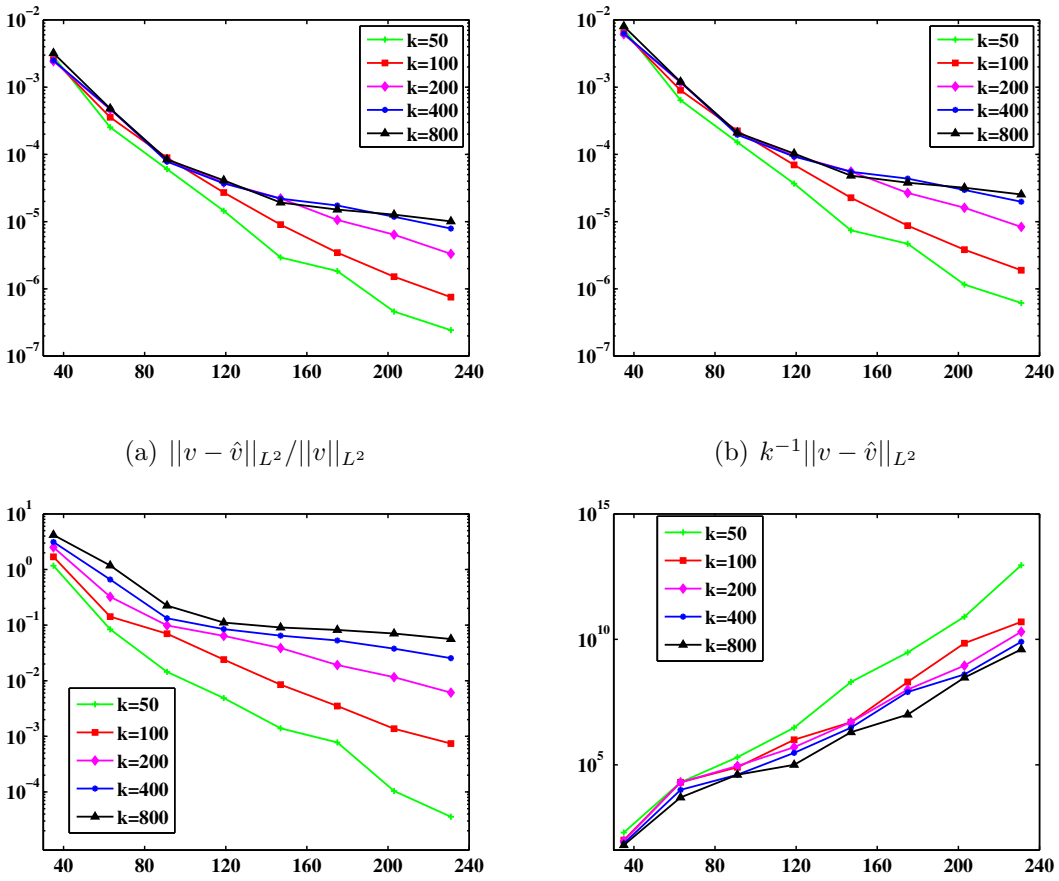

(a) $||v-\hat{v}||_{L^2}/||v||_{L^2}$ (b) $k^{-1}||v-\hat{v}||_{L^2}$

(c) Relative errors on $\Lambda_1^{DS}\cup\Lambda_2^{DS}$ (d) Condition numbers

Figure 4.10. Results using 7 regions with cosines.

From Figure 4.10, we observe that the cosine basis achieves slightly better errors than the exponential basis while resulting condition numbers are very similar. Compared to polynomial basis (Figure 4.4), condition numbers are far better and the similar error behavior retained. For moderate values of k, the shadow error is also improved. We finally note that the resulting errors of exponentials can be brought to the level of errors of this example by utilizing first small degree polynomials and then usual exponentials in the approximation successively.

Example 4.14. For a final example, we exercise all bases and report numerical results for $k = 400$ in the figure below.

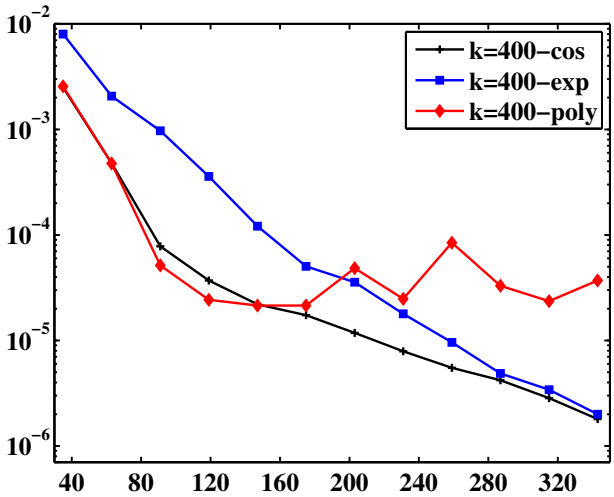

Figure 4.11. Relative errors using 7 regions with all basis functions.

It is clear that the polynomial basis stagnates and then oscillates from a certain point on whereas the other bases still preserve their accuracy upto the degrees of freedom considered.

5. Conclusion and Outlook

In this work, our main focus was to develop a robust algorithm for the problem of high frequency scattering by convex obstacles. To this end, we have considered boundary integral equation representations and studied numerical methods for integral equations of the second kind in a general framework.

In chapter two, Green's representation theorems for the solutions of the Helmholtz equation have been studied. Defining surface potentials and investigating their jump relations on the boundary, we deduced that solving the direct obstacle scattering problem, a special form of the exterior Dirichlet problem, is equivalent to finding solutions of the boundary integral equations (2.21) and (2.24). With the help of boundary integral equations, we proved the well-posedness of the exterior Dirichlet problem. It is important to note that combined field approach is preferred due to its invertibility for all wave numbers.

After casting the direct scattering problem into integral equations, we proceeded to investigate numerical methods for the integral equations of the second kind. In this context, we have considered three fundamental numerical methods; the Nyström method, the collocation method and the Galerkin method. Using the knowledge about operator approximations and interpolation/approximation theory, we established convergence results and error estimates for these methods under different assumptions. Regarding numerical experiments, we have discussed necessary implementation details and have tested the convergence orders of the methods by considering different scenarios.

In chapter four, we dealt with the direct obstacle scattering in high frequency regime. Armed with the knowledge from asymptotic analysis, we utilized wave number dependent hybrid approximation spaces to construct our convergent Galerkin-based numerical method. The convergence result, Theorem 4.4, provided us the flexibility to choose the number of regions sufficiently large to maintain a prescribed level of

accuracy with a very mild increase in the degrees of freedom. In addition, it has been numerically shown that the structure of the partition of unity is crucial for the numerical error and the condition number of the linear system. Yet an alternative scheme, using trigonometric polynomials instead of algebraic ones, was proposed at the end to remedy the emerging inaccuracy resulting from high condition numbers.

Throughout chapter 4, regarding the assembly of the Galerkin matrix, we are not interested in the efficient evaluation of high oscillatory integrals and used quadrature methods which are not k robust. For efficient oscillatory integration procedures we refer to [11, 34–37].

In all numerical experiments, we utilized the software MATLAB on a machine with an Intel (2.66 GHz) CPU. All MATLAB codes are written in a highly vectorized fashion. Moreover, in high frequency scenarios, we exploit the properties of the partition on unity to reduce the number of quadrature points for the numerical integration and use a naive parallelization concerning the assembly of the Galerkin matrix.

Future work could include incorporating efficient high oscillatory integration procedures to achieve better accuracy and efficiency in the numerical results. In addition, more sophisticated parallelization and preconditioning techniques can be used for assembling and solving the linear system. More importantly, the main subject of the ongoing work is the convergence analysis of the algorithm described in section 4.3 [27].

APPENDIX A: Integral Equations

The most basic types of integral equations are Fredholm equation of the first kind:

$$\int_D K(x,y)\,\varphi(y)\,dy = f(x), \quad x \in D,$$

and Fredholm equation of the second kind:

$$\varphi(x) - \int_D K(x,y)\,\varphi(y)\,dy = f(x), \quad x \in D.$$

In these equations the function φ is the unknown, and the kernel K and the right-hand side f are given functions. We regard them as operator equations $A\varphi = f$ and $\varphi - A\varphi = f$, respectively.

Definition A.0.1. *Let D be a nonempty compact subset of $\mathbb{R}^n$. The kernel K is said to be* weakly singular *provided it is defined and continuous for all $x, y \in D$, $x \neq y$, and there exists positive constants C and $\beta \in (0, n]$ such that*

$$|K(x,y)| \leq C|x-y|^{\beta-n}, \quad x, y \in D,\ x \neq y.$$

Correspondinly, suppose that the integral operator A is defined on $C(\partial D)$ then its kernel K is called weakly singular *if it is defined and continuous for all $x, y \in \partial D$, $x \neq y$, and there exists positive constants C and $\beta \in (0, n-1]$ such that*

$$|K(x,y)| \leq C|x-y|^{\beta-n+1}, \quad x, y \in \partial D,\ x \neq y.$$

Definition A.0.2. *A bounded linear operator $A : X \to Y$ from a normed space X into a normed space Y is called compact if it maps every bounded set in X to a relatively compact (precompact) set in Y.*

Theorem A.1. *Let $A : X \to X$ be a compact operator on a normed space X. Then $I - A$ is injective if and only if it is surjective. In such a case, the inverse operator $(I - A)^{-1} : X \to X$ is bounded* Fredholm Alternative [13].

Theorem A.2. (Neumann Series) *Let $A : X \to X$ be a bounded linear operator on a Banach space X with $||A|| < 1$. Then $I - A$ has a bounded inverse given by the series $(I - A)^{-1} = \sum_{k=0}^{\infty} A^k$* [5].

Theorem A.3. (Arzela-Ascoli) *Let $D \subset \mathbb{R}^n$ be a compact set. A set $U \subset C(D)$ is relatively compact if and only if it is bounded and equicontinuous* [5].

APPENDIX B: Function spaces

Definition B.0.3. *A function g defined on a domain $D \subset \mathbb{R}^n$ is said to be Hölder continuous with exponent $0 < \alpha \leq 1$ provided*

$$|g(x) - g(y)| \leq C|x - y|^\alpha, \quad x, y \in D$$

for some constant $C > 0$. The Hölder space $C^{0,\alpha}(D)$ is the space of all functions for which the norm

$$||g||_{0,\alpha} = ||g||_\infty + \sup_{\substack{x,y \in D \\ x \neq y}} \frac{|g(x) - g(y)|}{|x - y|^\alpha}$$

is finite. Similarly, $C^{1,\alpha}(D)$ is endowed with the norm

$$||g||_{1,\alpha} := ||g||_\infty + ||\nabla g||_{0,\alpha}.$$

For $m \in \mathbb{N}$, $C^{m,\alpha}(D)$ denotes the m-times Hölder continuously differentiable functions and $C_p^{m,\alpha}(2\pi)$ is the corresponding 2π-periodic $C^{m,\alpha}$ functions.

Theorem B.1. *Let $0 < \alpha < \beta \leq 1$ and D be compact. Then the embeddings $I^\beta : C^{0,\beta}(D) \to C(D)$ and $I^{\alpha,\beta} : C^{0,\beta}(D) \to C^{0,\alpha}(D)$ are compact* [5].

Definition B.0.4. *Let $0 \leq p < \infty$, then by $H^p[0, 2\pi]$ we denote*

$$H^p[0, 2\pi] := \left\{ \varphi \in L^2[0, 2\pi] \quad : \sum_{m=-\infty}^{\infty} (1 + m^2)^p |a_m|^2 < \infty \right\}.$$

where a_m is the m^{th} Fourier coefficient of φ.

Theorem B.2. (Sobolev Embedding) *For $p > 1/2$, the embedding of the Sobolev space $H^p[0, 2\pi]$ in the space $C_p(2\pi)$ of 2π-periodic continuous functions is compact* [5].

APPENDIX C: Auxiliary Results

Theorem C.1. *Let ∂D be of class C^2. Then there exists a constant $C > 0$ such that*

$$|\nu(x) \cdot \{x - y\}| \leq C|x - y|^2$$

[4, 5].

Proposition C.2. *The exact solution for the unit circle scattering with the direction $a = (1, 0)$ is given by*

$$v(t) = -\frac{2i}{\pi} \sum_{n=-\infty}^{\infty} \frac{e^{in\left(\frac{\pi}{2}+t\right)}}{H_n^{(1)}(k)}, \qquad t \in [0, 2\pi].$$

Proof. Let us assume that the circle is parametrized as $x = (\cos t, \sin t)$ so that

$$u^{inc}(x) = e^{ik\,x\cdot a} = e^{ik\,\cos t}.$$

The *Jacobi-Anger expansion* states [3]

$$e^{iz\,\cos\phi} = \sum_{n=-\infty}^{\infty} i^n\, J_n(z)\, e^{in\phi}$$

while the appropriate *addition formula* for cylindrical harmonics reads [43]

$$H_0^{(1)}(k\left|e^{i\phi} - e^{it}\right|) = \sum_{m=-\infty}^{\infty} J_m(k)\, H_m^{(1)}(k)\, e^{im(\phi-t)}.$$

Thus expanding the exact solution into a Fourier series

$$v(t) = \sum_{n=-\infty}^{\infty} c_n\, e^{int}$$

and plugging these into the integral equation

$$u^{inc}(x) = \int_{\partial D} \frac{i}{4}\, H_0^{(1)}(k|x-y|)\, v(y)\, ds(y)$$

yield

$$\sum_{n=-\infty}^{\infty} i^n\, J_n(k)\, e^{in\phi} = \frac{i}{4} \sum_{m,n=-\infty}^{\infty} J_m(k)\, H_m^{(1)}(k)\, e^{im\phi}\, c_n \int_0^{2\pi} e^{i(n-m)t} dt.$$

Using $\int_0^{2\pi} e^{i(n-m)t} dt = 2\pi\, \delta_{nm}$, we thus get

$$\sum_{n=-\infty}^{\infty} i^n\, J_n(k)\, e^{in\phi} = \frac{i\pi}{2} \sum_{n=-\infty}^{\infty} J_n(k)\, H_n^{(1)}(k)\; c_n\, e^{in\phi}.$$

The last line gives

$$v(t) = -\frac{2i}{\pi} \sum_{n=-\infty}^{\infty} \frac{i^n}{H_n^{(1)}(k)}\, e^{int} = -\frac{2i}{\pi} \sum_{n=-\infty}^{\infty} \frac{e^{in\left(\frac{\pi}{2}+t\right)}}{H_n^{(1)}(k)}.$$

□

REFERENCES

1. Colton, D. and R. Kress, *Inverse Acoustic and Electromagnetic Scattering Theory*, 2nd edition, Springer, New York, 1998.

2. Prem, K. K., *Fundamental Solutions for Differential Operators and Applications,* Birkhauser, Boston, 1996.

3. Abramowitz, M. and I. A. Stegun, *Handbook of Mathematical Functions*, Dover, New York, 1972.

4. Colton, D. and R. Kress, *Integral Equation Methods in Scattering Theory,* Krieger Publishing Company, 1992.

5. Kress, R., *Linear Integral Equations,* 2nd edition, Springer, New York, 1999.

6. Krantz, S. G. and H. R. Parks, *A Primer of Real Analytic Functions*, Birkhauser, Boston, 2002.

7. Rellich, F., "Über das asymptotische Verhalten der Lösungen von $\Delta u + \lambda u = 0$ in unendlichen Gebieten", *Jber. Deutsch. Math. Verein.*, 53, pp. 57-65, 1943.

8. Müller, C., *Spherical Harmonics,* Lecture Notes in Mathematics, 17, Springer, 1966.

9. McLean, W., *Strongly Elliptic Systems and Boundary Integral Equations,* Cambridge University Press, 2000.

10. Brakhage, H. and P. Werner, "Über das Dirihletsche Aussenraumproblem für die Helmholtzsche Schwingungsgleichgung", *Arch. der Math.*, 16, pp. 325-329, 1965.

11. Bruno, O. P., C. A. Geuizane, J. A. Monro, and F. Reitich, "Prescribed error tolerances within fixed computational times for scattering problems of arbitrarily high frequency: the convex case", *Philos. Trans. R. Soc. Lond. Ser. A Math. Phys.*

Eng. Sci., 362, pp. 629-645, 2004.

12. Kress, R., *Numerical Analysis*, Springer, New York, 1998.

13. Atkinson, K., *The Numerical Solution of Integral Equations of the Second Kind,* Cambridge University Press, Cambridge, 2009.

14. Hackbusch, W., *Integral Equations: Theory and Numerical Treatment,* Birkhauser, Basel, 1995.

15. Rivlin, T., *The Chebyshev Polynomials,* Wiley, New York, 1974.

16. Jackson, D., *The Theory of Approximation*, American Mathematical Society, 1930.

17. Kress, R. and I. Sloan, "On the numerical solution of a logarithmic integral equation of the first kind for the Helmholtz equation", *Numer. Math.*, 66, pp. 199-214, 1993.

18. Davis, P. J. and P. Rabinowitz, *Methods of Numerical integration*, Academic Press, Boston, 1984.

19. Nyström, E. J., "Über die praktische Auflösung von Integralglecihungen mit Anwendungen auf Randwertaufgaben", *Acta Math.*, 54, pp. 185-204, 1930.

20. Kress, R., "Minimizing the condition number of boundary integral operators in acoustic and electromagnetic scattering", *Q. J. of Mech. Appl. Math.*, 38, pp. 323-341, 1985.

21. Dunford, N. and J. T. Schwartz, *Linear Operators, General Theory*, Wiley-Interscience, 1988.

22. Lax, P., and A. Milgram, "Parabolic Equations", *Annals of Math. Studies*, 33, pp. 167-190, 1954.

23. Cea, J., *Approximation variatonelle des problemes aux limites*, Ph.D. Thesis, Ann. Inst. Fourier, 1964.

24. Hackbusch, W., *Multi-grid Methods and Applications,* Springer, Berlin, 1985.

25. Melrose, R. B. and M. E. Taylor, "Near peak scattering and the corrected Kirchhoff approximation for a convex obstacle", *Adv. Math.*, 55, pp. 242-315, 1985.

26. Keserci, S., *Analysis of convergent integral equation methods for high frequency scattering,* Master Thesis, Boğaziçi University, 2012.

27. Ecevit, F. and H. Ç. Özen, "A convergent algorithm for high-frequency scattering", (in preparation).

28. Domínguez, V., I. G. Graham, and V. P. Smyshlyaev, "A hybrid numerical asymptotic boundary integral method for high-frequency acoustic scattering", *Numer. Math.*, 106, pp. 471-510., 2007.

29. Langdon, S. and S. N. Chandler-Wilde, "A Galerkin boundary element method for high frequency scattering by convex polygons", *SIAM J. Numer. Anal.*, 2, pp. 610-640, 2007.

30. Spence, E. A., S. N. Chandler-Wilde, I. G. Graham, and V. P. Smyshlaev, "A new frequency-uniform coercive boundary integral equation for acoustic scattering", *Comm. on Pure and Appl. Math.*, 64, pp. 1384-1415, 2011.

31. Schwab, C., *p– and hp–finite element methods. Theory and Applications in Solid and Fluid Mechanics,* Oxford University Press, Oxford, 1998.

32. Keller, J. B., "Geometrical theory of diffraction", *J. Opt. Soc. Am.*, 52, pp. 116-130, 1962.

33. Timan, A. F., *Theory of Approximation of Functions of a Real Variable,* Dover, New York, 1994.

34. Iserles, A. and S. P. Norsett, "On quadrature methods for highly oscillatory integrals and their implementation", *BIT*, 44, pp. 755-772, 2005.

35. Bruno, O. P. and C. A. Geuizane, "An $\mathcal{O}(1)$ integration scheme for three-dimensional surface scattering problems", *J. Comp. Appl. Math.*, 204, pp. 463-476, 2007.

36. Huybrechs, D. and S. Vandewalle, "A sparse discretisation for integral equation formulations of high-frequency scattering problems", *SIAM J. Sci. Comput.*, 29, pp. 2305- 2328, 2007.

37. Domínguez, V., I. G. Graham, and V. P. Smyshlyaev, "Stability and error estimates for Filon-Clenshaw-Curtis rules for highly oscillatory integrals", *IMA J. Numer. Anal.*, 31, pp 1253-1280., 2011.

38. Ihlenburg, F., *Finite Element Analysis of Acoustic Scattering*, Springer, 1998.

39. Chandler-Wilde, S.N. and I. G. Graham, "Boundary integral methods in high frequency scattering", *Highly Oscillatory Problems*, Cambridge University Press, pp. 154-193, 2009.

40. Abboud, T., J. C. Nèdèlec, and B. Zhou, "Mèthode des èquations intègrales pour les hautes frèquencies", *C.R. Acad. Sci. Paris.*, 318, pp. 165-170, 1994.

41. Abboud, T., J. C. Nédélec, and B. Zhou, "Improvement of the integral equation method for high-frequency problems", *Proceedings of 3rd International Conference on Mathematical Aspects of Wave Propagation Problems*, SIAM, Phildelphia, 1995.

42. Giladi, E., "Asymptotically derived boundary elements for the Helmholtz equation in high frequencies", *J. of Comp. and Appl. Math.*, 198, pp. 52 74., 2007.

43. Chew, W. C., *Waves and fields in inhomogeneous media,* New York, IEEE Press, 1995.